Smithsonian Institution
Scholarly Press

SMITHSONIAN CONTRIBUTIONS TO MUSEUM CONSERVATION • NUMBER 5

The Noninvasive Analysis of Painted Surfaces

Scientific Impact and Conservation Practice

Edited by
Austin Nevin and Tiarna Doherty

SERIES PUBLICATIONS OF THE SMITHSONIAN INSTITUTION

Emphasis upon publication as a means of "diffusing knowledge" was expressed by the first Secretary of the Smithsonian. In his formal plan for the Institution, Joseph Henry outlined a program that included the following statement: "It is proposed to publish a series of reports, giving an account of the new discoveries in science, and of the changes made from year to year in all branches of knowledge." This theme of basic research has been adhered to through the years by thousands of titles issued in series publications under the Smithsonian imprint, commencing with Smithsonian Contributions to Knowledge in 1848 and continuing with the following active series:

Smithsonian Contributions to Anthropology
Smithsonian Contributions to Botany
Smithsonian Contributions to History and Technology
Smithsonian Contributions to the Marine Sciences
Smithsonian Contributions to Museum Conservation
Smithsonian Contributions to Paleobiology
Smithsonian Contributions to Zoology

In these series, the Smithsonian Institution Scholarly Press (SISP) publishes small papers and full-scale monographs that report on research and collections of the Institution's museums and research centers. The Smithsonian Contributions Series are distributed via exchange mailing lists to libraries, universities, and similar institutions throughout the world.

Manuscripts intended for publication in the Contributions Series undergo substantive peer review and evaluation by SISP's Editorial Board, as well as evaluation by SISP for compliance with manuscript preparation guidelines (available at www.scholarlypress.si.edu). For fully searchable PDFs of all open access series and publications of the Smithsonian Institution Scholarly Press, visit Open SI at http://opensi.si.edu.

SMITHSONIAN CONTRIBUTIONS TO MUSEUM CONSERVATION • NUMBER 5

The Noninvasive Analysis of Painted Surfaces

Scientific Impact and Conservation Practice

Edited by
Austin Nevin and Tiarna Doherty

Smithsonian Institution
Scholarly Press
WASHINGTON D.C.
2016

ABSTRACT

Nevin, Austin, and Tiarna Doherty. The Noninvasive Analysis of Painted Surfaces: Scientific Impact and Conservation Practice. *Smithsonian Contributions to Museum Conservation* number 5, viii + 81 pages, 43 figures, 5 tables, 2016.—While nondestructive and microdestructive analytical methods are often essential for the study and understanding of paintings, recent development in portable and noninvasive instrumentation has led to growing interest in the applicability of techniques to the study of paintings. Further, as new instrumentation becomes commercially available and more affordable, conservators and scientists are able to use noninvasive techniques for monitoring and analysis in new ways. A focus of the six papers in these proceedings is the interpretation of analytical results from portable instrumentation.

Cover images, from left: detail of the trapezoidal yellow form crossed by a blue bar showing small areas of exposed white underlayer (see Kokkori et al., Figure 5); detail of the *Beatus* initial on fol. 23v, painted by the Gaibana Master (see Ricciardi and Panayotova, Figure 1); and visible light image of sample in cross section from *The Dinner* (see Fife et al., Figure 3).

Published by SMITHSONIAN INSTITUTION SCHOLARLY PRESS
P.O. Box 37012, MRC 957
Washington, D.C. 20013-7012
www.scholarlypress.si.edu

Library of Congress Cataloging-in-Publication Data

Names: Nevin, Austin, 1978– editor. | Doherty, Tiarna, editor. | Smithsonian Institution Scholarly Press, publisher.

Title: The noninvasive analysis of painted surfaces : scientific impact and conservation practice / edited by Austin Nevin and Tiarna Doherty.

Other titles: Non-invasive analysis of painted surfaces | Scientific impact and conservation practice | Smithsonian contributions to museum conservation ; no. 5.

Description: Washington, D.C. : Smithsonian Institution Scholarly Press, 2016. | Series: Smithsonian contributions to museum conservation, ISSN 1949-2359 ; number 5 | Includes bibliographical references and index.

Identifiers: LCCN 2016027011

Subjects: LCSH: Painting—Conservation and restoration. | Fluorescence spectroscopy. | Paint materials—Analysis. | Colorimetry.

Classification: LCC ND1635 .N66 2016 | DDC 751.4--dc23 | SUDOC SI 1.57:5

LC record available at https://lccn.loc.gov/2016027011

ISSN: 1949-2367 (online); 1949-2359 (print)

Publication date (online): 9 November 2016

♾ The paper used in this publication meets the minimum requirements of the American National Standard for Permanence of Paper for Printed Library Materials Z39.48–1992.

Contents

Acknowledgments

The conference "The Non-Invasive Analysis of Painted Surfaces: Scientific Impact and Conservation Practice" was presented in partnership with the Lunder Conservation Center, the International Council of Museums–Committee for Conservation (ICOM-CC) Paintings Working Group and Scientific Research Working Group, and the Foundation of the American Institute for Conservation of Historic and Artistic Works. We thank Christopher Wayner, program coordinator at the Lunder Conservation Center, for assisting with the organization of the conference that was held in early 2014 and for coordinating all of the conference videos that are now available online. We thank Ginger Strader, director of the Smithsonian Institution Scholarly Press, and editor Deborah Stultz for their commitment in managing the publication of this volume.

Introduction

"The Non-Invasive Analysis of Painted Surfaces: Scientific Impact and Conservation Practice" was a conference designed to bring scientists and paintings conservators together to share current research. The two-day event was hosted by the Lunder Conservation Center at the Smithsonian American Art Museum and National Portrait Gallery in Washington, D.C., on February 20 and 21, 2014. Presented in partnership with the Lunder Conservation Center, the International Council of Museums–Committee for Conservation (ICOM-CC) Paintings Working Group and Scientific Research Working Group, and the Foundation of the American Institute for Conservation of Historic and Artistic Works, the meeting was attended by over 150 people. Current research in the field of conservation was presented by scientists, conservators, and companies that develop instrumentation that has compelling applications in the examination and analysis of paintings. Presentations and panel discussions were designed to highlight recent technological developments as well as challenges in interpreting data. All presentations were recorded and can be viewed online (https://www.youtube.com/playlist?list=PL7gn_68Hr4h_qnMshu8PN6wZdPrKoa6sL). Selected papers from the conference are presented in this volume.

A focus of the conference was the presentation of new instrumentation and applications, the integration of imaging and spectroscopic analysis, and the challenging interpretation of analytical results. Although nondestructive and microdestructive analytical methods are often essential for the study and understanding of paintings, recent developments in portable and noninvasive instrumentation have led to growing interest in the applicability of techniques to the study of paintings for the assessment of the environment and for optimizing conservation treatments. Indeed, as instrumentation becomes commercially available and more affordable, conservators and scientists are able to use noninvasive techniques for monitoring and analysis in new ways.

Research by conservators and scientists from different disciplines is found in many papers in this volume, as are case studies based principally on the use of nondestructive techniques for the study of paintings.

An instrument for the measurement of full-field images of paintings based on shearography is presented along with applications to the study of works at the Worcester Art Museum by Klausmeyer et al. These and similar optical metrology methods based on holographic interferometry are extremely powerful and yield convincing data on the immediate and long-term effects of environmental fluctuations on the surface of paintings. Data will surely inform future development of environmental guidelines.

Noninvasive nuclear magnetic resonance (NMR) is employed by Fife et al. in the assessment of two paintings that have significantly different treatment history. Data based on nuclear spin relaxation can be related to the rigidity of the canvases, which are quite different even though both paintings share a common stratigraphy. Indeed, the long-term effects of swelling of paint during cleaning are suggested to be responsible for the modification of the stiffness of the canvas. Nuclear magnetic resonance is likely to find other applications to the assessment of paintings and their conservation in the future.

In-depth case studies based on technical study of one or more paintings on different supports—parchment, wood, and canvas—constitute the main group of papers. Although spanning seven centuries, each of the case studies focuses on unique interdisciplinary methodologies for addressing specific questions related to technique, attribution, pigment degradation, and conservation. A common feature of all the papers presented is the need to unite point-like analytical methods with imaging techniques. Indeed, the strength of imaging or scanning techniques is that specific areas can be analyzed using point-like techniques, and noninvasive data can guide sampling.

Ricciardi and Panayotova present the study of illuminated manuscripts, comparing technical data acquired with noninvasive spectroscopy and imaging with codicological and art historical research. Albrecht et al. demonstrate the integration of analytical and imaging techniques for the study and attribution of fifteenth-century panel paintings. Mass et al. combine point-like X-ray fluorescence with imaging in different modalities to map the degradation of cadmium-based pigments from late nineteenth- and early twentieth-century paintings by Edvard Munch and Henri Matisse. Kokkori et al. present focused analytical research on a painting by Kazimir Malevich, harnessing a range of imaging and analytical techniques, including reflectance Fourier transform infrared spectroscopy, to study the composition of the paint he used and the methods he used to execute the seemingly simplistic shapes in the *Football Player*.

The contributions in this volume thus highlight many aspects of the application of noninvasive techniques to the study of paintings—their conservation, environment, and technique. Conservation science is a multidisciplinary field that relies on the close collaboration between conservators, physical scientists, and art historians. Some techniques are commercially available today, whereas others are still being developed by engineers and conservators for specific applications both in the laboratory and in the museum. There is still a strong need for access to instrumentation and expertise for conservators who do not have dedicated laboratories, and this is particularly important outside of the museum context. Portable and noninvasive techniques, including mobile laboratories, are thus promising solutions for the study of paintings when dedicated instrumentation is not present on site. With increased access to instrumentation the role of specialists remains integral to the correct interpretation of data gathered from complex art materials that have altered over time.

From the range of the six papers in this volume and the various applications of noninvasive methods it is clear that there is no unique toolkit of techniques or single approach based on techniques for the study of paintings and their conservation. The inspiring collection of work instead demonstrates ways in which conservators and conservation scientists can successfully work together.

Austin Nevin
Istituto di Fotonica e Nanotecnologie
Consiglio Nazionale delle Ricerche
Milano, Italy

Tiarna Doherty
Lunder Conservation Center
Smithsonian American Art Museum
Washington, D.C.

Quantifying and Mapping Induced Strain in Canvas Paintings Using Laser Shearography

Philip Klausmeyer,[1] Matthew Cushman,[1] Ivo Dobrev,[2] Morteza Khaleghi,[2,3] Ellery J. Harrington,[2] Xiaoran Chen,[2] and Cosme Furlong[2]*

ABSTRACT. Evaluation of museums' condition standards used for the exhibition of canvas paintings requires a quantitative technique capable of measuring strain induced by changes in temperature, relative humidity, and the thermomechanical effects of light, as well as the effects of ambient vibration. This paper presents advances in developing a customized shearography system for temporal characterization of strains that occur on canvas paintings when subjected to changes in exhibition conditions. The shearography system performs measurements of displacement derivatives along two orthogonal shearing directions and is synchronized with an IR camera to provide thermal maps of the area analyzed. Innovations incorporated into the system include a real-time temporal phase unwrapping algorithm, high-resolution fast Fourier transform methods to calibrate applied shearing levels, and algorithms to produce maps correlated to the temporal domain that locate strain vectors as they occur on the surface analyzed. This research also includes methods for isolating thermal-induced components from randomly induced mechanical vibrations through integration of IR imaging data. As a verification and exploration of the fault detection capabilities of our shearographic system, we have performed preliminary experiments that compare measured gradients of displacement with slopes of surface topology obtained by reflectance transformation imaging (RTI). Preliminary analysis indicates good correspondence between spatial patterns, indicative of surface cracks, in both shearographic and RTI data. The capability of the system to detect discontinuities in paint surfaces as well as to measure and map associated strain vectors as a function of changes in condition parameters is herein illustrated. Our multidomain approach, incorporating strain, thermal, and topographical data, has the potential to inform larger ongoing discussions regarding conservation standards for the exhibition of artwork as well as improving defect detection and evaluation of restoration techniques.

[1] Conservation Department, Worcester Art Museum, 55 Salisbury Street, Worcester, Massachusetts 01609, USA.

[2] Center for Holographic Studies and Laser micro-mechaTronics, Nanoengineering, Science, and Technology, Worcester Polytechnic Institute, 100 Institute Road, Worcester, Massachusetts 01609, USA.

[3] Stanford Biomedical Optics Group, 450 Serra Mall, Stanford University, Stanford, California 94305, USA.

[*] Correspondence: C. Furlong, cfurlong@wpi.edu

Manuscript received 15 August 2014; accepted 22 February 2016.

INTRODUCTION

Shearography is a full-field, nondestructive, noncontact, optical method that uses coherent light to conduct strain and vibration analysis (Hung, 1982). The method is highly sensitive for measuring load-induced surface displacement gradients and can effectively detect surface and subsurface discontinuities (Schnars and Jüptner, 1994; Steinchen and Yang, 2003; Lee et al., 2014). Although similar to holographic interferometry, shearography differs in that instead of measuring displacement, it measures gradients of displacement.

One of the primary advantages of shearography over holography is its relative insensitivity to environmental disturbances. Other advantages include range, mobility, versatility, ease, speed, and relative low cost. For these reasons, applications of shearography continue to grow, particularly as a method for defect detection in the aerospace, automotive, and

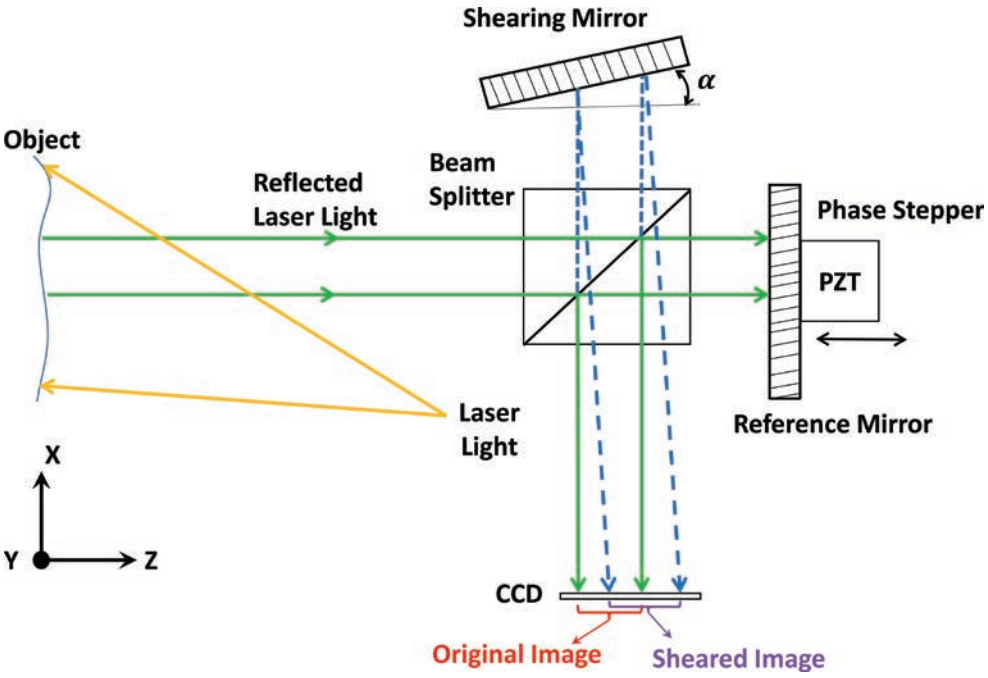

FIGURE 1. Schematic of shearography instrument and setup. The angle of α defines the measurement sensitivity.

wind power industries, where the performance of coatings and laminated surface construction is critical.

As a highly sensitive technique for measuring gradients of displacement, shearography also has great potential for applications in art conservation (Groves et al., 2009a, 2009b; Sfarra et al., 2011; Meybodi et al., 2012; Morawitz et al., 2013). In recent years, the majority of shearography-based research into art conservation applications has taken place in Europe, with the Institute for Technical Optics at Stuttgart University and the Foundation for Research and Technology–Hellas (FORTH) in Crete, Greece, each being research hotbeds. Most of the research has focused on detecting delamination or structural flaws in panel or wall paintings (Kalms and Jueptner, 2005; Morawitz et al., 2013). Tornari and her group at the Institute of Electronic Structure and Laser–FORTH spearheaded the development of a hybrid portable interferometry-shearography system entitled "MultiEncode: Multifunctional Encoding System for Assessment of Movable Cultural Heritage," in which a shearography-based system was developed to monitor the condition of paintings before and after transport (Groves et al., 2007; Tornari et al., 2009). This project also led to the development of a fringe database for using fringe patterns unique to each work as a method of authentication. Previous work (Georges et al., 2014) incorporating thermography, holography, and shearography has also indicated a multidomain approach to fault detection in complex multimaterial, multilayered objects with structural and mechanical complexity similar to that of paintings.

PRINCIPLES AND METHODS

The shearographic system allows for quantitative evaluation of deformations of an object and, more specifically, the spatial derivative, or slope, of the deformations. In general, the shearographic system allows for comparison between two or more distinct states of the object of interest, typically before and after application of a controlled excitation (Hung, 1982). The deformation of the object induces optical light path changes that lead to optical light phase changes in the optical setup of the shearographic system. Each state of the optical phase and intensity in the optical system, encoded within a shearographic interferogram, is recorded via a digital camera. By analyzing and comparing the phase differences between the interferograms, corresponding to each state of the object, the spatial gradient of the object's deformation can be quantified.

Optical Setup

Our shearographic setup, shown in Figure 1, is based on a Michelson interferometer and works by capturing laser light reflected from the optically rough (Hung, 1982) surface of an object, which is illuminated with an expanded laser beam. Some of the reflected laser light passes through a lens into the shearographic interferometer, where it is split into two identical beams and is later recombined at the camera sensor with a slight spatial offset (optical shear) between the two beams (Huang, 1997),

as shown in Figure 1. The interference between the two beams, forming the original and the sheared image, gives rise to an interferogram, which consists of spatially varying intensity and phase patterns, also known as fringes.

Measurements of Displacement Gradient through Optical Phase

The specific interference pattern at each moment in time is a result of multiple parameters, including the geometrical and optical characteristics of the environment and surfaces that the laser light passed through or reflected from, which means that the interference pattern is also dependent on the geometry of the object of interest. Any deformations in the object, as long as they alter the laser light path, will induce a corresponding change in the optical phase of the interference pattern at the camera sensor. On the basis of the optical configuration of our shearographic system, assuming the illumination and observation (z axis in Figure 1) directions are coaxial, the optical phase change $\Delta\Omega$ is related to the spatial gradient of displacement of the object $\frac{\delta w}{\delta s}$ along the observation direction of the system (Hung, 1982):

$$\Delta\Omega = \frac{4\pi}{\lambda}\frac{\delta w}{\delta s}\Delta s, \tag{1}$$

where λ is the optical wavelength, s and Δ are the direction and magnitude of the applied optical shear respectively, and w is the displacement of the object along the observation direction. Assuming that the observation direction of the shearographic system and the surface normal of the object (assuming an approximately flat object) are aligned, $\frac{\delta w}{\delta s}$ becomes proportional to the spatial derivative of the out-of-plane displacement of the object. Our shearographic optical setup allows for optical shear in vertical (x axis) and horizontal (y axis) directions as well as any combination of the two. This allows for individually extracting $\frac{\delta w}{\delta x}$ and $\frac{\delta w}{\delta y}$, corresponding to the vertical and horizontal spatial derivatives of the out-of-plane displacement of the object.

These displacement gradients partially define the full strain tensor S, which is composed of nine components, six shear strain and three tensile strain components located along the diagonal of the tensor, as described in the following equations(Chen, 2014):

$$S = \begin{Bmatrix} \frac{\partial u}{\partial x} & \frac{1}{2}\left(\frac{\partial u}{\partial y}+\frac{\partial v}{\partial x}\right) & \frac{1}{2}\left(\frac{\partial u}{\partial z}+\boxed{\frac{\partial w}{\partial x}}\right) \\ \frac{1}{2}\left(\frac{\partial v}{\partial x}+\frac{\partial u}{\partial y}\right) & \frac{\partial v}{\partial y} & \frac{1}{2}\left(\frac{\partial v}{\partial z}+\boxed{\frac{\partial w}{\partial y}}\right) \\ \frac{1}{2}\left(\boxed{\frac{\partial w}{\partial x}}+\frac{\partial u}{\partial z}\right) & \frac{1}{2}\left(\boxed{\frac{\partial w}{\partial y}}+\frac{\partial v}{\partial z}\right) & \frac{\partial w}{\partial z} \end{Bmatrix}, \tag{2}$$

Shearing in X and Y individually:

$$\boxed{\frac{\delta w}{\delta x} = \frac{\lambda\Delta\Omega}{4\pi\Delta x}} \tag{3a}$$

$$\boxed{\frac{\delta w}{\delta y} = \frac{\lambda\Delta\Omega}{4\pi\Delta y}} \tag{3b}$$

Measurements of Optical Phase Changes

Most camera sensors, including the one that is used in this setup (Pike-100B with KAI-1020 CCD sensor, AVT, Stadtroda, Germany), are sensitive only to the intensity, and not the phase, of the light. As a result, several methods have been developed for the retrieval of the light phase, and popular methods include fringe skeletonization (Osten et al., 1994), phase stepping (Creath, 1985), and Fourier transform–based methods (Takeda et al., 1982; Ge et al., 2001). Our shearographic system uses a custom-made automated phase sampling technique (Harrington et al., 2010, 2011), which is based on a four-step temporal phase sampling method (Creath, 1985). The four-phase-stepping approach is implemented on the basis of the need for developing a high-resolution, quantitative, and real-time measuring system. The method allows for quantification of the phase distribution of an interferogram by recording its intensity four times (at four camera frames), each with an incremental phase shift of 90° from the previous one. Each controlled phase step is achieved by a custom-made phase stepper (shown in Figure 1), the details of which are given later in this work. One set of four phase-stepped frames is related to the shape of the object at a particular state. The deformation of the object between any two states is related to the corresponding phase change, which is defined as follows (Chen, 2014):

$$\begin{aligned}\Delta\Omega(x,y) &= \Omega'(x,y) - \Omega(x,y) \\ &= \tan^{-1}\left[-\frac{(I_1-I_3)(I'_2-I'_4)-(I_2-I_4)(I'_1-I'_3)}{(I_1-I_3)(I'_2-I'_4)+(I_2-I_4)(I'_1-I'_3)}\right],\end{aligned} \tag{4}$$

where $I_{1,\ldots,4}$ are the four phase-stepped shearograms in the reference state and $I'_{1,\ldots,4}$ are the corresponding data in the deformed state. It can be seen that the phase change is calculated on the basis of only intensity information. In essence, four images are collected at the reference state, and four images are collected in the deformed state, and then this equation is calculated for every pixel at every time instance relative to another reference time instance. In the case of continuous measurements with thousands of data frames (each containing four images), the reference and deformed data frames may be defined arbitrarily by the user in order to compare the differences in the optical phase between two data frames, which, in turn, corresponds to the gradient of displacements that occurs between the two instants.

This optical phase sampling method assumes that during the capturing of the required four interferograms at each deformation state, the object and the surrounding environment are steady and do not induce a significant phase change on their own. The adequacy of this assumption has been verified through pilot tests in the museum environment based on the test setup described later in this chapter, as well as based on the literature (Kalms and Jueptner, 2005; Morawitz et al., 2013). This optical phase sampling method was chosen because of its superior spatial resolution, allowing for a quantification of the phase sampling at each pixel individually. The specific choice of the number of phase shifts and phase step size was defined on the basis of pilot studies of shearographic measurements on oil-on-canvas paintings in our laboratory settings

(Chen et al., 2014; Khaleghi et al., 2014) as well as literature (Kalms and Jueptner, 2005; Morawitz et al., 2013). Further work might be needed to find an optimal phase sampling technique and corresponding acquisition parameters; however, the ones used in this work were deemed sufficient for our preliminary work.

Temporal Unwrapping of Optical Phase Changes

Because of the use of the arctangent function in equation (4) to calculate phase differences, the resulting phase data "wraps" within a range of $-\pi$ to π radians, which causes spatial discontinuities in the spatial distribution of the measured phase across the recorded image. This wrapping of data is particularly challenging when measuring displacements that occur over an extended period, and as the displacement gradient increases, repeated wrapping occurs, and the resulting image becomes increasingly difficult to interpret. It is therefore necessary to demodulate or "unwrap" the data.

Existing spatial phase unwrapping algorithms have limited capabilities in the analysis of interferometric images of objects undergoing physical deformations that result in a large number of phase discontinuities (>50 cycles of phase across the field of view). The temporal phase unwrapping algorithms developed in this research and on the basis of existing methods (Huntley and Saldner, 1993) overcome this limitation. The basic idea behind the method is that the phase change at each pixel is measured as a function of time and is unwrapped along the temporal dimension independently of the neighboring pixels (Dobrev et al., 2012; Kreis, 2005). The temporal unwrapping method (Chen, 2014) relies on the assumption that the phase change between any two consecutive frames is between $-\pi$ and $+\pi$. This is an adequate assumption for this application because although the object may be undergoing large deformations, the temporal rate of the deformations is relatively slow. Typical significant changes for the range of our shearographic system and setup take >1 s to develop under typical testing conditions in museum settings, whereas the camera recording is done at 60 frames/s, resulting in <70 ms to capture a set of four images. The effects of random noise, which might contribute to significant phase variations between frames, has been suppressed with the use of spatial averaging filters with a size (i.e., 3 × 3 pixels) adjusted on the basis of the smallest features (i.e., <1 mm) that were considered to be important for this research. Although surface cracks could be much smaller, we assumed that their effect on the local deformation patterns will be sufficiently large in space to be detected by the shearographic system. Additionally, because of the inherited scalability of the optical system, analyzing a smaller region with a greater level of spatial detail and sensitivity is just a matter of adjusting the zoom lens or the shear, without any change in the overall analysis procedure.

Calibration of the Measurement Sensitivity

An important point to make from equation (1) is that the sensitivity of the system is highly affected by the amount of shear. Therefore, it is important to quantify the shear amount in order to convert the phase data from radians to appropriate engineering units.

This research implements a method based on the shift theorem of the Fourier transform that allows for the direct estimation of the shear amount without any pre- or postcalibration procedures (Figure 2). The technique is based on existing computer vision methods used to estimate camera motion during television broadcast (Bracewell et al., 1993; Licsár et al., 2003). The idea behind this method is that the 2D fast Fourier transform (FFT) of the superposition of an image and its sheared twin (i.e., the case of shearograms) will result in a 2D power spectrum, the magnitude of which is sinusoidally modulated with a period inversely proportional to the shear amount (Khaleghi et al., 2014). Typically, the images are captured individually and superimposed digitally, although in the case of shearograms, the two images are superimposed optically and are captured simultaneously, but this does not change the general principle of the method. For

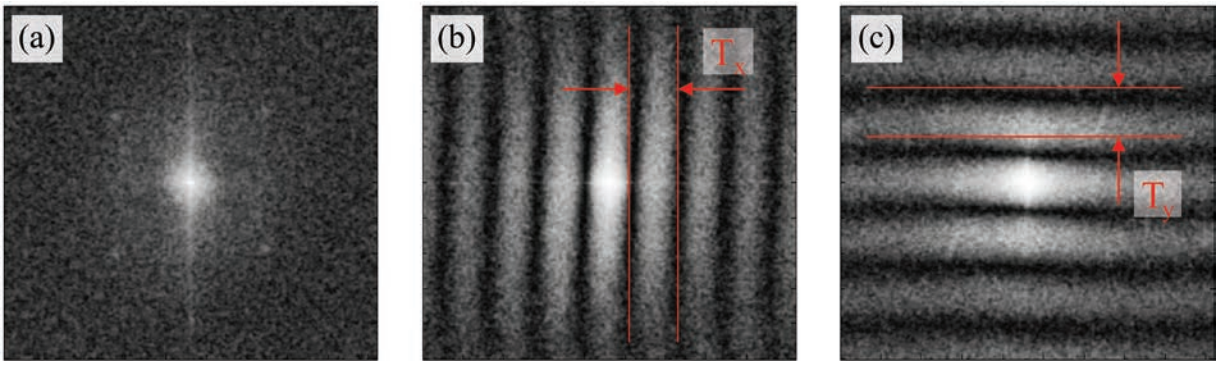

FIGURE 2. Illustration of the mathematical principle behind the automatic shear estimation algorithm. A power spectrum of the 2D FFT of a shearogram: (a) with no shear, (b) with shear in the horizontal (*x*) direction, and (c) with shear in the horizontal (*y*) direction. The corresponding modulation period is indicated (Chen, 2014).

example, for a horizontal shear (i.e., along the x direction), the relation between the period T_x of the modulation in the 2D FFT power spectrum (Figure 2b) and the shear amount x_0 can be expressed as (Chen, 2014)

$$x_0 \approx \Delta x \frac{N}{T_x}, \tag{5}$$

where Δx and N are the pixel size and number of pixels in the shear direction, respectively. By automatically extracting the period of the modulation in the FFT of the shearogram, we get the shear amount in the system. A novelty of our work (Khalegi et al., 2014; Dobrev et al., 2012; Chen, 2014) is in the development of automatic software for shear estimation and its application for shearography analysis. This tool greatly simplifies and accelerates the measurement procedures, as it does not require any calibration after each adjsutment of the shearographic system, thus allowing for rapid optimization of the recording parameters relative to the response of each new sample or loading procedure.

TEST SETUP

Initial tests in this research used shearography to see if a thermomechanical response could be detected on the surface of an oil painting as a result of simply turning on and off lights such as those used in a typical photography session. The setup mimicked the same configuration used at the time by the museum conservators for photographing works, the only difference being that the camera was replaced with the shearography instrument and workstation (Figure 3).

The shearography instrument constructed at Worcester Polytechnic Institute (WPI) is a mobile system that utilizes an adjustable tripod, a computer workstation, and an uninterrupted power supply (UPS) to power the system between relocations. In this case, the coherent light source is a 473-nm laser (50 mW, Diode-pumped solid-state [DPSS], Oxxius, Lannion, France), and the measuring head consists of a custom-built interferometer, a camera lens (zoom lens, 12.5–75 mm, model 53-153, Edmund Optics, Barrington, New Jersey, USA, and a camera (Pike F100B, AVT) interfaced directly to the computer workstation (Figure 3). The measuring head has an approximate size of 25 × 25 × 25 cm, excluding the lens and the IR camera, which can be easily removed or changed in accordance with the needs of each experiment. The size of the shearographic optical head, excluding the lens, laser, and IR camera, is 25 × 7 × 7 cm. The laser was mounted directly next to the lens, aligned approximately (i.e., <2° deviation) parallel to its optical axis. The laser beam, with a diameter of <0.3 mm, was expanded to a circular spot with a diameter of ~40 cm. The camera consists of a Truesense KAI-1020 CCD sensor, which has a resolution of 1,000 × 1,000 pixels at

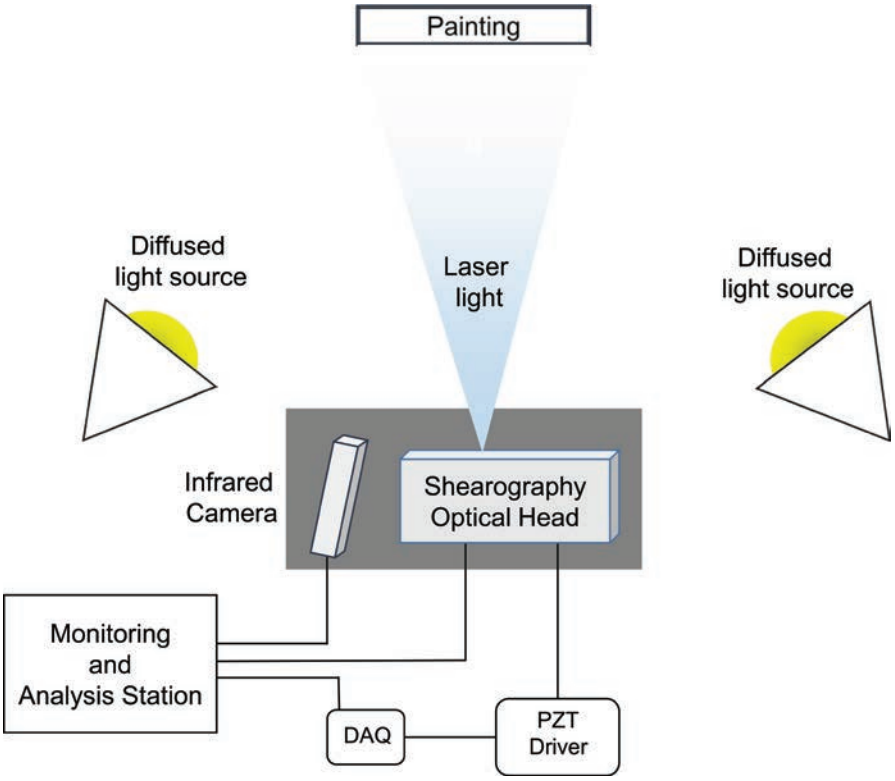

FIGURE 3. Schematic of the shearography setup during initial tests.

7.4-µm pixel pitch. The camera exposure time was 10 ms, with a frame rate of 60 frames/s. Phase shifting was achieved through a custom-made phase stepper based on a customized piezoelectric transducer (PZT; PAS005, Thorlabs, Newton, New Jersey, USA), driven by an analog output card (DAQ, NI USB-6343, National Instruments, Austin, Texas, USA) via a piezo controller (MDT694B, Thorlabs). All of the above components were combined into a compact optical head, shown in Figure 3.

Connectivity in the instrument includes firewire B from camera to laptop, USB 2.0 from DAQ to laptop, and Bayonet Neill-Concelman (BNC) cables from DAQ to PZT amplifier and camera (the camera triggers the DAQ, which then steps the PZT). The instrument is also equipped with an IR camera (FLIR A310) connected via GigE to the laptop in order to correlate thermal data with the shearography data. Excluding the IR camera, the instrument costs a few thousand dollars, the most expensive component being the camera. The control software was custom written at WPI (Harrington et al., 2011) and allows for the automatic continuous synchronization between camera frames and phase stepping, full control of all system settings (exposure, frame rate, recording speed, etc.), and storage of data and live display of the current phase map referenced to any desired frame.

A 473-nm, 50-mW laser was used essentially because it was the least powerful of the lasers available in the lab at the time in order to minimize the thermal excitation of the painting while providing sufficient illumination of the area of interest to allow shorter camera exposure times and higher recording speeds. The laser's coherence length is >10 m; however, a long-coherence laser is not necessary, and previous research (Falldorf et al., 2003) has shown the possible use of a white light source with limited coherence length (i.e., temporal coherence of <50 µm). One of the main constraints for use of a short-coherence light source is the maximum observable gradient of the object's surface, which is dependent on the applied shear and the direction of illumination (Falldorf et al., 2003). Tests with laser diodes from pointers, with a coherence length of <0.5 mm and a cost of <$10, indicate that sufficient amounts of shear can be achieved for quantitative analysis of flat objects (Chen, 2014), similar to pictures. Although this assumption may not hold at the steep walls of cracks on the paint surface, we assume that the cracks will influence the deformation of flat areas in their proximity, which in turn will be sufficient to estimate the location of the cracks within the spatial resolution of the system (i.e., <0.5 mm).

The initial setup (Kaleghi, et al. 2014) (Figure 4) positioned the system 1.8 m from the painting analyzed, allowing for the full field of view (FOV) range available with the objective lens. However, because of power limitations of the laser, the FOV was kept to 0.35 m, leaving the spatial resolution of the measurements to be 0.15 mm/pixel. The loading source in these initial tests was two Lowel Tota-lights with 500-W halogen bulbs, each equipped with a diffusing umbrella and positioned at 45° angles 2.3 m from the painting. The spectrum of the lights covers nearly the full visible range, including the laser's 473 nm, as well as a sufficient amount of infrared radiation for thermal excitation of the sample. The initial testing consisted of a 60-s loading period with the lights on, then a 60-s recording time immediately after turning the lights off (unloading period), which resulted in a 0.7°C increase in surface temperature of the painting in the loading cycle. Because of the high power of the lights compared to the laser, the shearographic system's camera saturated during the loading cycle. As a result, only the unloading period (lights off) was shearographically recorded.

The painting used throughout this research was an unlined, late nineteenth-century oil on canvas that is privately owned. The paint surface exhibits a network of craquelure and, to a lesser extent, drying cracks throughout, a few scattered paint losses, and a small puncture. The paint thickness varies from thin to areas with moderate impasto.

Previous work combining shearography and thermography has indicated the potential advantages of IR cameras in

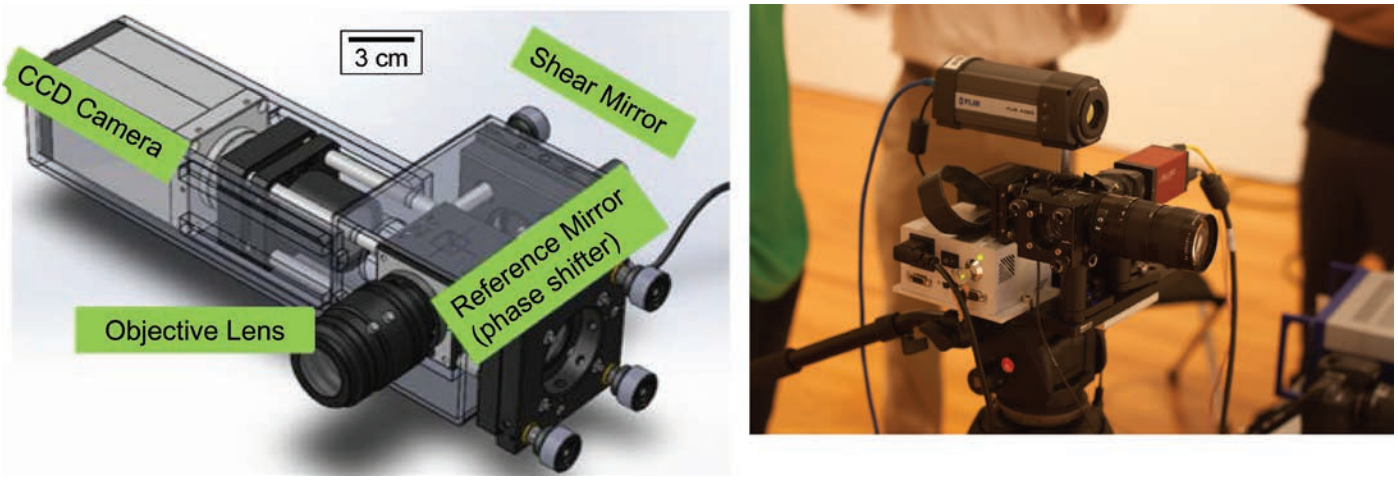

FIGURE 4. The CAD model of the instrument (left) and the realized instrument (right). (Chen, 2014; Chen et al., 2014)

shearographic inspection (Georges et al., 2014). The integrated IR camera enabled researchers to map the surface temperature of the painting throughout the process. The temperatures across the full surface of the painting, the frame, and the background wall were recorded. The temperature uniformity across the paint surface was within 0.2°C, and the average temperature change was within 0.3°C–0.6°C, with smaller changes at the periphery and larger changes at the center of the picture. The spatially varying temperature changes can be explained by better heat dissipation at the edge of the painting surface because of its proximity to the frame and stretcher structure. A 6-min equilibration period took place in between loading-unloading cycles, enabling researchers to start from the same temperature during each run.

CONTROLLED TEMPERATURE EXCITATION TESTING

Since the shearography system allows for recording with one shear direction at a time, at least two recordings are needed to capture the *X* (horizontal) and *Y* (vertical) components of the spatial gradient of the out-of-plane deformation individually. We verified the reliability of such a method by performing at least three measurements, each following the procedure described in the previous section, in each shear direction, which indicated a standard deviation of <5% of the maximum detected slope of deformation. The *X* and *Y* data sets were then combined to create a cumulative gradient of displacement map with a magnitude converted into microstrains, the unit preferred for representing such data (bottom row in Figure 5). The reference for all measurements, at each thermal cycle, was the first measurement (four phase-stepped frames) immediately after turning off the lights. Data in the bottom panels in Figure 5 refer to an example measurement made 10 s after turning off the lights. The data appear to indicate displacements that correspond to a dense crack network. Note the relatively large displacement gradients along the top and right margins roughly corresponding to the underlying stretcher bar support.

The 10-s time mark, indicated in Figure 5, roughly corresponds to the maximum spatial density of contours (fringes) of the wrapped phase (Figure 5, top middle panel) that could be still unwrapped via conventional spatial phase unwrappers (Ghiglia

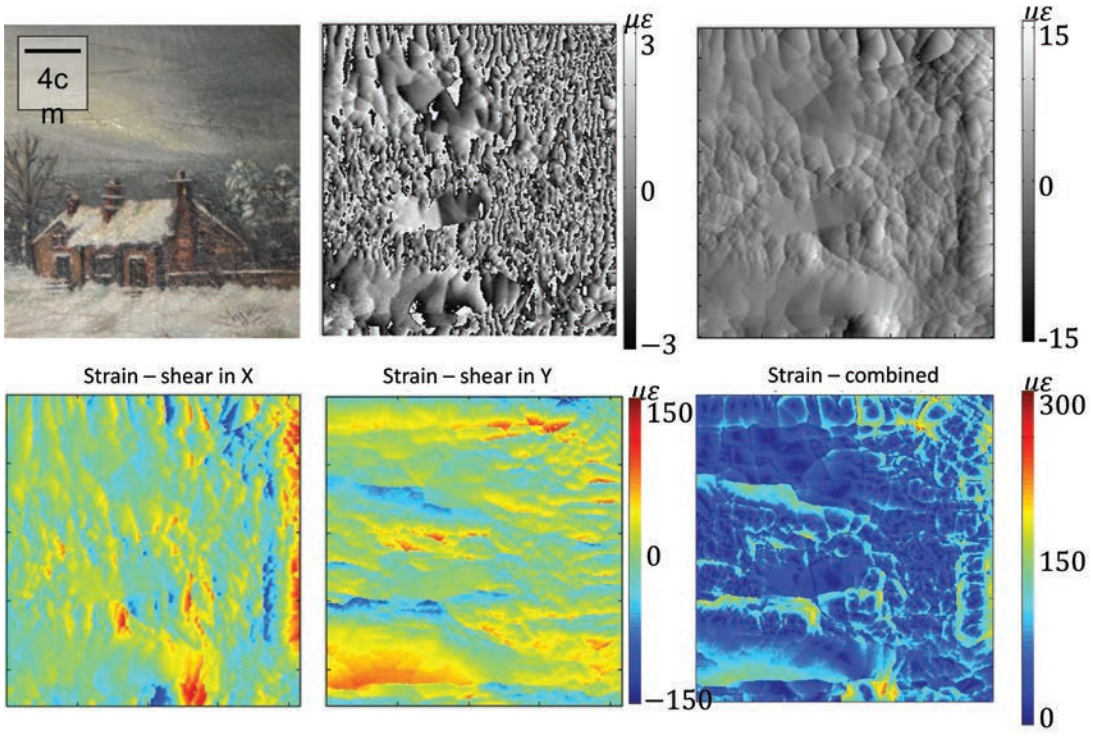

FIGURE 5. Analysis of an oil painting on canvas showing the transient response to thermal loading. An image of the upper right quadrant of the painting that was analyzed (top left) and the corresponding maps of wrapped and unwrapped optical phase measurements taken during a 10-s period of cooling immediately after turning the lights off (top middle and right). Color-coded gradient of displacement maps in the *X* and *Y* shear directions (bottom left and middle, respectively) and the absolute value of the combined gradients of displacement of both *X* and *Y* data sets with the scale in microstrains (bottom right). Painting analyzed: Untitled, oil on canvas, unknown artist, private collection.

and Pritt, 1998). However, since the response of the painting reached a relatively stable state only after 1 min, recordings were done for 60 s, at which point the spatial density of the wrapped phase contours becomes too high. Thus, only the temporal phase unwrapping algorithm was used for all recordings in this paper. The first 10 s have been presented as an illustration of the analysis approach, and a detailed analysis of the full 60-s cooling cycle will be included in a future work.

Temporal variations of the derived gradients of displacement can be viewed relative to each other in Figure 6. The ability to correlate strain to the temporal domain can be used not only to chart thermomechanical response but also to inform our understanding of equilibration properties of the object analyzed (Figure 6). This could be achieved by combining the full-field displacement gradient measurements with the full-field temperature data from the IR camera in order to obtain intrinsic material properties such as local heat coefficients and thermal time constants, which can be used to optimize the preservation conditions for each picture individually.

In order to provide more detailed information for the deformation pattern and cracks, we combined the magnitude and direction information of the combined data for both the *X* and *Y* deformation gradients into a single display, as show shown in Figure 7 (right), where corresponding color-coded arrows indicate the direction and magnitude of deformation gradients. It should be noted that although the vectors are expressed in plane, since they show the spatial direction of the highest slope of deformation, the deformations and the corresponding strains are occurring out of plane. Superposition of the resultant strain map on a ghost image of the area analyzed can help correlate gradients of displacement information with features present on the paint surface or under it.

IN SITU GALLERY TESTS

Following the tests that mimicked the Worcester Art Museum's lab photography setup, investigations shifted into the Worcester Art Museum galleries. On a two-day span in July, when the museum was closed to the public, a small painting on exhibit was replaced with the test painting, and the shearography instrumentation was set up in the gallery to monitor changes that occur over the course of a typical day-night cycle. In this case, the light loading was provided by broad washes of light from a pair of ceiling-mounted 50-W halogen bulbs 4 m away. For comparison, the same region of the test painting was analyzed. The combination of lower-power lights and the larger distance from the painting resulted in greatly reduced negative effects of the museum lighting to the shearographic system, such as local saturation and reduced fringe contrast, and allowed continuous operation regardless of the state of the lights. Preliminary noise floors tests of the shearography system under such conditions indicated ~λ/15 phase variation, equivalent to ~8 με.

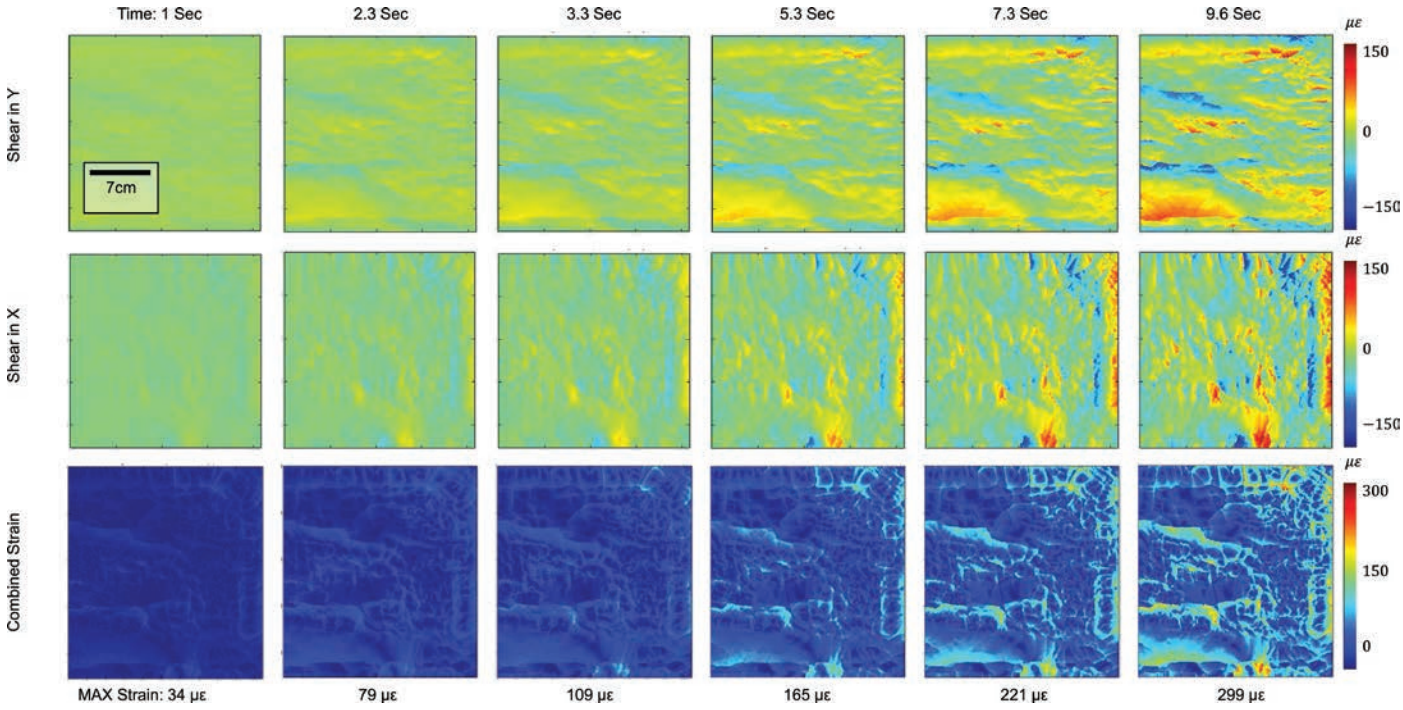

FIGURE 6. Gradient of displacement maps over a 10-s period of cooling when shear is in the *Y* direction (top row) and in the *X* direction (middle) and the resultant gradient of displacement maps when both shear directions are combined (bottom).

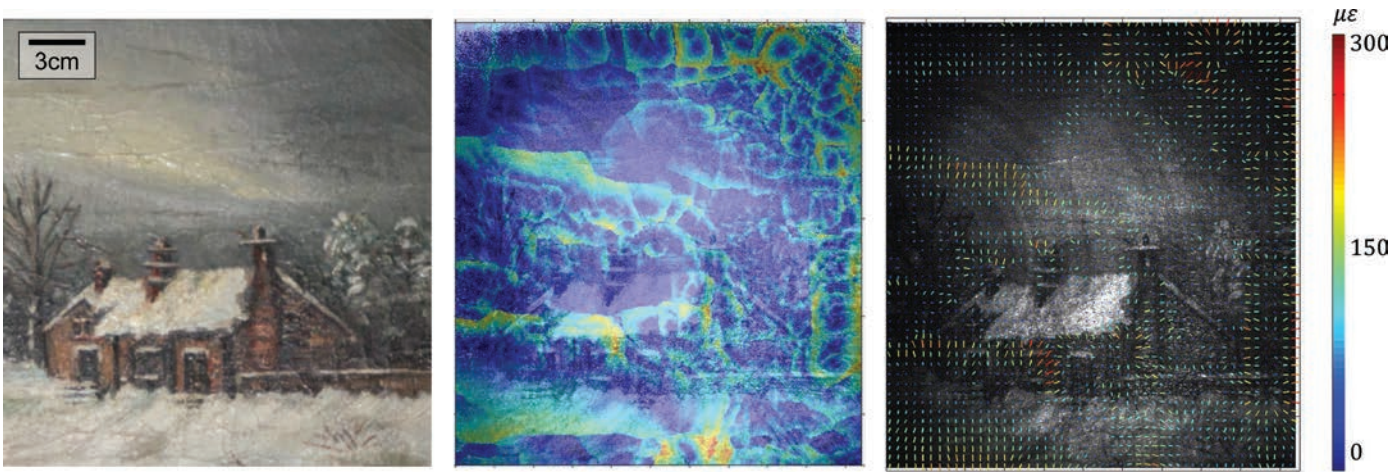

FIGURE 7. Representative in-plane laser shearography measurements of the upper right region of the painting analyzed (left). Color-coded strain map of same area indicating gradients of displacement originating along discontinuities in the paint film during a 10-s cooling period directly after thermal loading with photography lights (middle). The corresponding strain vector map indicating magnitude and direction of induced strain via color-coded arrows (right). Painting analyzed: Untitled, oil on canvas, unknown artist, private collection.

Setting appropriate acquisition parameters was a critical step, particularly regarding frame rate in order not to overwhelm the computer's memory capacity and the analyst's capacity to process the data. Data were taken in a time-lapse manner by making one measurement, consisting of four phase-stepped frames taken in a burst at 60 frames/s, every 10 s for a total duration of 27 hours, resulting in ~10,000 measurements (i.e., ~100 GB).

Temperature and relative humidity (%RH) data for the gallery were recorded internally in the museum's HVAC system throughout the course of the investigation and varied from 46.8% to 49.8% RH and from 23.1°C to 24.4°C. The recorded temperature and %RH timeline was also used to plot significant events, such as the beginning and ending of shearography analysis and when the lights were turned on or off (Figure 8, top). Shearography data were later analyzed to see if correlations exist between changes in gallery conditions and strain responses in the paint surface.

The amount of data acquired with the shearography instrument is substantial and presents a challenge for postprocessing. Ongoing work with processing software seeks to assist with this process. Efforts thus far have focused on examining data for correlations between detectable strain and changes in gallery lighting. Data revealed that even in the tightly controlled climate of the gallery, the paint surface underwent a detectable thermomechanical response when the lights were turned on or off (Figure 8, bottom row).

The maps in Figure 8 show that the greatest (i.e., 100–120 με range) strain incurred shortly after turning on the lights is along the edge of the canvas, whereas the center appears relatively stable. The reverse is true when turning off the lights. The low (i.e., 20 με) level of strain detectable (noise floor is <10 με) during the stable state, represented here by Figure 8a, is likely related to ambient vibration. As the analysis progressed, it became increasingly apparent that the sensitivity of the shearography instrument enables clear correlations to be drawn between exhibition conditions and physical changes in the painting.

Future work on this experiment will involve application of the temporal unwrapping software in a memory efficient way on the full data set. Once this is complete, the next step could be the comparison between the full shearographic data and the climate control parameters in order to analyze the response of the picture. Such a comparison could help us devise a scheme for the optimization of the climate control parameters to minimize strain fatigue on the painting while minimizing energy consumption.

CORRELATING SHEAROGRAPHY DATA TO TOPOGRAPHICAL FEATURES

The final component of this investigation explored how to improve capabilities for correlating shearography data with existing topographical features on the surface of paintings. This general problem is noted in the literature and was encountered firsthand when trying to relate shearography data to the network of cracks evident on the test painting. The images shown in Figure 8 of gradients of displacement and strain vector maps illustrate how processed shearography data can be overlaid with conventional camera images of the corresponding area. However, because of the lack of quantitative information about the topological features captured in conventional camera images, the encoded color information about the paintings surface may not be representative of the painting's surface topology and underlying

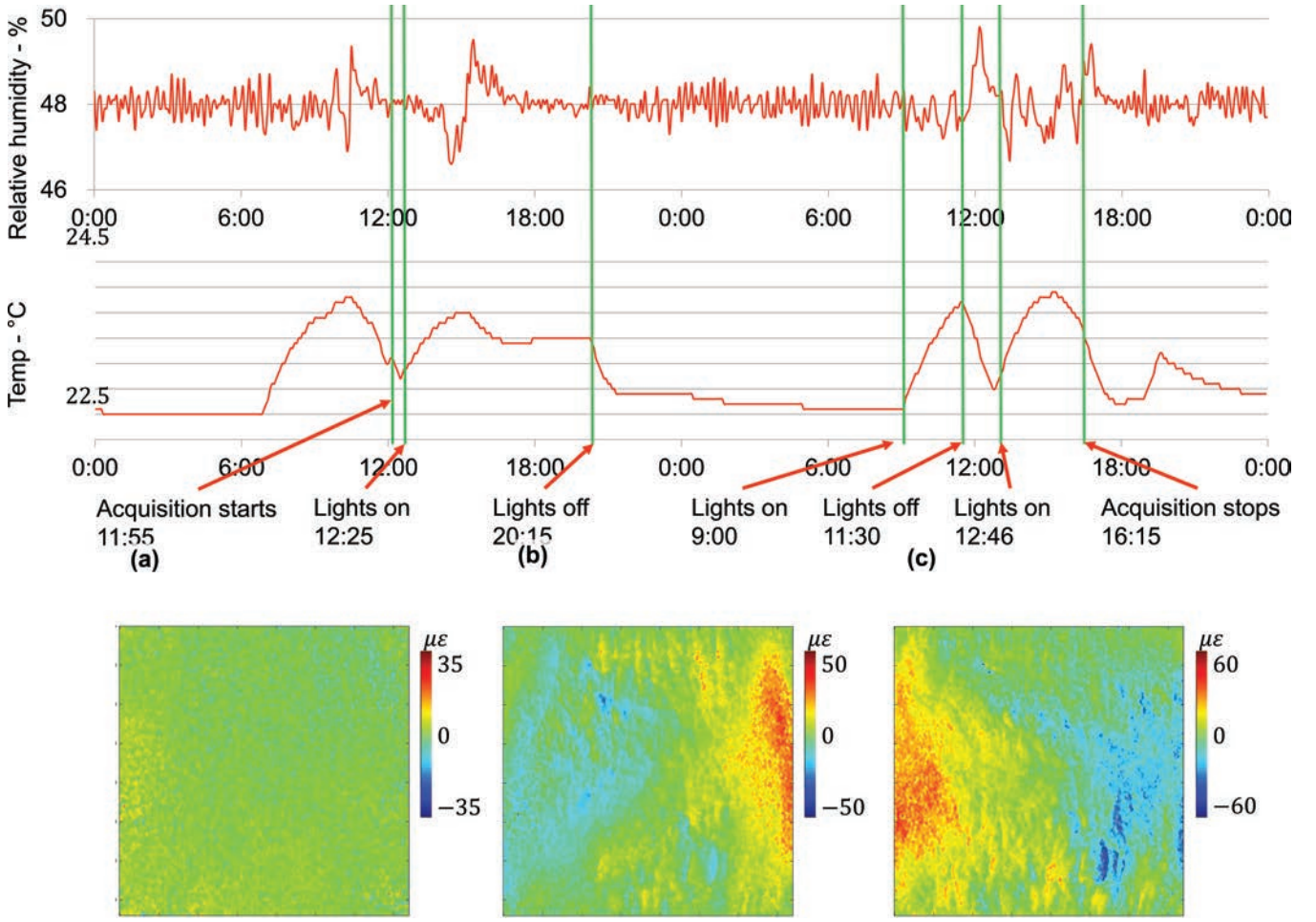

FIGURE 8. Temporal variation of the %RH and temperature over a 48-hour span (top). Arrows indicate start and stop times of shearography analysis, as well as times when lights were turned on or off. Three strain maps of the same upper right area of the test painting taken at different times: (a) 10 s before turning on the gallery lights, (b) 10 s after turning on the lights, and (c) 10 s after turning off the lights.

structure. The discrepancy between color information and surface topography makes a direct comparison with shearographic data more difficult to interpret.

In order to facilitate comparison with a greater level of detail, we utilized the visually rich surface imaging technique of reflectance transformation imaging (RTI), and we explored it as a possible compliment to shearography data. Because of limitations with the FOV of the available RTI system (lighting array system designed by the Cultural Heritage Imaging Corp., San Francisco, California, USA), only about 50% of the area, as shown in the previous two experiments, was available for comparison with the shearographic system. For direct side-by-side comparison with the gradient of displacement maps, the specular enhancement viewing function available in RTI viewing software (RTIViewer V1.1, Cultural Heritage Imaging Corp.) was initially considered, as it enhances the visible details of the topography of the paint surface (Figure 9, middle). However, in order to remove any subjectivity in relating gradients of displacement to physical features on the painting, other approaches were considered. The improved functionality of the most recent RTI viewing software allows one to generate per-pixel surface normal data, which quantifies the in-plane and out-of-plane slope of the shape of the painted surface. The surface normal is related to the slope of the surface shape and therefore can be interpreted as a collection of two pieces of information: the magnitude and the direction of the slope of the local shape. A slope with larger magnitude indicates steeper surface features such as those at the crack boundaries and walls. For this reason, magnitude information was extracted from the surface normal data and further color coded such that deep blue or red indicates high positive or negative slope and green indicates no or very little slope of the surface topography (Figure 9, right).

Our main hypothesis behind such an approach is that surface cracks, detectable through the RTI surface normal data, will

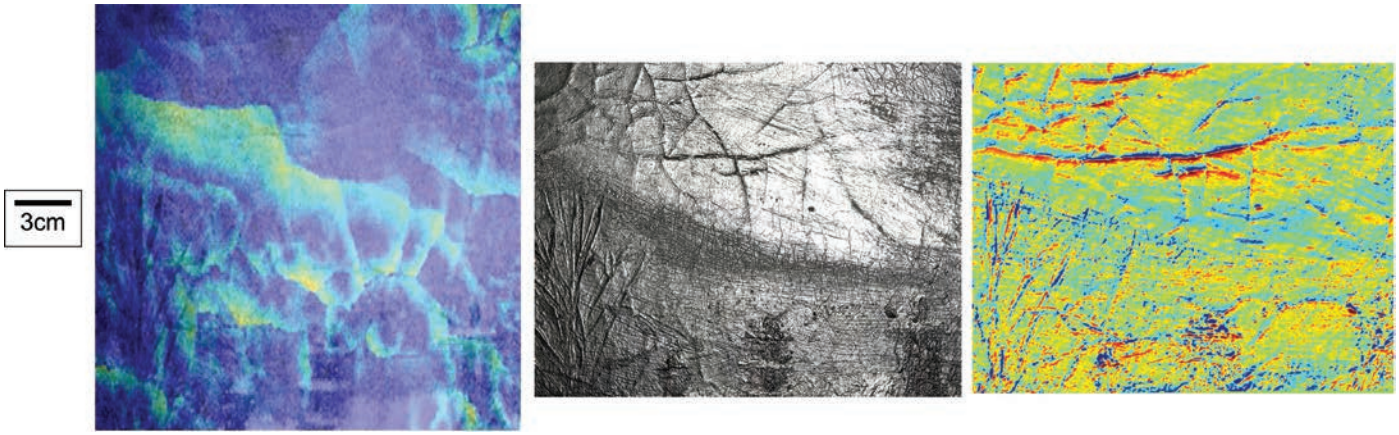

FIGURE 9. Side-by-side comparison of a shearography-generated gradient of displacement map with ghost overlay (left) and RTI-generated views of the same paint surface as seen with specular enhancement (middle) and as a contrast-enhanced surface normal map (right). A comparison between the RTI and shearographic (abbreviated as "shear") data is shown in Figure 10. A direct pixel-to-pixel comparison required spatial transformation of the RTI data and scaling of both data sets. Although the RTI data offered 80 times more spatial information (80 megapixels versus 1 megapixel in our shearographic setup), it was reduced and spatially transformed in order to facilitate direct comparison with shearographic data. This reduction was also done in order to focus on spatially larger and potentially more significant features. The reduction was done through affine transformations of the RTI data to the shearographic data set while using linear interpolation to spatially resize and compress the RTI image. The affine transformation was defined through manual selection of similar spatial points in both image sets. Additionally, for comparison with the RTI data, the absolute of the combined strain data was used in order to enhance regions of large positive or negative strain (both indicated with red in Figure 10), indicative of cracks. Since two data sets are coming from two different domains with different engineering units, we normalized each cross section to a range of 0 to 1 to facilitate comparison. After these manipulations, small details of the painting surface were used to generate and plot cross-section data of the RTI and shearographic data for comparison (graph in Figure 10).

produce a significant strain pattern in their close vicinity, which will be detectable with our shearography system. On the other hand, cracks close to the surface, but without visual indication via the RTI system, will also produce a significant strain pattern in their vicinity, which would affect the surface strain pattern and in turn would also be detectable by the shearographic system.

The first part of this hypothesis is supported by an example of details shown in Figure 10, where there is a clear correspondence between the strong gradient of displacement present and the presence of a high spatial slope indicative of a crack. On the other hand, the second part of our hypothesis is supported by other details analyzed, which showed areas with little to no correlation between shear and RTI data, possibly because of the presence of subsurface discontinuities that are not related to surface topographical features. To our knowledge, this may well be the most exacting correlation between topography and load-induced strain done for the surface of a canvas painting to date. This approach not only could locate damage or imperfections in the layered structure, providing insight into the time-based thermodynamics of painted surfaces by mapping the actual magnitude and direction of displacements, but also it could allow for correlation of such findings with physical features visible on the paint surface. This blend of different quantitative data analyses from different domains could be an effective predictor of where strain-induced damage such as crack propagation is likely to occur in paint surfaces. Future work will incorporate more rigorous comparison between shearographic and RTI data based on visible and subsurface paint defects. Additionally, work will be expanded via correlation with other domains, such as X-ray and optical coherence tomography (OCT), to further confirm the effectiveness of the blend of RTI and shearography data and to establish better testing methods and detection procedures.

CONCLUSIONS

The shearography system developed at WPI provides researchers with the ability to quantify and map induced strain using gradients of displacement. Directional vectors of these gradients of displacement can also be mapped in order to better understand the response of painted surfaces to different loadings. Temporal unwrapping algorithms of displacement gradients enable researchers to directly correlate displacement response to events in time. Furthermore, a complementary approach using shearography and RTI provides a more exacting degree of correlation between displacement gradients and surface topography.

Ultimately, the aim is to combine future work involving material fatigue and failure thresholds with multidomain

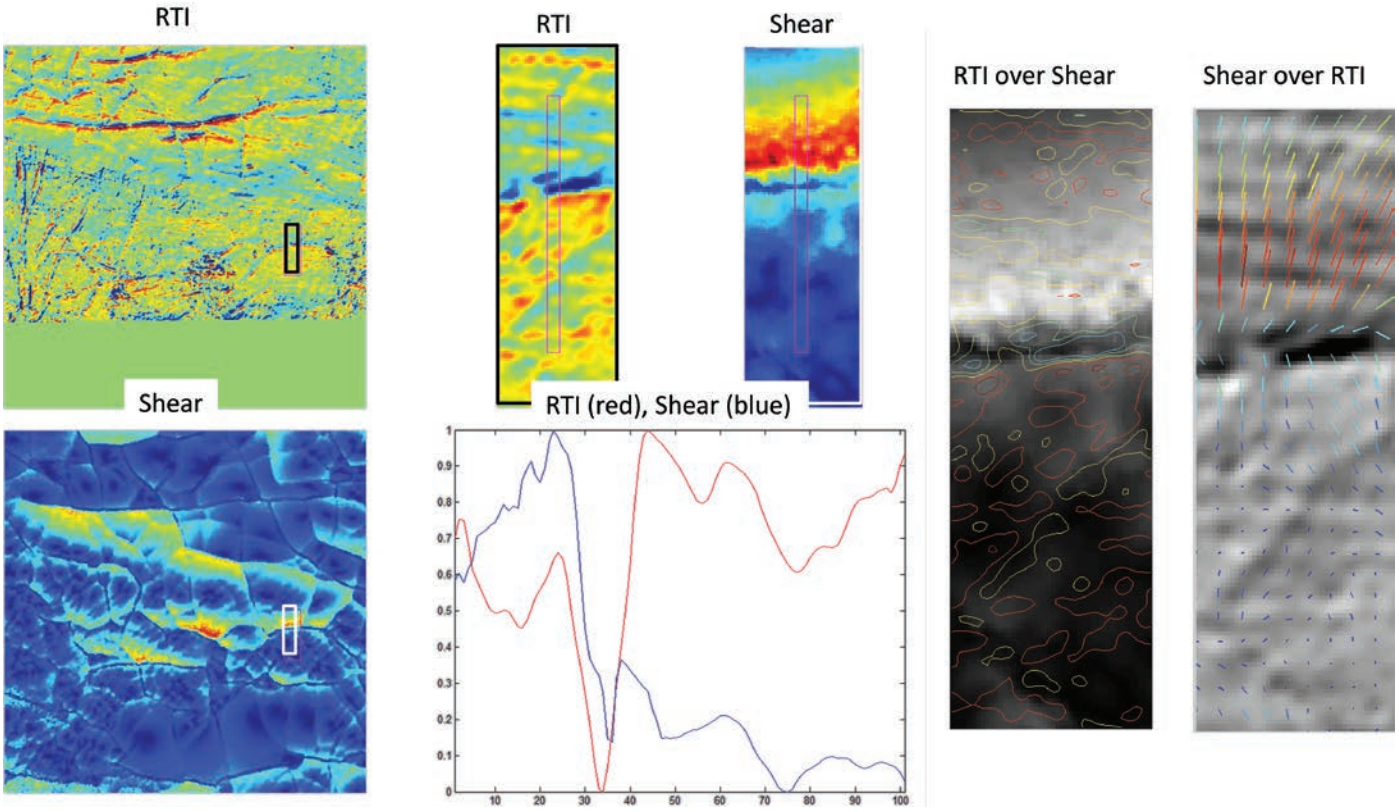

FIGURE 10. Map of RTI-generated slope magnitudes (top left) and the corresponding absolute of the gradient of displacement (strain) map (bottom left), where red indicates large negative or positive strain and blue indicates low strain. The top middle panel shows details of areas outlined in the corresponding maps. Within each detail is a smaller outline of the data plotted in the graph below. The data sets in the graph are normalized to facilitate comparison. On the right are overlays; "RTI over Shear" shows color-coded surface slope data overlaid onto a grayscale map of the shearography data, whereas "Shear over RTI" shows the color-coded strain vectors overlaid onto an RTI-generated image of the slope of the topology, where white and black indicate large positive or negative surface slope and gray indicates nearly no surface slope.

shearography-based measurements in order to make fully informed recommendations on how to optimize a sustainable approach for climate control standards in museums.

REFERENCES

Bracewell, R. N., K. Y. Chang, A. K. Jha, and Y. H. Wang. 1993. Affine Theorem for Two-Dimensional Fourier Transform. *Electronics Letters*, 29(3):304. http://dx.doi.org/10.1049/el:19930207.

Chen, X. 2014. Computational and Experimental Approach for Non-destructive Testing by Laser Shearography, Master's thesis, Worcester Polytechnic Institute, Worcester, MA.

Chen, X., M. Khaleghi, I. Dobrev, W. Tie, and C. Furlong. 2014. Structural Health Monitoring by Laser Shearography: Experimental and Numerical Investigations. *Experimental and Applied Mechanics*, 6:149–155. http://dx.doi.org/10.1007/978-3-319-06989-0_20.

Creath, K. 1985. Phase-Shifting Speckle Interferometry. *Applied Optics*, 24(18):3053–3058. http://dx.doi.org/10.1364/AO.24.003053.

Dobrev, I., C. Furlong, M. Flores, P. Hefti, and E. J. Harrington. 2012. Design of a Shearography-Based Defect Detection System for Structural Health Monitoring. *Proc. SEM*, *Advancement of Optical Methods in Experimental Mechanics,* (42):131–134.

Falldorf, C., W. Osten, and E. Kolenovic. 2003. Speckle Shearography Using a Multiband Light Source. *Optics and Lasers in Engineering*, 40(5):543–552. http://dx.doi.org/10.1016/S0143-8166(02)00080-5.

Ge, Z., F. Kobayashi, S. Matsuda, and M. Takeda. 2001. Coordinate-Transform Technique for Closed-Fringe Analysis by the Fourier-Transform Method. *Applied Optics*, 40(10):1649–1657. http://dx.doi.org/10.1364/AO.40.001649.

Georges, M. P., J.-F. Vandenrijt, C. Thizy, I. Alexeenko, G. Pedrini, B. Vollheim, I. Lopez, I. Jorge, J. Rochet, and W. Osten. 2014. Combined Holography and Thermography in a Single Sensor through Image-Plane Holography at Thermal Infrared Wavelengths. *Optics Express,* 22(21):25517–25529. http://dx.doi.org/10.1364/OE.22.025517.

Ghiglia, D. C., and M. D. Pritt. 1998. *Two-Dimensional Phase Unwrapping: Theory, Algorithms, and Software*. Hoboken, NJ: Wiley.

Groves, R. M., X. Liu, S. Hackney, L. Ameng, X. Peng, and W. Osten. 2009a. 2.5 D Virtual-Reality Visualisation of Shearography Strain Data from a Canvas Painting. *Proceedings of SPIE*, 7391:10–16.

Groves, R. M., W. Osten, M. Doulgeridis, E. Kouloumpi, T. Green, S. Hackney, and V. Tornari. 2007. Shearography as Part of a Multi-functional Sensor for the Detection of Signature Features in Movable Cultural Heritage. *Proceedings of SPIE*, 6618:661810.

Groves, R. M., B. Pradarutti, E. Kouloumpi, W. Osten, and G. Notni. 2009b. 2D and 3D Non-destructive Evaluation of a Wooden Panel Painting Using Shearography and Terahertz Imaging. *NDT & E International*, 42(6):543–549. http://dx.doi.org/10.1016/j.ndteint.2009.04.002.

Harrington, E., I. Dobrev, N. Bapat, J. M. Flores, C. Furlong, J. Rosowski, J. T. Cheng, C. Scarpino, and M. Ravicz. 2010. Development of an Optoelectronic Holographic Platform for Otolaryngology Applications. *Proceedings of SPIE*, 7791:77910J.

Harrington, E., C. Furlong, J. J. Rosowski, and J. T. Cheng. 2011. "Automatic Acquisition and Processing of Large Sets of Holographic Measurements in Medical Research." In *Optical Measurements, Modeling, and Metrology,* vol. 5, pp. 219–228. New York: Springer. http://dx.doi.org/10.1007/978-1-4614-0228-2_26.

Huang, J. R., H. D. Ford, and R. P. Tatam. 1997. Slope Measurement by Two-Wavelength Electronic Shearography. *Optic and Lasers in Engineering*, 27:321–333. http://dx.doi.org/10.1016/0143-8166(95)00124-7.

Hung, Y. Y. 1982. Shearography: A New Optical Method for Strain Measurement and Nondestructive Testing. *Optical Engineering*, *21*(3):213391. http://dx.doi.org/10.1117/12.7972920.

Huntley, J. M., and H. Saldner. 1993. Temporal Phase-Unwrapping Algorithm for Automated Interferogram Analysis. *Applied Optics*, 32(17):3047–3052. http://dx.doi.org/10.1364/AO.32.003047.

Kalms, M., and W. Jueptner. 2005. A Mobile Shearography System for Non-destructive Testing of Industrial and Artwork Components. *Key Engineering Materials,* 295–296:165–170. http://dx.doi.org/10.4028/www.scientific.net/KEM.295-296.165.

Khaleghi, M., I. Dobrev, E. J. Harrington, P. Klausmeyer, M. Cushman, and C. Furlong. 2014. "Long-Term Effects of Cyclic Environmental Conditions on Paintings in Museum Exhibition by Laser Shearography." In *Advancement of Optical Methods in Experimental Mechanics*, vol. 3, pp. 283–288. New York: Springer. http://dx.doi.org/10.1007/978-3-319-00768-7_36.

Kreis, T. 2005. *Handbook of Holographic Interferometry: Optical and Digital Methods*. Weinheim: Wiley-VCH. http://dx.doi.org/10.1002/3527604154.

Lee, J. R., J. Molimard, A. Vautrin, and Y. Surrel. 2004. Application of Grating Shearography and Speckle Shearography to Mechanical Analysis of Composite Material. *Composites Part A: Applied Science and Manufacturing*, 35(7):965–976. http://dx.doi.org/10.1016/j.compositesa.2004.01.023.

Licsár, A., L. Czúni, and T. Szirányi. 2003. "Adaptive Stabilization of Vibration on Archive Films." In *Computer Analysis of Images and Patterns,* pp. 230–237. ed. N. Petkov and M. Westenberg. Berlin: Springer-Verlag.

Meybodi, M. K., I. Dobrev, P. Klausmeyer, E. J. Harrington, and C. Furlong, 2012. Investigation of Thermomechanical Effects of Lighting Conditions on Canvas Paintings by Laser Shearography. *Proceedings of SPIE*, 8494:84940A. http://dx.doi.org/10.1117/12.958089.

Morawitz, M., N. Hein, I. Alexeenko, M. Wilke, G. Pedrini, C. Krekel, and W. Osten. 2013. "Optical Methods for the Assessment of Transport and Age Induced Defects of Artwork." In *Fringe 2013*, pp. 951–956. Berlin: Springer. http://dx.doi.org/10.1007/978-3-642-36359-7_180.

Osten, W., W. P. O. Jüptner, and U. Mieth. 1994. Knowledge-Assisted Evaluation of Fringe Patterns for Automatic Fault Detection. *Proceedings of SPIE*, 2004:256–268. http://dx.doi.org/10.1117/12.172599.

Schnars, U., and W. P. Jüptner. 1994. Digital Recording and Reconstruction of Holograms in Hologram Interferometry and Shearography. *Applied Optics*, 33(20):4373–4377. http://dx.doi.org/10.1364/AO.33.004373.

Sfarra, S., P. Theodorakeas, C. Ibarra-Castanedo, N. P. Avdelidis, A. Paoletti, D. Paoletti, and X. Maldague. 2011. Importance of Integrated Results of Different Non-destructive Techniques in Order to Evaluate Defects in Panel Paintings: The Contribution of Infrared, Optical and Ultrasonic Techniques. *Proceedings of SPIE*, 8084:80840R. http://dx. doi.org/10.1117/12.889335.

Steinchen, W., and L. Yang. 2003. *Digital Shearography: Theory and Application of Digital Speckle Pattern Shearing Interferometry*. Bellingham, WA: SPIE Press.

Takeda, M., H. Ina, and S. Kobayashi. 1982. Fourier-Transform Method of Fringe-Pattern Analysis for Computer-Based Topography and Interferometry. *Journal of the Optical Society of America,* 72:156–160. http://dx.doi.org/10.1364/JOSA.72.000156.

Tornari, V., E. Bernikola, K. Hatziyannakis, W. Osten, R. M. Grooves, M. Georges, T. Cedric, G. M. Hustinx, J. Rochet, E. Kouloumpi, M. Doulgeridis, T. Green, and S Hackney. 2009. "Multifunctional Encoding System for Assessment of Movable Cultural Heritage." In *Fringe 2009*, edited by W. Osten and M. Kujawinska, pp. 1–8. Berlin: Springer. http://dx.doi.org/10.1007/978-3-642-03051-2_113.

Evidence for the Accumulative Effect of Organic Solvent Treatments on Paintings and What to Do about It: A Case Study of Two "Identical" Seventeenth-Century Paintings Using Single-Sided Nuclear Magnetic Resonance

Gwendoline Fife,[1] Bascha Stabik,[1] Bernhard Blümich,[2] Renè Hoppenbrouwers,[1] and Tyler Meldrum[3]*

ABSTRACT. Two paintings made by the same artist in 1616 to depict *The Dinner* and *The Dance* celebrations of the *Pipenpoyse Wedding* were examined at Stichting Restauratie Atelier Limburg, Maastricht, Netherlands. In addition to a shared provenance these paintings demonstrated similarities in their composition and identical materials and techniques. However, the paintings exhibited dramatic differences in their condition, and inconsistencies between their previous treatments were apparent. One of the paintings, *The Dinner*, had undergone repeated surface treatments of varnishing and varnish removal, whereas the other, *The Dance*, had never been varnished. The paintings thus presented an opportunity to potentially examine the accumulative effects of paint surface treatments using organic solvents. Detailed depth profiles of the two paintings were measured using single-sided nuclear magnetic resonance (NMR). This type of NMR is sensitive to physical properties of the material such as hardness and is a contact-free technique. The T_2 relaxation times, indicative of the hardness or stiffness of a material, were found to be different for the two paintings and consistent with the observed visual and tactile differences. With regard to these findings the contribution from the repeated exposures to natural resins and organic solvents during paint surface treatments is considered. Various developments in current conservation practice have aimed to restrict the penetration of solvent into paint films and thereby reduce related solvent effects. Initial findings from investigations using single-sided NMR on model paint films to compare the effects of such adapted approaches are presented.

INTRODUCTION

Varnishing and varnish removal are the most common treatments applied to the overall surface of oil paintings involving organic solvents. Various methods and analytical techniques have been previously employed to investigate the effects of organic solvents on oil paint films (Stout, 1936; Jones, 1965; Maschelein-Kleiner and Deneyer, 1981; Stolow, 1985; Erhardt and Tsang, 1990; Hedley et al., 1990; Michalski, 1990;

[1] Stichting Restauratie Atelier Limburg, Avenue Ceramique 224, 6221 KX Maastricht, Netherlands.

[2] RWTH Aachen University, Institute of Technical and Macromolecular Chemistry, Worringerweg 1, 52062 Aachen, Germany.

[3] The College of William & Mary, Department of Chemistry, 540 Landrum Dr., Williamsburg, Virginia 23185, USA.

* Correspondence: G. Fife, gwenfife26@hotmail.com

Manuscript received 27 May 2014; accepted 22 February 2016.

Tsang and Erhardt, 1992; Phenix, 1998; Tumosa et al., 1999; Phenix and Sutherland, 2001; Sutherland, 2001; Phenix, 2002a, 2002b; Fuesers and Zumbühl, 2008; Zumbühl et al., 2010; Zumbühl, 2014).[1] Their results have been highly beneficial to our field in developing our conceptual modeling and understanding of paint films and the potential negative effects from solvents. From a practitioner's perspective, examining how the magnitude of these "invisible" solvent effects can be influenced by our techniques and practices is a pertinent focus, and this paper shall describe the novel application of single-sided nuclear magnetic resonance (NMR) in this endeavor. A case study of two "identical" seventeenth-century paintings examined with single-sided NMR and experiments on a simple painting model will be discussed.

Analytical Methods

In an NMR experiment, a sample is placed in a large, homogeneous magnetic field, and the response to that field is measured, producing a spectrum. Interpretation of that spectrum reveals the structure of the molecule of interest. Although chemical identification of compounds is tremendously powerful, the technique is not an analytical panacea. One particularly pertinent drawback is the size of the sample—most magnets accommodate samples only millimeters across, not entire paintings. Reducing an NMR apparatus to its simplest components, one needs just three things: a sample, a magnet, and a radio-frequency coil (an antenna). If two or more permanent magnets are cleverly arranged next to each other, the field between them can be made fairly flat and homogeneous in a region *above the magnets themselves*. This offset of the magnets and their magnetic field allows for an unconventional geometry of an NMR experiment—one in which the sample sits atop, rather than within, the device. Using these single-sided magnets, samples of arbitrary geometry can be analyzed to probe certain physical properties of a material. The field homogeneity is, however, not good enough to give chemical information: chemical shifts, the most common way to identify functional groups in and the structure of molecules using NMR, are inaccessible with single-sided magnets. Single-sided NMR *can* access information about the relaxation rates of nuclear magnetization following the application of radio-frequency radiation; these relaxation rates indicate physical properties of the system.

The relaxometric data that single-sided NMR experiments generate comprise signals that decay with time. From that decay, one can extract two significant parameters: the signal amplitude and the rate of signal decay. The signal amplitude, designated A, indicates the quantity of proton-containing material in the measured location, whereas the rate of signal decay, evaluated by the NMR parameter T_2, indicates the strength of the intermolecular network. In samples with a small value of T_2 (rapid signal decay), there is a strong intermolecular network, often associated with a stiff or brittle material. A large T_2 (slow signal decay) may suggest a softer material (Bloembergen et al., 1948). Thus, depth profiles with T_2 and A show the strength of the intermolecular network at different positions within the thickness of a painting.[2]

The sensitive region of the single-sided magnet used in these studies (Blümich et al., 1998) has an area of approximately 6.25 cm^2 and an adjustable thickness of between 10 and 500 µm for a sample volume of up to 0.3 mL. In addition, it is positioned between 1 and 5 mm above the surface of the magnet. If one suspends a sample just above the magnet but below the sensitive region and makes repeated measurements while moving the magnet down, a signal profile can be generated as a function of the depth through the sample.

EXPERIMENTAL OVERVIEW

Varnish removal may be undertaken for a number of reasons, including conservation of the original materials (e.g., by allowing better consolidation), improvement of the painting aesthetically, or enabling a more accurate and sensitive restoration campaign using stable materials. Varnish layers may be (re)applied for saturation, isolation of original materials from subsequent restoration, or protection of the paint surface. Given the potential side effects from solvents (e.g., swelling, loss, or movement of low-molecular-weight components) such treatments involve risk assessment. Since the conscientious conservator will aim to minimize any potential risks to an acceptable level before varnish removal is undertaken, any observable changes to original materials during treatment are unacceptable. Concern instead lies with the risk of engendering subtle long-term effects, invisible at the point of treatment yet indicated by previous research (Maschelein-Kleiner and Deneyer, 1981; Stolow, 1985; Erhardt and Tsang, 1990; Hedley et al., 1990; Michalski, 1990; Tsang and Erhardt, 1992; Phenix, 1998; Tumosa et al., 1999; Phenix and Sutherland, 2001; Sutherland, 2001; Phenix, 2002a, 2002b; Fuesers and Zumbühl, 2008; Zumbühl et al., 2010; Zumbühl, 2014) and, from our experience, observable when examining previously treated paintings. However, given the individuality of each painting, the complexity of its structure, and the number of unknowns in its lifetime, it is not possible to quantitatively correlate these specific aspects of treatment history with current condition.

For measuring the effects of previous treatment, the real-life equivalent of an experimental "control" would be ideal. Such a control could comprise two paintings made a long time ago by the same artist with the same materials and techniques and at same the time, with the only difference being only one had never undergone organic solvent–based treatments (varnish application and removals). Extraordinarily, in 2011 two paintings arrived at Stichting Restauratie Atelier Limburg (SRAL)—as part of a larger treatment project from the Fries Museum in Leeuwarden, Netherlands—displaying exactly these characteristics. Called *The Dinner* (212 × 124 cm) and *The Dance* (218 × 130 cm; from the *Pipenpoyse Wedding* set), the paintings were attributed to the same artist, were very similar compositionally (Figure 1),

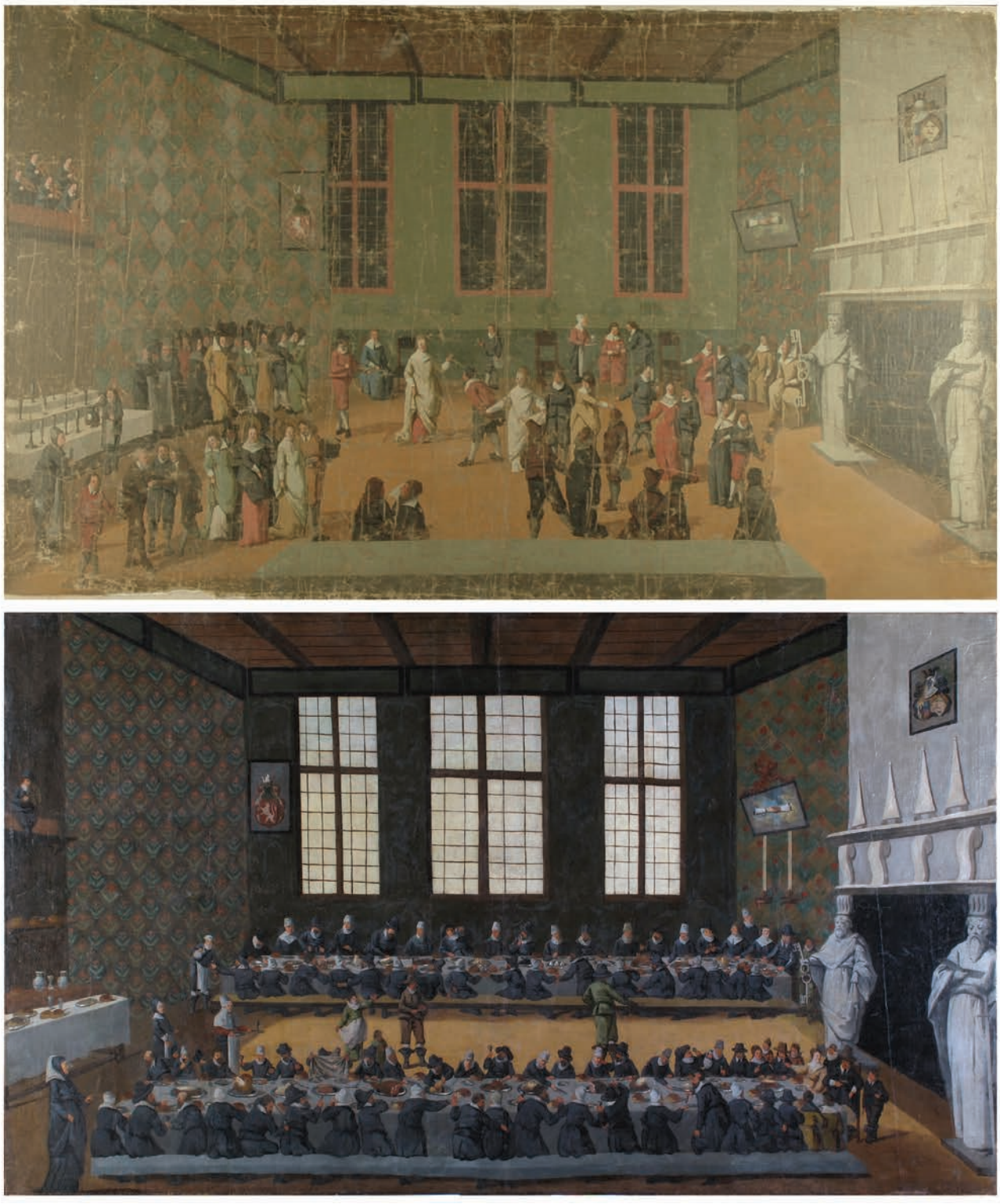

FIGURE 1. (top) *The Dance* (218 × 130 cm) and (bottom) *The Dinner* (212 × 124 cm) from the *Pipenpoyse Wedding* Set (1616), artist unknown. The surface of *The Dance* has never been varnished or otherwise treated with organic solvents. In contrast, *The Dinner* has undergone numerous solvent-based varnish removals. For legibility of the images, paintings are shown here after SRAL treatments. Paintings: Fries Museum, Leeuwarden, Netherlands. Photographs courtesy of Stichting Restauratie Atelier Limburg (SRAL).

had very similar dimensions, and were both dated 1616. As part of an originally larger series they were known to have hung together in the big hall in the Liauckamastate in Friesland until the estate was demolished in 1824, after which they remained in the family collection until going in 1963 to the Fries Museum. No further information regarding the specific environments experienced by the two paintings is known, nor is there any existing documentation regarding previous treatments. Apart from local tear repairs in *The Dinner*, the only structural treatments for both paintings involved restretching: two for *The Dance* and three for *The Dinner*. Regarding surface treatments, *The Dinner* was varnished with natural resins and cleaned (although unevenly) at least twice, and there were numerous overpaints visible above the first varnish layer. With *The Dance*, there were no indications that its surface had ever been varnished or otherwise treated with organic solvents.

Various visual, material, and technical examinations were carried out on these paintings, and they constitute the first set of experimental materials with the single-sided NMR that will be discussed here. For NMR measurements, each individual painting was positioned on an easel in its normal vertical position, and identical data acquisition parameters were used for measuring both paintings.[3] With the magnet mounted on a lift to control horizontal positioning it was placed parallel to and as close as possible to the surface of each painting in turn.

The second sample set consists of 2.5 × 2.5 cm sections cut from a very simple, unvarnished, and uniform painting model consisting solely of a single red oil paint layer (containing lead white, chalk, and red ochre) on sized linen canvas, naturally aged for around 10 years. Since in normal working practice only a low level of invisible solvent effects can be anticipated during an individual varnish removal (Phenix and Sutherland, 2001), these model samples were subjected to deliberately extreme solvent exposures to allow a comparative examination of resulting solvent movement and the potential solvent effects induced by different varnish removal techniques. Although not typically employed for varnish application or removal, 1-methoxy-2-propanol was selected for these tests precisely because it caused a slow (and initially optically invisible) but ultimately high swelling of the model paint layer with a significant period prior to dissolution.

The two techniques selected for comparison were application of free solvent in a swab—hereafter referred to as free solvent—and a version of SRAL's tissue gel composite method (Fife et al., 2010, 2011). With this latter technique—hereafter referred to as thickened solvent—the thickened solvent (3% w/v using hydroxypropyl cellulose) was applied in a tissue, with a secondary absorbent tissue step. Pretesting was carried out, and a desirable time exposure of 30 seconds was determined for the application of both techniques. NMR and gravimetric measurements were carried out both immediately before and after each technique application (Fife, 2015). During NMR testing, samples were placed between two microscope slides to maintain correct position and avoid solvent loss during measurement.[4]

RESULTS AND DISCUSSION: SET 1

Each painting comprised two canvas pieces with a central seam. In *The Dinner* all sides had been cut, and the painting had been made smaller. In *The Dance*, since there was one painted turnover edge with original threading holes, a loom size of 110 cm could be calculated. The canvas support of *The Dance* was highly flexible and light in color, indicating less oxidation of fibers. No resin residues were observable in normal and ultraviolet light examinations. In contrast, the canvas of *The Dinner* was embrittled, and evidence of resin appeared throughout the structure, with residues observable (in accordance with surface crack pattern) on the canvas reverse.

Aside from surface dirt and mechanical damage caused by previous folding, the paint and ground layers in *The Dance* had an excellent condition overall. There was also a noticeable lack of cracking on the paint surface (Figure 2). In contrast, *The Dinner* showed typical "age" cracks in the paint film across the surface. It appeared more brittle and was also more glossy and saturated.

Infrared reflectography indicated no technical differences in the preparatory underdrawing of the paintings. Twelve samples were removed from comparable areas of each painting for further examination in cross section with visible and ultraviolet light microscopy, with staining tests.[5] X-ray fluorescence of both paintings surfaces (at 26 spots) was further carried out.[6] The combined findings from these analyses confirmed an identical painting technique and pigment palette (lead white, vermilion, red lead, earth pigments, carbon black, and calcium carbonate in ground) with the same layer buildup and oil binder. A comparable area in both paintings, a red flower on the background wallpaper, was selected for NMR measurements. A sample from each painting was subsequently removed from this same area to quantify the individual layer thicknesses for correlation with the NMR-generated profiles.[7] Optical microscopy gave comparable paint plus ground layer depth measurements, and elemental mapping using energy-dispersive x-ray spectroscopy (EDX) verified identical pigment compositions (Fife and Meldrum, 2014). Scanning electron microscopy (SEM) indicated some condition differences: the paint and ground layers in *The Dinner* sample showed cracks, fissures, and pores, and the layers appeared less discrete (Figure 3).

Single-sided NMR measurements, carried out in the nominated 2.5 × 2.5 cm area in both paintings, were taken at 15-µm increments throughout the thickness of each painting. The results are shown in Figure 4 and include both signal intensity A (top) and T_2 (bottom).[8] In *The Dance* the signal intensity was somewhat variable across the painting, with a gradient of increasing T_2 values toward the rear of the painting. In *The Dinner* the signal amplitude was larger but similarly variable as in *The Dance*.[9] The T_2 value in *The Dinner* was small and constant throughout 600 µm below the painting surface and increased dramatically at the back of the canvas.

The Dance's paint was stiffest at the surface of the paint film with then a smooth gradient of decreasing stiffness through

FIGURE 2. Details (ordinary light, before SRAL treatment) of the paint surfaces of (top) *The Dance* and (bottom) *The Dinner*. There was a noticeable lack of cracking on the paint surface of *The Dance*, whereas *The Dinner* showed typical age cracks in the paint film across the surface.

depth of ground, whereas *The Dinner* is uniformly stiff, as stiff as the uppermost surface of *The Dance*, throughout almost its entire depth.

Studies of oil paint films have shown that after initial drying, oxidation reactions continue in the polymeric oil network

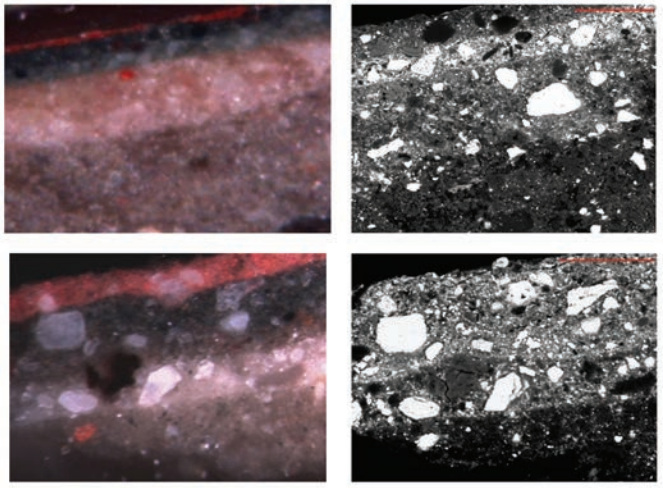

FIGURE 3. Visible light and scanning electron photographs of comparable samples in cross section from (top) *The Dance* and (bottom) *The Dinner*. The red scale bar denotes 50 μm. The similarity of materials and techniques employed in both paintings can be observed. In *The Dinner* layers appear less discrete, and microfissures can be observed.

whereby lower-molecular-weight (LMW) components can be formed. These LMW components (e.g., free fatty acids and glycerol) can have a plasticizing effect, are potentially mobile and extractable, and can undergo further reactions (such as the complexation of free fatty acids with metal ions to create metal soaps). The production of LMW species, their further mobility (and potential loss), and specific reactions within the paint and ground layers will depend on both internal factors (e.g., the nature of the pigments, the binder, their relative concentration, manufacturing methods) and external factors (e.g., treatments and environmental effects; Van den Berg, 2002; Keune and Boon, 2007; Van Loon, 2008).

It is proposed that the stiffness gradient in *The Dance* is consistent with a natural aging process with greater retention of plasticizing LMW components within the body of the paint and ground and their gradually increasing loss toward the paint surface. The constant T_2 value throughout the paint and ground layers of *The Dinner* painting may rather indicate less of these components within the deeper paint and ground layers. Since the pigments, binder, and layer buildup were identical within the paint and ground layers between the two paintings, differences can only be reasonably accounted for by external factors. The effect of the previous surface treatments cannot be quantified since specific environmental factors for each painting remain unknown. However, it is hypothesized that the mobility (and or subsequent reaction or loss) of LMW components in the paint and ground layers of *The Dinner* was likely enhanced by solvent penetration during previous varnish applications and varnish removals, significantly contributing to its current condition.

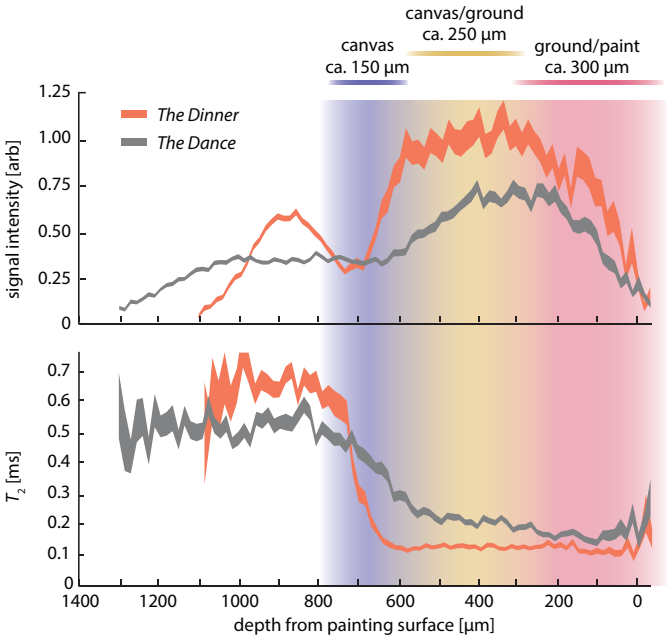

FIGURE 4. Depth profiles of both (top) signal intensity *A* and (bottom) T_2 for *The Dinner* and *The Dance* are shown. *The Dance* is in gray, whereas *The Dinner* is in orange; the width of the lines indicates the range of the 95% confidence intervals for both parameters. The T_2 profile of *The Dinner* shows a constant T_2 value of ~0.10 ms for the top 600 µm of the painting (0–600 µm on the horizontal axis), with an abrupt change in T_2 at a depth of 600 µm. The peak in the signal intensity depth profile for *The Dinner* between 700 and 1,100 µm is from a piece of tape that was placed on the back of the painting prior to measurement to give a location reference. The T_2 profile of *The Dance* shows a smooth gradient of T_2 values throughout the thickness of the painting, ranging from 0.15 ms near the surface to ~0.25 ms toward the rear of the paint/ground layer region. Distances are accurate to within 100 µm.

Previous research has demonstrated the influence of the resin on the level of LMW component extraction by the solvent in which it was applied (Tsang and Erhardt, 1992; Phenix and Sutherland, 2001). However, the effects of penetrating resin material on the mechanical structure of the painting and, ultimately, the visual appearance of the painting are also shown here. Examining specifically the regions of ground and canvas in both paintings, in *The Dance* there was a gradual gradient in decreasing stiffness through the ground and to the back of the canvas; in *The Dinner* the steeper gradient in this equivalent region indicates some stiffening within the canvas itself that is likely due to the natural resin varnish having impregnated the canvas fibers. The NMR data from the ground and canvas layers (lowest ~400 µm), alongside the visual and technical results, give a strong indication of the effect of resin residues on the mechanical differences evident between the two paintings.

In varnish removal, solvents could serve to increase penetration of resin residues into the paint, ground, and canvas. This potentially presents a cumulative effect not only from the solvents but also, and perhaps critically, from the resin residues.

The case study here suggests the relatively extreme effects of resin varnishes and their residues and thereby inspires further questions, including whether the resin effects can be halted or even reversed and if different treatment approaches to remove the resin more effectively from the entire structure could be beneficial. Whether this should be a weightier consideration in our varnish removal treatments depends on the acceptable risk from solvent exposure.

RESULTS AND DISCUSSION: SET 2

Whether this risk from the accumulative effects of solvents in paint films can be reduced by relatively simple adaptations in our varnish removal techniques is a crucial question and is the focus of the experiments described below. Small pieces of the red oil paint on canvas model (Figure 5) were measured using single-sided NMR (Fife, 2015). Figure 6 shows profiles for both free- and thickened-solvent–treated model samples that experienced similar mass gains (5.3% and 5.5%, respectively) immediately after treatment. By subtracting the pretreatment fit data from the posttreatment data two measurable effects from the treatments can be observed. The T_2 of both treated samples similarly increased by approximately one order of magnitude, whereas the profile of signal intensity *A* showed peak widths of ~260 µm for

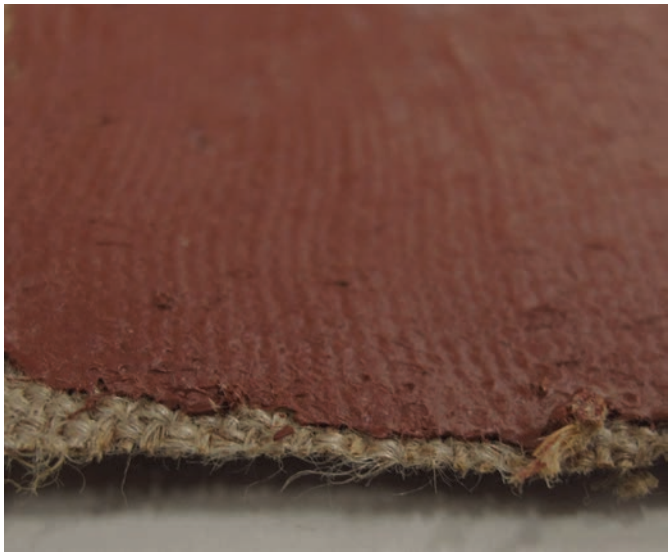

FIGURE 5. Detail of model paint film: single red oil paint layer (containing lead white, chalk, and red ochre) on sized linen canvas, naturally aged for around 10 years.

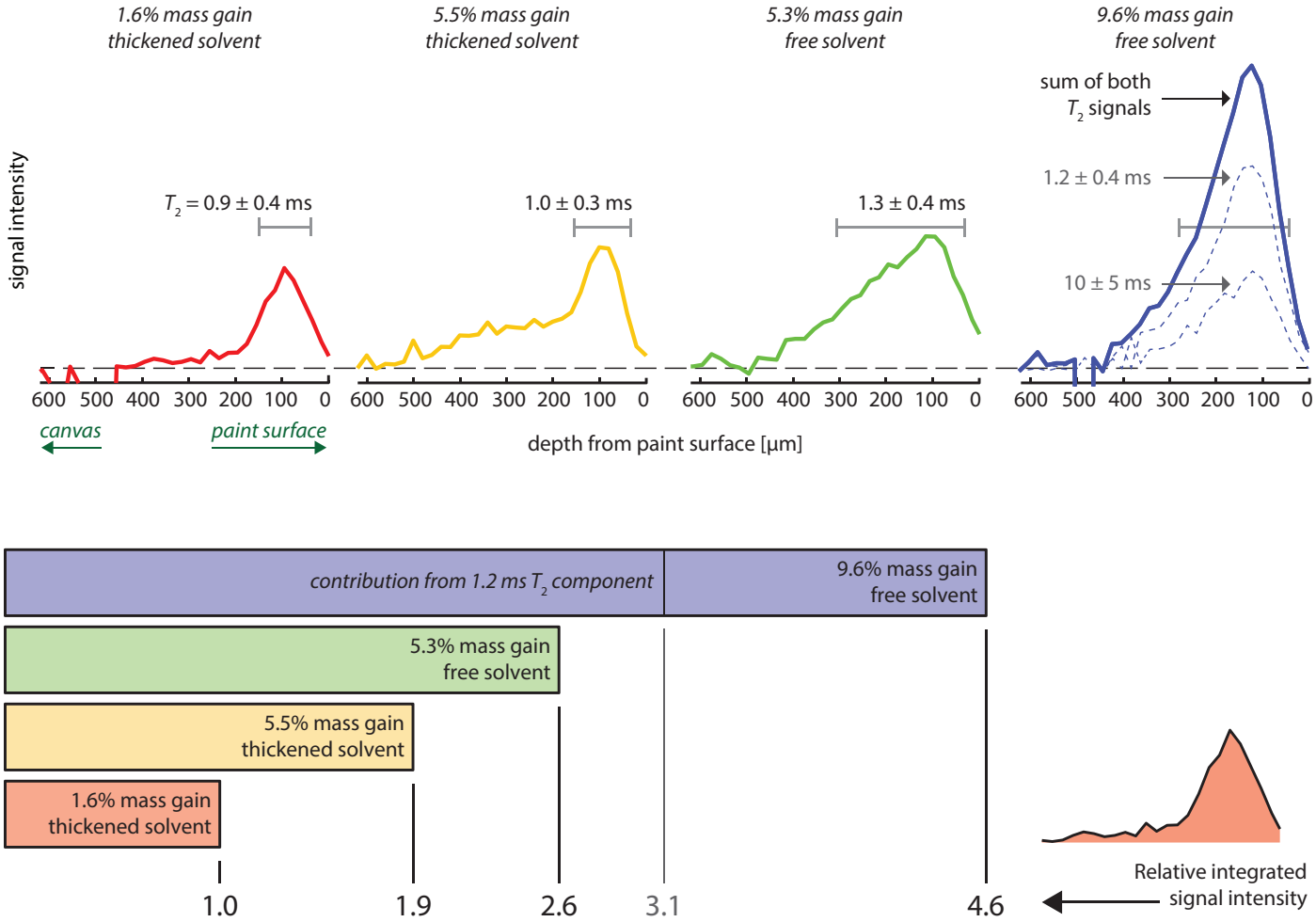

FIGURE 6. A comparison of the effects on the model paint films from different treatments with free and thickened solvents. Four treatments were applied to identical pieces of the model, two thickened-solvent treatments (with a 1.6% and a 5.5% mass gain immediately following treatment) and two free-solvent treatments (5.3% and 9.6% mass gain). (top) The thickened-solvent treatments had a narrower range of effect (~100 µm, red and yellow) than the free-solvent treatments (~260 µm, green and blue), determined by the full width at half maximum value and indicated by the horizontal gray bars. In addition, the three treatments with the smallest percentage gain in mass showed only one T_2 value following treatment at approximately 1.0 ms. In contrast, the free-solvent treatment with a 9.6% mass gain (blue) resulted in two different T_2 values, one consistent with the other treatments' values at 1.2 ms and another at 10 ms. This second T_2 suggests a different solvent interaction in this sample. (bottom) Integrating the effect of the different solvent treatments shows that the mass change percentage is directly related to the amount of effect observed. All integrated values are normalized to the thickened-solvent treatment with the 1.6% mass gain.

free solvent and 100 µm for thickened solvent (full width at half maximum value).

Other data from similar experiments on the identical sample material with the same experimental conditions and NMR parameters also provide insights into the potential effects engendered by these different solvent application methods (Figure 6). When two identical samples were both treated with thickened solvent (1-methoxy-2-propanol) but with different mass changes (i.e., more thickened solvent was applied and retained in one of the samples), the T_2 profiles exhibited no differences within experimental error. The signal intensity for both samples followed a comparative curve over their depths, with a higher profile in the sample with the higher mass gain. In a comparison of similar data from two identical samples treated with free solvent (but, again, exhibiting different mass changes of 5.3% and 9.6%), the signal intensity for both samples again followed comparative curves with an increased profile in the sample with greater mass gain. But this time, in the sample where more free solvent had been applied and retained, an additional T_2 signal was observed (1.2 ± 0.4 and 10 ± 5 ms).

In these comparative experiments on model paint films using single-sided NMR, relative differences between the application methods could be observed. Although the maximum level (i.e., depth) of solvent penetration is found to remain comparable between two different techniques, the quantity of penetration is reduced with the thickened-solvent application. This is considered a significant finding for practice since it is the *relative magnitude* of solvent effects we aim to reduce by adapting application methods and techniques.

Solvent penetration with both techniques may follow a similar physical model of infiltration (by diffusive and capillary penetration; Michalski, 1990), but it appears that in the case of the thickened solvent application the amount of penetrating solvent is hindered by the gel matrix (in this case, hydroxypropyl cellulose). This correlates with the gravimetric result that indicates a restricted effective evaporation from the gel matrix.[10] In practice, it is observed that when using free solvent, immediate penetration of liquid solvent can occur, resulting in its appearance in wet patches on the back of the canvas. Thickened solvent cannot be observed in this way and, in combination with the results presented here, may indicate that in the deeper region (below 200 μm) the solvent is not present in liquid form but as more dispersed particles. This difference may result in reduced solvent effects caused by transport processes, but since the samples immediately after both application methods nonetheless show similar T_2 profiles, the ultimate effect of the different application methods on the painting model samples must be compared in further experiments.

A further interesting result is the additional signal observed when the free solvent is applied with a swab technique as opposed to the thickened solvent in tissue composite method. The nature of this secondary type of signal cannot be unambiguously described with these experiments. It did not occur with the thickened solvent (even when in relative excess), and it is plausible that a specific swelling mechanism (such as solvent clusters forming in the medium or around particles, etc.) results in the ground matrix when excess "free" solvent has been applied. What is unambiguous is that the observed signals are not free solvent in a bulk state as this solvent has a T_2 in bulk solution of 22.65 ms—much larger than any signal observed with either treatment method.

It must be iterated that the region of highest signal intensities (peaks) for both techniques should, in practice, not be in the painting layers (as in the unvarnished model) but in the varnish being removed. These findings indicate that accurate timing of a thickened solvent's contact with the surface is advised to maximize the benefits of reduced solvent within the paintings layers.

CONCLUSIONS AND FURTHER WORK

The NMR data correlated well with those from the other technical and visual examinations and provided greater information on the mechanical properties within the paintings' layers, enabling further interpretations. The combined results supported the premise that *The Dance* could be considered a 400-year-old untreated control for *The Dinner*. Some investigations were beyond the scope of this current study, but samples from both paintings have been retained for eventual further analyses.

An argument is provided for conservators to carefully consider the mechanical properties of any conservation material to be applied to the surface. The case study here indicates that treatment-induced changes within the layers of *The Dinner* plausibly contributed to the development of observable mechanical cracks within the paint film. It is hypothesized that the potential for natural resins to induce undesirable changes may be more significant than is currently considered in much practice not only for varnishing but also in varnish removal. The continuing effect of resin remaining within the entire painting structure is not necessarily illuminated in cleaning discussions. Perhaps considered obvious, it nonetheless deserves explicit discussion in research and in practice. Approaches which not only reduce solvent penetration, but increase removal of these previously applied materials merit deliberation.

Utilizing only single-sided NMR, these experiments did not aim to provide an in-depth study of solvent effects or to illustrate the level of effects that would be seen in practice. However, the NMR data can aid in our conceptual modeling of the effects incurred by different application methods. Single-sided NMR has proven to be a valuable tool to compare selected varnish removal techniques and to better understand changes and the locations of those changes within the painting structure.

It is also suggested that other types of conservation treatments that may induce a change (desired or otherwise) in the physical properties of the original materials, such as the lining or consolidation of paintings, may be more easily examined with single-sided NMR. With this analytical technique the penetration of conservation materials might be assessed, and profiles might be compared to indicate the efficacy of a particular material and/or treatment approach under consideration.

On the basis of our experimental findings continuing work includes comparative measurements after the simulation of multiple cleanings (and full solvent evaporation) to clarify if the different local conditions apparent in the painting model samples result in different longer-term (cumulative) effects. Investigating the nature of the solvent in a swollen film environment would be beneficial, as would comparative studies for the introduction of resins. Ultimately, comparative experiments on varnished painting models would be highly informative

Acknowledgments

The following are gratefully thanked for their contributions: Dr. Paul van Kan for assistance with SEM-EDX analysis at SRAL, Marlies Stoter at the Fries Museum for providing information regarding provenance of the paintings, the Alexander von Humboldt Foundation for their generous financial support, Dr. Erich Uffelman for pXRF analysis, the National Science Foundation for a grant funding nondestructive instrumentation (NSF MRI 0959625), and the Lenfest Summer Grant program at

Washington and Lee University for funding Dr. Uffelman's travel to the Netherlands with the pXRF.

NOTES

1. Methods and analytical techniques previously used to investigate the effects of organic solvents on oil paint films include dimensional changes, gravimetric studies, stress-strain measurements, differential scanning calorimetry, thermal mechanical and dielectric measurements, radioisotopic labeling, and various and combined chromatographic and spectroscopic methods.
2. Because of the dependence on experimental parameters, A and T_2 values can only be related within comparative studies in which the experimental parameters are kept constant. For accuracy in applications within laminar and nonhomogeneous systems it may be advisable to correlate depth profiling via the examination of layer thicknesses in a removed sample(s).
3. For NMR experimental details, see G. R. Fife, B. Stabik, A. E. Kelley, J. N. King, B. R. Blümich, R. Hoppenbrouwers, and T. Meldrum, "Characterization of Aging and Solvent Treatments of Painted Surfaces Using Single-Sided NMR," *Magnetic Resonance in Chemistry*, 53 (2015): 58–63, doi:10.1002/mrc.4164.
4. For both free and thickened solvents, the sample mass decreased exponentially with solvent evaporation. Half-lives of 72 min for the free solvent and 116 min for the thickened solvent were determined.
5. Samples were stained with Alexa Fluor (proteins), Rhodamine B (lipids), and triphenyltetrazolium chloride (carbohydrates).
6. E. Uffelman (Washington and Lee University) used a Bruker Tracer III-SD, Rh anode X-ray tube with with an oval spot size of 4 × 6 mm, and collection parameters of 40 kV, 11 μA, and 180s for spectrum accumulation.
7. The total thickness of each painting was measured using calipers of 700 ± 100 μm. Layer thicknesses were calculated in removed samples (i.e., without canvas) using an analytical light microscope. Paint layers were 40 ± 20 μm; ground layers were 200 ± 100 μm. With a resolution of 15 μm over a 2.5 × 2.5 cm area, location can be determined ±100 μm. Although specific layers cannot be specified with these certainties, the upper 300 μm can be considered the paint/ground region, with the lower 400 μm being the ground/canvas region.
8. The shoulder region in the signal intensity depth profile of *The Dance* between 650 and 1,100 μm is from the lining canvas adhered to the back of the painting during SRAL's treatment in 2012. A mist lining technique was used whereby the original painting is subjected to minimal solvent exposure (from reverse), low pressure, and no increased temperature.
9. Increased signal intensity observed throughout the depth of *The Dinner* may indicate resin content.
10. It has been previously shown using radioisotopically labeled solvents (Stulik, D., D. Miller, H. Khanjian, N. Khandekar, R. Wolbers, J. Carlson, and W.C. Petersen. *Solvent Gels for the Cleaning of Works of Art: The Residue Question,* ed. V. Dorge [Los Angeles: Getty Conservation Institute, 2004]) that free solvent is retained longer in paint films than thickened solvent. The converse result shown here is most likely due to the unvarnished nature of the model and incomplete clearing procedures employed. These two factors allow for significantly more gel residues remaining on the painting model surface than would be anticipated in practice; thus, the previous research findings are not disputed.

REFERENCES

Bloembergen, N., E. Purcell, and R. Pound. 1948. Relaxation Effects in Nuclear Magnetic Resonance Absorption. *Physical Review,* 73:679–712. http://dx.doi.org/10.1103/PhysRev.73.679.

Blümich, B., P. Blümler, G. Eidmann, A. Guthausen, R. Haken, U. Schmitz, K. Saito, and G. Zimmer. 1998. The NMR-Mouse: Construction, Excitation, and Applications. *Magnetic Resonance Imaging,* 16:479–484. http://dx.doi.org/10.1016/S0730-725X(98)00069-1.

Stulik, D., D. Miller, H. Khanjian, N. Khandekar, R. Wolbers, J. Carlson, and W.C. Petersen. 2004. *Solvent Gels for the Cleaning of Works of Art: The Residue Question.* ed. V. Dorge. Los Angeles: Getty Conservation Institute.

Erhardt, D., and J. S. Tsang. 1990. The Extractable Components of Oil Paint Films. *Studies in Conservation,* 35(suppl. 1):93–97. http://dx.doi.org/10.1179/sic.1990.35.s1.021.

Fife, G., and T. Meldrum. 2014. The Non-Invasive Analysis of Painted Surfaces: Scientific Impact and Conservation Practice. YouTube video, 37:09. Posted by Smithsonian American Art Museum, 1 April. https://www.youtube.com/watch?v=qDee6QUc0gg (accessed September 2015).

Fife, G. R., B. Stabik, A. E. Kelley, J. N. King, B. R. Blümich, R. Hoppenbrouwers, and T. Meldrum. 2015. Characterization of Aging and Solvent Treatments of Painted Surfaces Using Single-Sided NMR. *Magnetic Resonance in Chemistry*, 53:58–63. doi:10.1002/mrc.4164.

Fife, G. R., J. Van Och, K. Seymour, and R. Hoppenbrouwers. 2010. "Tissue Gel Composite Cleaning at SRAL." In *Cleaning 2010: New Insights into the Cleaning of Paintings,* ed. Fuster-López. L., A. E. Charola, M. F. Mecklenburg, and M. T. Doménech-Carbó. pp. 85–86. Valencia, Spain: Imprenta Llorens.

Fife, G. R., J. Van Och, B. Stabik, N. Miedema, K. Seymour, and R. Hoppenbrouwers. 2011. "A Package Deal: The Development of Tissue Gel Composite Cleaning at SRAL." In *ICOM-CC 16th Triennial Meeting Abstracts*, *Lisbon, Portugal, September 19–23 2011*, ed. J. Bridgland, p. 172. Lisbon: Critério.

Fuesers, O., and S. Zumbühl. 2008. "The Influence of Organic Solvents on the Mechanical Properties of Alkyd and Oil Paint." Paper presented at 9th International Conference on NDT of Art, Jerusalem, Israel, 25–30 May. http://www.ndt.net/article/art2008/papers/219Fuesers.pdf (accessed 8 May 2014).

Hedley, G., M. Odlyha, A. Burnstock, J. Tillinghast, and C. Husband. 1990. A Study of the Mechanical and Surface Properties of Oil Paint Films Treated with Organic Solvents and Water. *Studies in Conservation,* 35(suppl. 1):98–105. http://dx.doi.org/10.1179/sic.1990.35.s1.022.

Jones, P. 1965. The Leaching of Linseed Oil Films in Isopropyl Alcohol. *Studies in Conservation,* 10:119–128

Keune, K., and J. Boon. 2007. Analytical Imaging Studies of Cross-Sections of Paintings Affected by Lead Soap Aggregate Formation. *Studies in Conservation,* 52:161–176. http://dx.doi.org/10.1179/sic.2007.52.3.161.

Maschelein-Kleiner, L., and J. Deneyer. 1981. "Contribution à l'etude des solvants utilisés en conservation." In *ICOM-CC 6th Triennial Meeting Preprints*, *Ottawa, 21st–25th September 1981,* ed. D. Grattan, pp. 1–10. Paris: International Council of Museums.

Michalski, S. 1990. A Physical Model of the Cleaning of Oil Paint. *Studies in Conservation,* 35 (suppl. 1):85–92. http://dx.doi.org/10.1179/sic.1990.35.s1.020.

Phenix, A. 1998. Solubility Parameters and the Cleaning of Paintings: An Update and Review. *Zeitschrift für Kunsttechnologie und Konservierung,* 12:387–409.

———. 2002a. Cleaning of Paintings. *V&A Conservation Journal Online*. Spring, Issue 40. http://www.vam.ac.uk/content/journals/conservation-journal/issue-40/building-models-comparative-swelling-powers-of-organic-solvents-on-oil-paint-and-the-cleaning-of-paintings/ (accessed 8 May 2014).

———. 2002b. The Swelling of Artists' Paints in Organic Solvents. *Journal of the American Institute for Conservation,* 41:43–90.

Phenix, A., and K. Sutherland. 2001. The Cleaning of Paintings: Effects of Organic Solvents on Oil Paint Films. *Studies in Conservation,* 46:47–60. http://dx.doi.org/10.1179/sic.2001.46.2.47.

Stolow, N. 1985. "Solvent Action." In *On Picture Varnishes and Their Solvents,* pp. 47–116. Washington, D.C.: National Gallery of Art.

Stout, G. 1936. A Preliminary Test of Varnish Solubility. *Technical Studies in the Field of Fine Arts* 4:146–161.

Sutherland, K. 2001. Solvent Extractable Components of Oil Paint Films. Ph.D. thesis, University of Amsterdam, Amsterdam.

Tsang, J. S., and D. Erhardt. 1992. Current Research on the Effects of Solvents and Gelled and Aqueous Cleaning Systems on Oil Paint Films. *Journal of the American Institute for Conservation,* 31:87–94. http://dx.doi.org/10.1179/019713692806156457.

Tumosa, C., J. Millard, D. Erhardt, and M. Mecklenburg. 1999. "Effects of Solvents on Physical Properties of Paint Films." In *ICOM-CC 12th Triennial Meeting Preprints*, *Lyon, 29th August–3rd September 1999,* ed. D. Grattan, pp. 347–352. London: James & James.

Van den Berg, J. D. J. 2002. Analytical Chemical Studies on Traditional Linseed Oil Paints. Ph.D. thesis, University of Amsterdam, Amsterdam.

Van Loon, A. 2008. Colour Changes and Chemical Reactivity in Seventeenth-Century Oil Paintings. Ph.D. thesis, University of Amsterdam, Amsterdam.

Zumbühl, S. 2014. Parametrization of the Solvent Action on Modern Artists' Paint Systems. *Studies in Conservation,* 59:24–37. http://dx.doi.org/10.1179/2047058413Y.0000000099.

Zumbühl, S., E. Ferreira, C. Scherrer, and V. Schaible. 2010. "The Non-ideal Action of Binary Solvent Mixtures on Oil and Alkyd Paint." In *Cleaning 2010: New Insights into the Cleaning of Paintings*, ed. Fuster-López. L., A. E. Charola, M .F. Mecklenburg, and M. T. Doménech-Carbó, pp. 43–44. Valencia, Spain: Imprenta Llorens.

A Holistic, Noninvasive Approach to the Technical Study of Manuscripts: The Case of the Breslau Psalter

Paola Ricciardi and Stella Panayotova*

ABSTRACT. This paper discusses the cross-disciplinary study of a richly illuminated thirteenth-century manuscript (Fitzwilliam Museum, MS 36-1950), combining codicological, art historical, and noninvasive technical analyses. Each of this psalter's 294 pages is decorated with illuminations including 28 full-page miniatures, 10 large historiated initials, 168 small miniatures, and a variety of figural and ornamental motifs in the margins. The volume's extensive and diverse decorative program poses challenges to the attribution of its numerous illuminations as well as the amount of analytical data needed to help clarify its method of production and to inform its long-term preservation. Needing to prioritize, the first phase of our investigation, whose results are discussed here, focused on the full-page miniatures and the historiated initials. The analytical protocol employed a cross-disciplinary methodology including paleographical, textual, historical, art historical, and codicological analyses, which were interpreted together with the results of photomicroscopy, infrared imaging, visible and near-infrared reflectance spectroscopy, and X-ray fluorescence spectroscopy. Focused on 38 illuminations, this comprehensive investigation produced an extraordinary amount of data, which had to be cross-referenced and analyzed in a comparative way. The preliminary results of this extensive investigation have so far produced a much clearer picture about the structure and authorship of the decoration, and they are presented here as an example of an integrated approach to the study of illuminated manuscripts.

INTRODUCTION

Technical analysis of works of art is usually undertaken for two main purposes: to establish the histories of production, use, and meaning of objects, including dating, localization, ownership, and later modifications, and to understand the material nature of objects in view of their preservation. In the case of illuminated manuscripts, for which the focus of the technical examination is often the decoration, the main motivation behind scientific analyses is to answer historical and art historical questions. The inherently "conservative" approach to manuscripts employed by most conservators today means that the exact knowledge of the pigments and painting techniques used in a manuscript has limited practical impact on its treatment.[1]

Knowledge of the painting materials and techniques used in manuscripts can provide a wealth of information on production methods and artists' skills (and, occasionally, identity), allowing for synchronic and diachronic comparisons of practices both within and across artistic media and geographical areas. It can also contribute to broader discussions of material culture, art patronage, and the trade of luxury goods. In addition, it can help explain observed degradation phenomena and inform decisions regarding the long-term preservation of manuscripts, if not their interventive conservation.

Department of Manuscripts and Printed Books, The Fitzwilliam Museum, Trumpington Street, Cambridge CB2 1RB, UK.

* Correspondence: P. Ricciardi, pr364@cam.ac.uk

Manuscript received 17 August 2014; accepted 22 February 2016.

Despite major technological developments in recent years that allow reliable, *noninvasive* identification of many artists' materials (Miliani et al., 2007, 2010; Vagnini et al., 2009; Delaney et al., 2010; Rosi et al., 2010; Ricciardi et al., 2012), the scientific analysis of works of art on parchment and paper remains an underdeveloped field in comparison to the extensive analyses carried out on other artifacts, especially easel paintings (Neate et al., 2011). One main reason is the widespread conservation requirement to employ only noninvasive analytical methods to examine manuscripts, avoiding sampling, which is commonly practiced on paintings.[2] Even when noninvasive analytical equipment is available, the experimental setup needs to be planned for and adapted to individual manuscripts in order to avoid physical stress or compromising their integrity.[3]

This paper discusses the cross-disciplinary investigation of a richly illuminated thirteenth-century manuscript, the Breslau Psalter (Fitzwilliam Museum, MS 36-1950).[4] It offers an example of an integrated approach to manuscript studies, combining methods from a range of well-established disciplines, such as codicology, paleography, history, and art history, with noninvasive technical analyses. The goal is to explore the production methods of this complex manuscript and clarify the nature of collaboration between the large number of artists entrusted with its ambitious illustrative program.

THE BRESLAU PSALTER

The Old Testament book of 150 Psalms was a central liturgical and devotional text throughout the medieval period. This manuscript, made in thirteenth-century Breslau in Silesia (Wrocław in modern-day Poland), is one of the most richly illuminated extant psalters (Morgan and Panayotova, 2009: vol. 1, cat. no. 75; Morgan et al., 2011: vol. 1, cat. no. 44). Each of its 294 pages (147 folios) boasts figural representations and lavish ornamentation. Twenty-eight full-page framed miniatures, most facing one another in pairs, are grouped in 10 sections, each introducing one of the standard text divisions beginning with Psalms 1, 26, 38, 51, 52, 68, 80, 97, 101, and 109. These psalms also received 10 large historiated initials—scenes depicted within the first letter of the psalm's opening word. One hundred sixty-eight small framed miniatures adorn the margins of all remaining psalms and the canticles (songs from the Old and New Testaments). The calendar and litany of saints and the borders throughout the volume are populated with hundreds of small scenes and marginal figures. This extraordinary repertoire presents serious challenges to—and exciting opportunities for—in-depth analyses of artistic collaboration and manuscript production.

Trying to identify all artists' materials and painting techniques in this manuscript would equal the task of characterizing the production of a large painting workshop. Faced with a staggering amount of analytical data, we decided to prioritize the 28 full-page miniatures and the 10 historiated initials for the first phase of our investigation. Only the results obtained on these elements of the decoration are discussed here.

ANALYTICAL PROTOCOL

The variety of painting materials—natural and synthetic, organic and inorganic—employed by illuminators requires the use of multiple, complementary analytical methods in order to clarify their identity. The wish to characterize artists' painting techniques calls for an even larger set of analytical tools. For a comprehensive interpretation of the manuscript's methods of production, the technical data need to be considered alongside codicological, textual, art historical, and broader historical analyses.

The investigation of the Breslau Psalter employed the following cross-disciplinary methodology:

- paleographical analysis of the script for features suggestive of a place and date of origin
- textual analysis of the contents for evidence of liturgical use, patronage, and intended ownership
- historical analysis of the patronage to clarify the dynastic, aristocratic, and ecclesiastical context of production
- art historical analysis of stylistic, compositional, and iconographic features to formulate questions for the technical analyses
- codicological analysis of the manuscript's structure to help clarify artistic collaboration
- photomicroscopy, focusing on the buildup of flesh tones and on the presence of mixtures
- infrared imaging, to investigate the presence and appearance of underdrawing and pentimenti
- spectroscopic analysis by fiber-optic reflectance spectroscopy (FORS) in the ultraviolet–visible–near-infrared range (UV-vis-NIR: 350–2,500 nm)
- X-ray fluorescence (XRF), X-ray diffraction (XRD), and Raman spectroscopy analysis on selected sites.[5]

Although still ongoing, these analyses have already produced a clearer picture about the decoration's authorship, which is presented below.

Summary of Paleographical, Textual, and Historical Analyses

The dating and localization of the manuscript was determined by combined paleographical, textual, and historical analyses. The script, a compressed version of Gothic book hand (textualis), and specific letter forms point to thirteenth-century central Europe. The liturgical texts establish that the psalter was made between 1255 and 1267 in Breslau, Silesia (Morgan and Panayotova, 2009: vol. 1, cat. no. 75). A prayer composed for a woman and mentioning "God's servant Henry" (fol. 146r) has been linked to the daughter of Duke Albert of Saxony, Helen, who married Henry III, Duke of Breslau, around 1257. Although relatively few saints specific to Saxony feature in the calendar, several saints associated with Prague grace the litany, pointing to Helen's mother-in-law, Anna Přemyslid, who died in 1265. Sister of Wenceslas I of Bohemia, Anna was the duchess of Henry II of Breslau and mother of Henry III and Vladislav, archbishop of

Salzburg. Helen's marriage and Anna's death may narrow the date range to 1257–1265 if the manuscript was intended for the young bride and commissioned by her mother-in-law.

Art Historical Analysis

The Breslau Psalter is the most richly illuminated in a group of manuscripts made north of the Alps but containing the work of an artist who illuminated an epistolary copied in 1259 for Padua Cathedral by the scribe Giovanni da Gaibana.[6] The northern migration of the Paduan style has been associated with Anna Přemyslid's younger son, Vladislav, who studied in Padua before becoming archbishop of Salzburg in 1265 and presumably brought the Gaibana Master with him. If the psalter was begun by 1265, the year Anna Přemyslid died and Vladislav arrived in Salzburg, it would be the earliest of the deluxe Gaibana-style manuscripts illuminated north of the Alps. Given its extensive pictorial program, work may have continued for several years, perhaps under the auspices of Vladislav (Bossetto, 2010; 2015). The full-page *B*(*eatus*) initial for Psalm 1 (fol. 23v, Figure 1), the most accomplished illumination in terms of style, painting technique, composition, and iconography, is unanimously attributed

FIGURE 1. The *Beatus* initial on fol. 23v, painted by the Gaibana Master. Fitzwilliam Museum, MS 36-1950. Silesia, Breslau, ca. 1255–1267 © The Fitzwilliam Museum, Cambridge.

to the Gaibana Master. His work is characterized by dignified figures with icon-like expressions; elegant drapery with hems defined by crisp white lines and folds forming rhythmical or nestled patterns, often accentuated by thick impasto, creating a relief effect; juxtapositions of luminous colors in fabrics, highlighted in white, geometrically shaped areas and shaded in darker, transparent glazes; soft modeling of faces, with layers built in gradation from a dark gray undertone through carefully blended flesh color to red shading and white highlights; flesh and facial features outlined in red; and the flowering, broccoli-like trees considered to be the artist's signature feature.

Ten other images are often attributed to the Gaibana Master (denoted GM in the figures and tables): the full-page miniature of Christ and the Apostles and the historiated initial for Psalm 38 (fols. 49v and 51r, Figure 2), as well as eight small miniatures. Although their style is closely related to that of the Gaibana Master, they display differences in the modeling of faces and drapery, and their execution falls short of the refinement seen on fol. 23v, suggesting the involvement of an associate. Analysis of the materials and techniques in these images could clarify the stylistic observations and inform broader enquiries: Was the associate a disciple trained in the Gaibana Master's painting techniques or a local artist absorbing the Paduan style? Did they collaborate on the psalter, sharing materials and perhaps premises, or did they work independently?

Until now, scholarship has focused exclusively on the images attributed to the Gaibana Master and their importance in transmitting a new wave of Byzantinizing style and iconography from the Veneto to regions north of the Alps (Bossetto, 2010; 2015; Mariani Canova et al., 2014: no. 12). All remaining figural scenes—well over 200 images—have been ascribed to local Breslau-based artists without discussing the nature of their work or their relationship to the Gaibana Master (Wormald and Giles, 1982: 416; Morgan and Panayotova, 2009: vol. 1, cat. no. 75).

FIGURE 2. The full-page illumination on fol. 49v and the historiated initial on fol. 51r, both traditionally attributed to the Gaibana Master but most likely painted by one of his associates. Fitzwilliam Museum, MS 36-1950. Silesia, Breslau, ca. 1255–1267 © The Fitzwilliam Museum, Cambridge.

The present study is the first attempt to examine closely all 38 major illuminations. Apart from the three usually attributed to the Gaibana Master, the remaining 35 seem to have been painted by seven main artists and three assistants (fols. 40r, 64r, 104r) working in a homogeneous style. Their figure style, facial types, modeling of fabrics, and compositional organization of the pictorial space are consistent with contemporary Silesian illumination. Lest we create new "masters of" at this preliminary stage of research, we shall assign letters to these hands, listed here with the illuminations attributed to them:

A: fols. 18r (Figure 3), 19v, 50r, 73r, 74v, 86r, 87v, 99r, 100v
B: fols. 15v, 16r (Figure 3), 21v, 22r
C: fols. 17v, 20r, 62r
D: fols. 59v (Figure 3), 60r, 61v, 63v
E: fols. 39v, 103v
F: fols. 72v, 75r (Figure 3), 85v, 88r, 98v, 101r, 113v, 116r
G: fols. 114r, 115v

The work of these artists will be discussed below, bringing the technical analyses to bear on the art historical observations. We shall attempt to characterize their palettes, techniques, and professional relationships while addressing a number of questions. Was the manuscript a workshop product, undertaken by a master with his assistants or a collaborative project between independent artists? Did the Gaibana Master make a guest appearance, or was he an integral member of the team? What was the extent of interaction between the Breslau artists and the illuminators working in the Italian style? Was there a two-way exchange of ideas and technical expertise or simply a Paduan influence on the Breslau artists? Was any influence or exchange limited to stylistic borrowing, or did it run deeper—into the choice of specific materials and the adoption of painting techniques? Did the illuminators work side by side, dipping their brushes into the same paints? Or were separate leaves dispatched to individual artists, presumably working at different premises? The codicological study of the volume may help answer this last question and inform the subsequent discussion, which will integrate the technical analyses with the remaining investigation.

Codicological Analysis

The manuscript consists of 21 quires—gatherings of parchment sheets folded in half, stacked inside one another, and accommodating distinct sections of text and images. Quires 3–19 contain the psalms and all major illuminations discussed here.[7] Ten of these quires are regular quaternions, composed of four folded sheets (bifolios), making eight leaves (folios), or 16 pages. Quires 7 and 15 are also quaternions, but an additional leaf (singleton) with a full-page miniature has been tucked inside each of them (fols. 50, 103). Quires 8, 9, 10, 12, and 14 vary in composition, from two to five folded sheets (4 to 10 folios); each was designed in view of accommodating full-page miniatures before main division psalms with historiated initials. The manuscript's structure was determined by the desire for lavish illumination. The full-page miniatures are painted on only one side of the leaves, a feature reserved for deluxe manuscripts and intended to avoid an image on one side of the leaf bleeding through. Although the thick parchment of the Breslau Psalter could have supported images on both sides of a leaf without visual interference, the decision to employ this layout demonstrates that no expense was spared in the manuscript's design and execution.

Another codicological feature reveals different—and evolving—methods of work adopted by individual artists. In the earlier part of the volume, red or black frames on the reverse of miniatures delineate the painted space, a practice common to earlier and contemporary German manuscripts. The frames accompany miniatures by Breslau illuminators but not those by the Gaibana Master and his associate. In the later part of the manuscript, the Breslau illuminators abandoned the traditional frames, perhaps an aesthetic decision made under Paduan influence.

The division of labor among the artists confirms that the quires were the volume's main building blocks in terms of pictorial design as well as textual content. Although two or more artists collaborated within many quires, miniatures on pages belonging to the same double sheet were painted by a single artist, as illustrated in Table 1. Hand A illuminated the central double sheets in four quires, whose other miniatures were supplied by three distinct illuminators: hands B and C in quire 3 and hand F in quires 10, 12, and 14. Hand A also provided a miniature on a singleton added to quire 7 between images by the Gaibana Master's associate.

The division of labor is more complex in the case of double sheets containing a miniature and a historiated initial. Usually, both were painted by the same illuminator, hand F. In one instance, however (fols. 59v and 62r in quire 8), the miniature and the historiated initial were painted by hands D and C, respectively. All other historiated initials lack major illumination on the conjoint leaf.

Technical Investigation

The 38 miniatures and initials selected as the focus of our investigation were analyzed with a range of imaging and spectroscopic methods, some in more detail than others. Because of the quantity of information needed, we privileged the use of FORS in the UV-vis-NIR range to carry out an extensive survey of painted areas on these illuminations.[8] Reflectance spectroscopy has been successfully used in recent years to identify a large number of pigments, inks, and paint binders on easel paintings as well as on works of art on parchment and paper (Strlič et al., 2010; Ricciardi et al., 2012, 2013a, 2013b; Aceto et al., 2014; Delaney et al., 2014; Vetter and Schreiner, 2014). Each spectrum can be collected within a matter of seconds, and often, the identification of the main components of the paint layer is immediate, making FORS an ideal tool for preliminary technical analysis of manuscripts (Aceto et al., 2012, 2014).

FIGURE 3. The full-page illuminations on fols. 18r, 16r, and 59v and the historiated initial on fol. 75r, here attributed to four different artists. Fitzwilliam Museum, MS 36-1950. Silesia, Breslau, ca. 1255–1267 © The Fitzwilliam Museum, Cambridge.

TABLE 1. Relationship between the quire structure and the position and attribution of the 28 full-page illuminations (FP) and 10 historiated initials (HI) in the Breslau Psalter. S indicates an inserted singleton.

Q3		15v	FP	B
		16r	FP	B
		17v	FP	C
		18r	FP	A
		19v	FP	A
		20r	FP	C
		21v	FP	B
		22r	FP	B
Q4		23v	HI	GM
Q6		39v	FP	E
		40r	HI	assistant
		49v	FP	GM's associate
Q7	S	50r	FP	A
		51r	HI	GM's associate
		59v	FP	D
		60r	FP	D
		61v	FP	D
Q8		62r	HI	C
		63v	FP	D
		64r	HI	assistant
Q10		72v	FP	F
		73r	FP	A
		74v	FP	A
		75r	HI	F
Q12		85v	FP	F
		86v	FP	A
		87v	FP	A
		88r	HI	F
Q14		98v	FP	F
		99r	FP	A
		100v	FP	A
		101r	HI	F
Q15	S	103v	FP	E
		104r	HI	assistant
Q16		113v	FP	F
		114r	FP	G
		115v	FP	G
		116r	HI	F

Reflectance Spectroscopy: Results on the Breslau Psalter

Reflectance spectroscopy allowed the identification of a number of pigments used in the majority of the 38 illuminations analyzed, as exemplified by the sample spectra from fol. 49v (Figure 4): ultramarine (spectrum A) can be recognized in most blue areas by its characteristic absorption centered at 600 nm, followed by a rise in reflectance with the transition edge between about 700 and 720 nm. In a small number of dark/dull blue areas, ultramarine appears to have been mixed with (or possibly layered over) azurite (spectrum B), whose presence is clearly revealed by absorption bands at 1,493, 2,285, and 2,353 nm. A mixture of azurite with a yellow pigment (as yet unidentified) was also used in a few green areas (spectrum C), although the green pigment of choice was verdigris (spectrum D), characterized by a broad absorption centered at 700 nm followed by a slow rise in reflectance, peaking at about 1,320 nm. All red areas were painted using vermillion (spectrum E), identified by its sharp transition edge at 595–600 nm. A greater variety of pigments was used to paint yellow areas, which are, however, relatively scarce throughout the manuscript. The combined use of FORS, XRF, and Raman spectroscopy reveals the presence of orpiment on four folios in quire 3 and of a yellow earth or ochre on four folios in quire 8 and suggests the use of an organic yellow dye on 14 other folios throughout the manuscript. No yellow areas are present on the remaining 16 folios analyzed.

In addition to the blue, green, and yellow areas, FORS analyses also identified pigments and mixtures in the flesh tones and white/blue beards of the figures, revealing different patterns in the use of materials. Overall, the technical analyses suggest the presence of six distinct "palettes," allowing a preliminary division of the miniatures into groups as summarized in Table 2.[9] For example, Figure 5 shows a selection of FORS spectra of flesh tones relative to six different folios, and Figure 6 shows the corresponding photomicrographs. The FORS analysis alone cannot identify all the components of these complex mixtures, but it helps separate the flesh-tone spectra into groups and identify at least some of the individual pigments that characterize each group. Flesh tones on folios 16r and 18r are characterized by the presence of large amounts of woad,[10] as indicated by the strong absorption maximum around 660 nm followed by a sharp rise in reflectance. Smaller amounts of woad can be identified also on fol. 59v. Flesh tones on fol. 49v instead contain azurite, as indicated by the presence of absorption bands at about 2,285 and 2,353 nm, along with a less noticeable band at 1,492 nm. Finally, flesh tones on fols. 23v and 75r do not seem to contain any blue pigments, but rather are characterized by the presence of iron oxide–containing pigments (earths or possibly ochres). The spectra from fols. 18r, 23v, and 49v also show an additional absorption band at about 2,305 nm, probably related to the presence of a lipid-containing paint binder, most likely egg yolk (Ricciardi et al., 2012).[11]

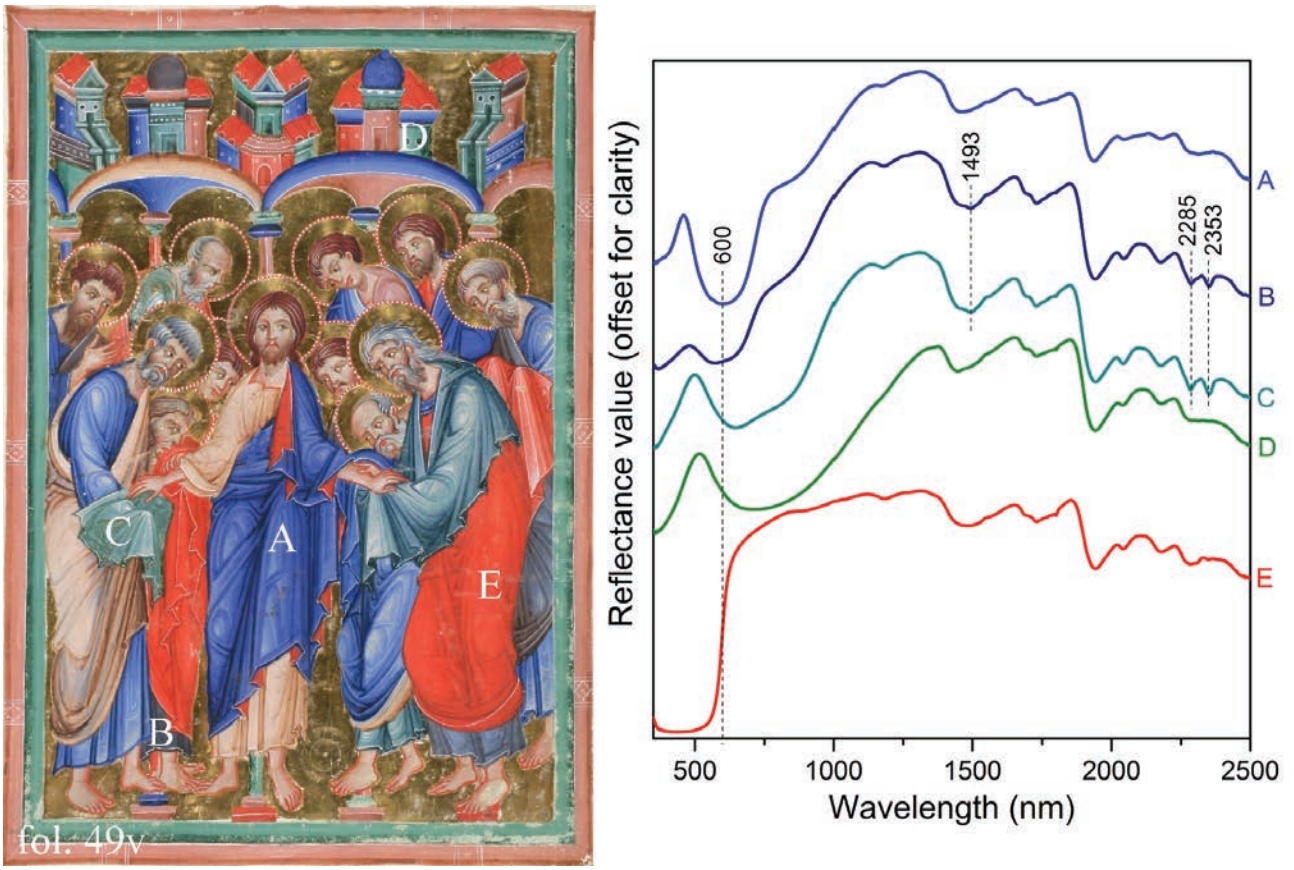

FIGURE 4. Sample FORS spectra from blue, green, and red areas on fol. 49v. See text for an interpretation of each spectrum. Fitzwilliam Museum, MS 36-1950. Silesia, Breslau, ca. 1255–1267 © The Fitzwilliam Museum, Cambridge.

TABLE 2. Grouping of the major illuminations in the Breslau Psalter based on the results of technical analyses, a list of the signature pigments and mixtures for each group, and attribution to individual artists. A dash (—) indicates the absence of a specific color or feature in the folio(s).

Category	Folios[a]	Artists	Blue	Green	Yellow	Flesh tones	Beards
1	23v	GM	ultramarine	verdigris	—	earths	—
2	49v, 51r	GM's associate	ultramarine, azurite	verdigris, azurite mixture	—	azurite	azurite
3	18r, 19v, 50r, 73r, 74v, 86r, 87v*, 99r, 100v*	A	ultramarine	verdigris	organic/—	woad	ultramarine
4	15v, 16r*, 17v, 20r, 21v*, 22r, 62r*, 64r	B, C	ultramarine	verdigris	orpiment/—	woad	woad
5	59v, 60r, 61v, 63v	D	ultramarine	verdigris	earth/ochre	woad	ultramarine
6	39v, 40r, 72v, 75r, 85v, 88r, 98v, 101r, 103v, 104r, 113v, 114r, 115v, 116r	E, F, G	ultramarine	verdigris, azurite mixture	organic/—	earths	ultramarine

[a]No blue beards or yellow areas are present in the folios marked by an asterisk (*), meaning that they could match both categories 3 and 4. Their assignment here is based on the presence of bright pink (present on all other folios in category 3) versus a muted tan color (typical of folios in category 4) in the fabrics.

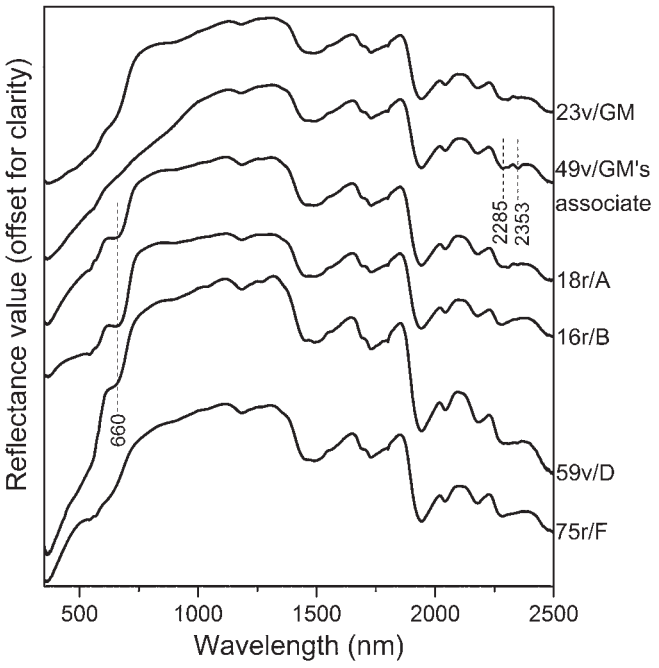

FIGURE 5. Sample FORS spectra of flesh tones on six different folios, each by a different artist and corresponding to one of the groups listed in Table 2.

DISCUSSION

A systematic comparison of the information obtained by the different methods employed for this cross-disciplinary study reveals considerable agreement between the art historical, codicological, and technical analyses for the majority of illuminations examined. Tables 1 and 2 summarize the overall results.

The results of the technical analyses support the art historical differentiation between the Gaibana Master, responsible for fol. 23v, and the associate who illuminated fols. 49v and 51r. The Gaibana Master's use of a delicate violet color, obtained with a mixture of vermillion and ultramarine blue, is unique in the manuscript. Another major difference is the painting of flesh: unlike the Gaibana Master, who chose earth pigments, his associate made prolific use of azurite in flesh tones and beards, as well as in blue areas and green mixtures. None of the Breslau artists favored azurite, despite—or perhaps because of—its wide availability in central Europe. The varying choices of blue pigments suggest that the Gaibana Master, his associate, and the Breslau artists worked independently; they were neither supplied with nor expected to share the same materials.

Although the associate emulated the Gaibana Master's style successfully, his choice of materials, especially for the flesh and beards, is markedly different. This difference suggests that he was neither a disciple trained by the Gaibana Master nor a close collaborator on the Breslau Psalter, sharing pigments and presumably premises. Nevertheless, the close and confident adherence to the Paduan style implies ready access to the Gaibana Master's work. If the associate did not come with the Gaibana Master from Padua, he may have encountered him upon his arrival in Salzburg. Although the Gaibana Master contributed a single image in quire 4, the associate painted 10, including small miniatures in quires 6 and 7.[12] These quires may have been sent to Salzburg, or both artists may have visited Breslau, with the associate perhaps staying on and transmitting his knowledge of the Gaibana Master's style and iconography to the Breslau artists.

Among the seven local artists, two stand out as the most accomplished: hands A and B. They share certain features with the Gaibana Master and his associate: the nestled folds, impasto outlines and shading glazes on fabrics, and the red outlines of flesh and facial features. However, their faces lack delicacy. Without careful blending, the modeling of flesh reveals the layers, shading, and highlights. Hand A introduces monumental figures, gold-tooled and painted halos, and liquid gold over details first colored in green, all implying that he might have been trained as a panel painter rather than an illuminator.[13] He favors trichromatic highlights on green drapery, white scumble on blue fabrics, bright pink robes, and light yellow areas painted with an organic dye. His pink flesh tones have blue undertones obtained with woad, whereas the blue/gray beards of his older characters contain ultramarine blue. The use of large amounts of woad in flesh tones is shared by hand B, who, unlike hand A, uses the same pigments for beards and prefers soft tan as a surface hue for faces. His figures are elegant but less imposing in proportion to the overall pictorial space. His range of greens is more limited and of inferior technical execution, with large areas of flaking pigment revealing the underdrawing. His pink fabrics are transparent and muted in hue. Hand C follows the first two artists closely, but his style is dry and linear, his crowded compositions lead to oversights (the domes on fol. 17v are suspended in thin air), and his dwarflike figures are devoid of elegance, their exaggerated facial features bordering on the grotesque. His palette is the same as the one employed by hand B.

Hand D, who was responsible for a cluster of four miniatures, emulated the delicate facial expressions and broccoli-like trees of the Gaibana Master, but his drapery folds are as schematic and his compositions as crowded as those of hand C. He also mixed woad in his flesh tones, but his palette is strongly characterized by the use of an ochre pigment in yellow areas.

The remaining three artists all employed the same palette, characterized by the lack of blue pigments in their flesh tones. Hand F painted eight large images in four clusters, collaborating with hand A in three of them (quires 10, 12, 14). His salient features include gold-tooled frames, elongated figures with small heads, elaborately knotted belts and "ankle warmers," and gray outlines of limbs; the few exceptions to the latter include the miniature on fol. 72v, where the artist adhered to the red outlines employed by all other artists and painted a hem in liquid gold, perhaps to mirror those by hand A on the facing page.

FIGURE 6. Micrographs (originally taken at ×7.5 magnification) of the flesh tone areas whose FORS spectra are shown in Figure 5.

Hands E and G painted two miniatures each. Hand E is identified as the only artist in the manuscript to outline red drapery folds in black. Hand G emulated hand A's stylistic features[14] but appears to display a strong interest in the Gaibana Master's iconography,[15] whereas the remaining local artists seem less inclined to borrow directly from the Gaibana Master or his associate.

The authorship of the three historiated initials on fols. 40r, 64r, and 104r remains problematic. It is possible that they were painted by three different artists who may have been among the illuminators responsible for the minor decoration throughout the volume.[16] Although the production of this deluxe manuscript was carefully planned and managed, the completion of such an ambitious decorative program required the involvement of numerous artists, resulting in individual idiosyncrasies within the overall design.[17]

Furthermore, as in the case of the Gaibana Master and his associate, stylistic similarities between the Breslau artists do not always correspond to shared materials and techniques. Hand A's accomplished work, prominent role throughout the volume, and stylistic influence on his collaborators suggest that he was an established artist, probably entrusted with managing the provision of the major illuminations. His choice of materials, however, was not followed by hands B and C, who adhered to his style, or by hand F, who collaborated with him in three quires. Likewise, hand D stands in isolation from other artists in his pigment preferences. Conversely, the use of a common palette did not always result in an artistic homogeneity: hands E, F, and G employed the same pigments but retained their individual stylistic peculiarities. By contrast, hands B and C shared not only stylistic features but also specific painting materials and techniques.

CONCLUSIONS

The combined codicological, art historical, and technical analyses of the 38 major illuminations in the Breslau Psalter demonstrate the benefits of an integrated, cross-disciplinary approach. The benefits are particularly clear in the case of this exceptionally complex manuscript involving numerous illuminators and combining stylistically and geographically distinct artistic traditions.[18] The integrated approach answered many of the questions about production methods and artistic collaboration.

The illuminators of the major images do not seem to have belonged to a single workshop. Some of them were independent artists (hand D), others may have been regular collaborators (hands B and C), and yet others seem to have come together for this project (hands E, F, and G). All of them were most likely gathered to ensure the timely completion of the ambitious decorative program. The brief, but brilliant, guest appearances of the Gaibana Master and his associate were probably intended to speed up the process and enhance the quality of the final product. Rather than a two-way exchange of ideas and technical skills, their interaction with the German artists resulted in borrowing of isolated stylistic and iconographic features by some, but not all, of the local illuminators. Hand A, probably a painter at the ducal court, may have overseen the project, but without imposing a uniformity of style, materials, or techniques. Some of the illuminators (hands E, F, and G) may have worked side by side, sharing pigments, but others probably received individual bifolios dispatched to their own premises.

These preliminary suggestions, based on the partial analyses of 38 images, may be modified by cross-disciplinary analyses of the small miniatures and marginalia at the next stage of research. This next step may establish the degree of interaction between the main artists discussed above and the lesser hands responsible for the minor decoration. Future work will also focus on the identification of brown and pink/tan pigments, as well as paint binders. An enriched and refined characterization of painting materials and techniques in both the major and minor decoration would offer a truly comprehensive understanding of this complex volume and provide a sound foundation for the analyses of contemporary manuscripts.

NOTES

1. The exact knowledge of paint binders, however, may have a stronger impact on conservation treatments, which is just one of the reasons why the noninvasive identification of paint binders on manuscripts is one of the most pressing challenges faced by conservation science at present.
2. The fragility and light sensitivity of the paint layers, as well as the physical shape and dimensions of the manuscripts, greatly reduce the number of analytical methods that can be used on bound volumes. The technical analysis of manuscript cuttings and individual leaves that were cut out of their parent manuscript at some point in the past is easier from the practical point of view and more similar to the analysis of small panel paintings. The issues of fragility and light sensitivity, however, are still present, as are the additional complications in the interpretation of spectroscopic data discussed further on in this paper in the section on reflectance spectroscopy.
3. For a discussion and suggestions for appropriate analytical protocols for the analysis of manuscripts, see Maurizio Aceto, Angelo Agostino, Gaia Fenoglio, Monica Gulmini, Valentina Bianco, and Eleonora Pellizzi, Non invasive Analysis of Miniature Paintings: Proposal for an Analytical Protocol, *Spectrochimica Acta Part A,* 91 (2012): 352–359, http://dx.doi.org/10.1016/j.saa.2012.02.021; Paola Ricciardi and John K. Delaney, Combining Visible and Infrared Imaging Spectroscopy with Site-Specific, in-Situ Techniques for Material Identification and Mapping, *Revista de História da Arte, Série W,* 1 (2011): 252–261.
4. The most recent discussions of the manuscript's illumination and patronage are Fabio L. Bossetto, *Il Maestro del Gaibana: un miniature del Duecento fra Padova, Venezia e l'Europa* (Milan: Silvana Editoriale, 2015); Nigel Morgan and Stella Panayotova, *A Catalogue of Western Book Illumination in the Fitzwilliam Museum and the Cambridge Colleges,* part 1 (London: Harvey Miller, 2009), vol. 1, cat. no. 75; Nigel Morgan, Stella Panayotova, and Suzanne Reynolds, *A Catalogue of Western Book Illumination in the Fitzwilliam Museum and the Cambridge Colleges*, part 2 (London: Harvey Miller, 2011), vol. 1, cat. no. 44; Stella Panayotova (ed.), *Colour: The Art and Science of Illuminated Manuscripts* (London: Harvey Miller, 2016), cat no. 26 and 119–135. They sum up earlier discussions and list all essential previous literature, which is not repeated here for lack of space. The technical analysis was carried out within the context of the MINIARE (Manuscript Illumination: Non-Invasive Analysis, Research and Expertise) research project (http://www.miniare.org).
5. Combined XRF-XRD measurements were carried out by Philippe Walter and Hélène Rousselière from the Laboratoire d'Archéologie Moléculaire et Structurale in Paris, within the context of the CHARISMA-MOLAB (Cultural Heritage Advanced Research Infrastructures: Synergy for a Multidisciplinary Approach to Conservation and Restoration—Mobile Laboratory) project. Raman analyses were undertaken by Andrew Beeby and Kate Nicholson from Durham University.
6. Biblioteca Capitolare, MS E 2, Padua, Italy; Giordana Mariani Canova, Marta Minazzato, and Federica Toniolo, *I Manoscritti Miniati della Biblioteca Capitolare di Padova*, vol. 1 (Padua: Istituto per la Storia Ecclesiastica Padovana, 2014), no. 12.
7. For an introduction to codicological analysis, see Bernhard Bischoff, *Latin Palaeography: Antiquity and the Middle Ages* (Cambridge: Cambridge University Press, 1990), 5–45, http://dx.doi.org/10.1017/CBO9780511809927.
8. The FORS analysis was carried out using a FieldSpec4 spectroradiometer (ASDi/Panalytical) with a bifurcated fiber-optic probe, with the ability to collect reflectance spectra between 350 and 2,500 nm. Each spectrum was the average of 64 measurements; over 600 painted areas of about 3 mm in diameter were surveyed by this method.
9. In the case of flesh tones, in particular, the table lists only the main or most characteristic component of each complex mixture.
10. The presence of woad, rather than indigo, can be hypothesized on the basis of the geographic origin of this manuscript. However, FORS, like many other techniques, cannot distinguish between these two colorants.
11. The spectral evidence suggests the presence of a paint binder different from the one (or ones) used in other parts of the decoration. Such evidence is most clear in areas of flesh on several folios (e.g., 18r, 23v, 49v, 73r, 74v, and 100v), all of which have been attributed to the Gaibana Master, to his assistant, and to hand A, as well as in the beards of figures on fol. 23v. There is certainly scope for further investigation; we hope among other things to perform Fourier transform infrared spectroscopy analysis and near-infrared hyperspectral imaging on these areas to help clarify the nature of this material and to verify the extent of its presence at least across the 38 major illuminations.
12. Technical examination of these small miniatures still has to be undertaken, but the art historical analysis strongly suggests that they were painted by the Gaibana Master's associate.
13. Should the substantial presence of an egg yolk binder be confirmed on folios painted by hand A, this information would additionally support the suggestion that he may have been trained as a panel painter and as such very familiar with egg tempera as a painting medium.
14. These include his monumental figures, chromatic juxtapositions, drapery folds, and halos.
15. For example, he transferred the Gaibana Master's Byzantine iconography of the Deësis, showing the Virgin and St. John the Baptist interceding with Christ for human salvation (fol. 23v), into his own composition (fol. 115v).
16. Their overall palette is most similar to the work of hands B and C (fol. 64r) and E, F, and G (fols. 40r and 104r), respectively. However, the initial on fol. 40r includes a facial type and the sophisticated handling of green

characteristic of hand A, suggesting that the leading Breslau artist may have collaborated with an assistant on this image. The possible collaboration of different artists on the same miniature exemplifies the Breslau Psalter's complexity.

17. Among these differences are the absence or presence (in black or red) of frames on the versos of full-page miniatures, the insertion of two miniatures on singletons (fols. 50r, 103v), the marked increase of whimsical marginalia from quire 11 onward, the presence of orange areas painted with red lead only on one bifolio (fols. 127–134), and the stylistic change in the small miniatures in quires 17–19.
18. The initial phase of this work has already highlighted the pressing need for a flexible tool allowing for coherent storage, structure, annotation, and visualization of the large amount of text, images, and analytical data in different formats generated during the project. An initial step has been taken during the "Digital Layers" project, which has resulted in the development of a digital image annotation tool and an online research resource (www.fitzmuseum.cam.ac.uk/illuminated) which features, among others, the Breslau Psalter. The need to better integrate imaging and analytical technologies used by conservators and cultural heritage scientists for the study of works of art was also the topic of an experts' meeting held at the Getty Conservation Institute in 2013. One of its most immediate outcomes was a report including a review of case studies and a list of recommendations for future research on this topic, posted on the institute's website (http://www.getty.edu/conservation/our_projects/integrating_imaging.html, accessed 3 August 2016).

REFERENCES

Aceto, Maurizio, Angelo Agostino, Gaia Fenoglio, Monica Gulmini, Valentina Bianco, and Eleonora Pellizzi. 2012. Non invasive Analysis of Miniature Paintings: Proposal for an Analytical Protocol. *Spectrochimica Acta Part A,* 91:352–359. http://dx.doi.org/10.1016/j.saa.2012.02.021.

Aceto, Maurizio, Angelo Agostino, Gaia Fenoglio, Ambra Idone, Monica Gulmini, Marcello Picollo, Paola Ricciardi, and John K. Delaney. 2014. Characterisation of Colourants on Illuminated Manuscripts by Portable Fibre Optic UV-Visible-NIR Reflectance Spectrophotometry. *Analytical Methods,* 6:1488–1500. http://dx.doi.org/10.1039/c3ay41904e.

Bossetto, Fabio L. 2010. Splendori a corte: Il Salterio Thompson di Cambridge. *Alumina* 30:6–17.

Bossetto, Fabio L. 2015. *Il Maestro del Gaibana: un miniatore del Duecento fra Padova, Venezia e l'Europa*. Milan: Silvana Editoriale.

Bischoff, Bernhard. 1990. *Latin Palaeography: Antiquity and the Middle Ages*. Cambridge: Cambridge University Press. http://dx.doi.org/10.1017/CBO9780511809927.

Delaney, John K., Paola Ricciardi, Lisha D. Glinsman, Michelle Facini, Mathieu Thoury, Michael Palmer, and E. René de la Rie. 2014. Use of Imaging Spectroscopy, Fiber Optic Reflectance Spectroscopy, and X-ray Fluorescence to Map and Identify Pigments in Illuminated Manuscripts. *Studies in Conservation,* 59(2):91–101. http://dx.doi.org/10.1179/2047058412Y.0000000078.

Delaney, John K., Jason G. Zeibel, Mathieu Thoury, Roy Littleton, Michael Palmer, Kathryn M. Morales, E. René de la Rie, and Ann Hoenigswald. 2010. Visible and Infrared Imaging Spectroscopy of Picasso's *Harlequin Musician*: Mapping and Identification of Artist Materials *in Situ*. *Applied Spectroscopy,* 64(6):584–594. http://dx.doi.org/10.1366/000370210791414443.

Mariani Canova, Giordana, Marta Minazzato, and Federica Toniolo. 2014. *I Manoscritti Miniati della Biblioteca Capitolare di Padova*. 2 vols. Padua: Istituto per la Storia Ecclesiastica Padovana.

Miliani, Costanza, Francesca Rosi, Brunetto G. Brunetti, and Antonio Sgamellotti. 2010. In Situ Noninvasive Study of Artworks: The MOLAB Multitechnique Approach. *Accounts of Chemical Research,* 43(6):728–738. http://dx.doi.org/10.1021/ar100010t.

Miliani, Costanza, Francesca Rosi, Aviva Burnstock, Brunetto G. Brunetti, and Antonio Sgamellotti. 2007. Non-invasive in-Situ Investigations Versus Microsampling: A Comparative Study on a Renoirs Painting. *Applied Physics A,* 89(4):849–856. http://dx.doi.org/10.1007/s00339-007-4222-3.

Morgan, Nigel, and Stella Panayotova. 2009. *A Catalogue of Western Book Illumination in the Fitzwilliam Museum and the Cambridge Colleges*. Part 1. London: Harvey Miller.

Morgan, Nigel, Stella Panayotova, and Suzanne Reynolds. 2011. *A Catalogue of Western Book Illumination in the Fitzwilliam Museum and the Cambridge Colleges*. Part 2. London: Harvey Miller.

Neate, Sarah, David Howell, Richard Ovenden, and A. M. Pollard, eds. 2011. *The Technological Study of Books and Manuscripts as Artefacts*. Oxford: Archaeopress.

Panayotova, Stella (ed.). 2016. *Colour: The Art and Science of Illuminated Manuscripts*. London: Harvey Miller.

Ricciardi, Paola, and John K. Delaney. 2011. Combining Visible and Infrared Imaging Spectroscopy with Site-Specific, in-Situ Techniques for Material Identification and Mapping. *Revista de História da Arte Série W,* 1:252–261.

Ricciardi, Paola, John K. Delaney, Michelle Facini, and Lisha Glinsman. 2013a. Use of Imaging Spectroscopy and in Situ Analytical Methods for the Characterization of the Materials and Techniques of 15th Century Illuminated Manuscripts. *Journal of the American Institute for Conservation,* 52(1):13–29. http://dx.doi.org/10.1179/0197136012Z.0000000004.

Ricciardi, Paola, John K. Delaney, Michelle Facini, Jason G. Zeibel, Marcello Picollo, Suzanne Lomax, and Murray Loew. 2012. Near Infrared Reflectance Imaging Spectroscopy to Map Paint Binders in Situ on Illuminated Manuscripts. *Angewandte Chemie International Edition,* 51:5607–5610. http://dx.doi.org/10.1002/anie.201200840.

Ricciardi, Paola, Anuradha Pallipurath, and Kristine Rose. 2013b. It's Not Easy Being Green: A Spectroscopic Study of Green Pigments Used in Illuminated Manuscripts. 2010. An Integrated Spectroscopic Approach for the Non-invasive Study of Modern Art Materials and Techniques. *Applied Physics A,* 100:613–624. http://dx.doi.org/10.1007/s00339-010-5744-7.

Strlič, Matija, Linda Cséfalvayová, Jana Kolar, Eva Menart, Joanna Kosek, Caroline Barry, Catherine Higgitt, and May Cassar. 2010. Non-destructive Characterisation of Iron Gall Ink Drawings: Not Such a Galling Problem. *Talanta,* 81(1–2):412–417. http://dx.doi.org/10.1016/j.talanta.2009.12.017.

Vagnini, Manuela, Costanza Miliani, Laura Cartechini, P. Rocchi, Brunetto G. Brunetti, and Antonio Sgamellotti. 2009. FT-NIR Spectroscopy for Non-invasive Identification of Natural Polymers and Resins in Easel Paintings. *Analytical and Bioanalytical Chemistry,* 395:2107–2118. http://dx.doi.org/10.1007/s00216-009-3145-6.

Vetter, Wilfried, and Manfred Schreiner. 2014. A Fiber Optic Reflection-UV/Vis/NIR-System for Non-destructive Analysis of Art Objects. *Advances in Chemical Science,* 3(1):7–14.

Wormald, Francis and Phyllis M. Giles. 1982. *A Descriptive Catalogue of the Additional Manuscripts in the Fitzwilliam Museum Acquired between 1895 and 1979 (Excluding the McClean Collection)*. Cambridge: Cambridge University Press.

Unraveling the History of Two Fifteenth-Century Spanish Panels

Marya Albrecht,[1] Melissa Daugherty,[2] Saskia van Oudheusden,[3] Lieve d'Hont,[4] Kate Seymour,[5] Michael Rief,[6] Ray Marchant,[7] and Erich Uffelman[8]*

ABSTRACT. This paper presents the results of a technical investigation of two panel paintings from the collection of the Suermondt-Ludwig-Museum, Aachen, formerly attributed to a Burgundian workshop and more recently to an unknown Spanish workshop. The study applied methods of noninvasive analysis that aimed to understand the painting process and the conservation history and to reevaluate the attribution of the panels. Noninvasive analysis was carried out using stereomicroscopy, ultraviolet fluorescence, raking light topographical studies, X-radiography, infrared reflectography, and portable X-ray fluorescence. Microsamples were taken for examination of layers and material analysis using scanning electron microscopy–energy dispersive X-ray spectroscopy and Fourier transform infrared spectroscopy. The results of the technical study informed both the attribution of the works to the Kingdom of Aragon, Catalonia, or the Province of Valencia and decisions for the conservation treatment of the panels. The study also corroborated that the paintings are remnants of a much larger unknown altarpiece. At present, no workshop attribution can be established, but it is clear that the paintings are characteristic of a small group of master artists-craftsmen practicing at the end of the fifteenth century.

[1] Mauritshuis/Atelier Albrecht, Henry Hagalaan 22, 2273 DT Voorburg, The Netherlands.

[2] Restauratie Atelier Daugherty, Paramaribostraat 61, 1058 VH Amsterdam, The Netherlands.

[3] Cultural Heritage Agency of the Netherlands/ Saskia van Oudheusden Schilderijenrestauratie, Sint Jorisstraat 10, 5211 HB 's-Hertogenbosch, The Netherlands.

[4] Hamilton Kerr Institute Cambridge, Hoge Zand 12 2512 EM, The Hague, The Netherlands.

[5] Stichting Restauratie Atelier Limburg, Avenue Ceramique 224, 6221 KX Maastricht, The Netherlands.

[6] Suermondt-Ludwig-Museum, Wilhelmstraße 18, D-52070 Aachen, Germany.

[7] London Studio, The Hamilton Kerr Institute/ Simon Bobak Conservation, 153A Ebury St., London SW1W 9QN, UK.

[8] Department of Chemistry and Biochemistry, Washington and Lee University, 204 W Washington St., Lexington, Virginia 24450, USA.

* Correspondence: M. Albrecht, marya.albrecht @live.nl

Manuscript received 29 October 2015; accepted 22 February 2016.

INTRODUCTION

This paper presents the results of a technical examination of two panel paintings depicting biblical scenes from the lives of St. John the Evangelist and St. John the Baptist: *St. John the Evangelist Drinking from a Poisoned Chalice* and *The Beheading of St. John the Baptist*.[1] The panels belong to the collection of the Suermondt-Ludwig-Museum in Aachen, Germany (Figure 1).[2] The panels came to the conservation studios of the Stichting Restauratie Atelier Limburg (SRAL) in Maastricht, the Netherlands, for research and treatment in 2012.

The panels were donated to the museum in 1914 by Louis (Ludwig) Beissel (1842–1914), an entrepreneur and friend of Robert Frederick Suermondt (1844–1919), son of the founder of the museum.[3] The panels are unattributed, and few pertinent archival documents exist, certainly none preceding accession. Except for the material evidence on the panels themselves, only two brief records dating to the latter part of the twentieth century provide any information on prior conservation treatments.[4]

The panels were attributed on accession to a medieval Burgundian workshop.[5] However, in the catalog to the 2006 exhibition *El Greco, Velázquez, Goya: Five Centuries of Spanish Masterpieces* at the Szépművészeti Múzeum (Museum of Fine Arts), Budapest, attribution of *St. John the Evangelist* to a Burgundian master practicing in France or the

FIGURE 1. Unknown master. (left) *St. John the Evangelist Drinking from the Poisoned Chalice* (GK84a) and (right) *The Beheading of St. John the Baptist and the Feast of Herod* (GK84b). Circa 1475. Photographs before treatment. Image: SRAL.

Low Countries was dismissed on the basis of stylistic analysis.[6] Instead, solely on the basis of connoisseurship, Spanish authorship was proposed.

The present study reexamines the question of the origins of the panels, investigating the original materials and techniques used to create the works, the condition of the panels, and their condition history. A number of methods for technical examination were employed to provide answers to specific questions. Resources were limited in terms of both access to advanced analytical equipment and finances. The results of the undertaken technical

study were contextualized by reviewing the contemporary (Spanish) cultural and historical milieu, as described in original sources and through a literature study. Combining the outcomes of both investigations permitted a more holistic approach wherein the conclusions of each study supported the other.

ICONOGRAPHY

The panels depict the feast of Herod with the decapitation of St. John the Baptist and St. John the Evangelist drinking from a chalice containing a poisoned liquid. These two well-established events in the lives of these saints are described in the New Testament (Matthew 14:1–12[7] and the Acts of John,[8] respectively). Placing the two Suermondt-Ludwig panels in this narrative provided a starting point for the iconographical investigation. The panels show scenes from the end of one saint's life and the key event in the other saint's life. A photograph from 1914 shows both paintings displayed in one frame, which consists of a partitioned rectangular construction with two elaborate, pinnacled canopies.[9] However, juxtaposing the panels in this frame is discordant with iconographical convention. In altarpieces dedicated to more than one saint, medieval protocol would show a similar number of scenes for each saint and odd numbers would prevail. Thus, the presence of one image central to the life of one saint and a martyrdom image of another saint suggests that scenes are missing. Prominent additional scenes from the lives of these saints would include, for St. John the Evangelist, his martyrdom (immersed in a vat of boiling oil), the raising of Drusiana, and the writing of the Book of Revelation on the island of Patmos and, for St. John the Baptist, the annunciation to Zacharias, the saint living in the wilderness, and the baptism of Christ.[10]

Therefore, when considered in an iconographical context, it is likely that the panels once formed part of a larger altarpiece dedicated to the lives of St. John the Baptist and St. John the Evangelist. The panels are thus two surviving fragments of a much larger whole. Both Saints John were very popular in fifteenth-century Spain, and there are many examples of large and small retablos dedicated to them in the region the researchers focused upon: the Kingdom of Aragon, Catalonia, and Valencia.[11, 12] One example is the 1432 Vinaixa (Les Garrigues, Catalonia) *Altarpiece of the Saints John* by the Catalan master Bernat Martorell (died 1452), in which the lives of both saints are depicted in the lateral columns.[13] The story of each saint begins in the upper tier and culminates in the lower corners of the *sotto banco*. The moment of St. John the Evangelist's martyrdom as he is boiled in oil is shown on the left, and the decapitation of St. John the Baptist is depicted on the right. The imagery depicted in Martorell's retablo is similar to that in the two existing Suermondt-Ludwig panels.

The Martorell example is typical of late medieval Spanish altarpieces. Large pictorial altarpieces (retablos) of this period from the northeastern coastal provinces of Spain often consisted of several sections in which a narrative is used to educate the illiterate viewer. The section above the altar is called the *banco*.[14] The slightly wider central portion of the retablo is dedicated to the patron saint of the altarpiece, a triumphant Christ, or the Virgin Mary and is crowned with an *ático* depicting the Calvary. This section is flanked by vertical columns called *calles*, which contain narrative scenes, separated by gilded carved wooden traceries showing moments in the lives of the saints. Three-dimensional canopies often top the altarpiece. These are called *guardapolvo*. Larger altarpieces also contained a *sotto banco* directly above the altar. This typically shows important acts of the saints, such as their martyrdom, flanking a resurrected or entombed Christ. The authors presume that the missing sections of the Suermondt-Ludwig altarpiece would conform to this template. This context was considered when interpreting the results of the technical examination.

STRUCTURAL EXAMINATION OF THE PANEL: SUPPORT CONSTRUCTION AND PREPARATION

The starting point for the technical investigation was an assessment of the condition of the panels, including the wooden supports, and the materials used for ground and paint layers. The original wooden support used for *St. John the Evangelist* (see Figure 2) is badly damaged by wood-boring insects and past treatments; however, close examination provided information about its original construction. The support of *St. John the Baptist* provided no additional information as it was removed entirely when the decorative layers were transferred to a new support in the 1970s.[15] However, traces of the original construction are still evident in the preparatory and paint layers used for both panels. These will be described below in the appropriate context.

Panel Construction

The original panel support of *St. John the Evangelist* now consists of two pinewood boards of ~4 cm thick. The boards differ in width, measuring 41 and 9 cm, respectively, from left to right and are butt joined with one centrally placed wooden dowel.[16] The height of the panel is roughly 104 cm (Figure 3). The top and bottom edges are not parallel to each other. The decorated surface does not extend to any of the edges of the panel, and the undecorated wood differs in extent on each side. The two vertical edges of the decorative surface (at the canvas level, see below) show signs of being cut with a sharp edge, such as a knife. The scene is framed at the top by a typical superimposed carved and gilded wooden tracery attached directly to the wooden support. The three-dimensional architectural framework that is typically situated between the narrative scenes has been removed. There are marks, however, along the border of the decorated surface that indicate these were present on both vertical edges. The architectural elements were intended to be three-dimensional and provide a "space" or "niche" in which the scene is played. The tracery spatially links the depicted scene with the architectural frame, as shown in the reconstructed frame in the 1914 archival

FIGURE 2. Reverse of the original support of *St. John the Evangelist*. Image: SRAL.

photograph and in contemporary exemplars. The reverse of the panel is covered with a number of nonoriginal coatings in white (earlier) and in red (later), providing evidence of past nonoriginal cross-board supporting systems. The bottom edge of the panel is beveled at the reverse to a distance of ~10 cm and is badly damaged. There are (three) plugholes inserted into this undecorated bottom edge, likely to fix the support into a framing element. Saw marks are clearly visible on three edges (top, left, and right) of the panel. Dissected insect tunnels are present along the right-hand edge.[17] The larger board contains the pith of the tree trunk and (badly damaged) sapwood on both edges.

The presence of these typically discarded elements of the timber suggests that the carpenter who constructed the large retablo used the source material, thick unprocessed pinewood boards, economically, as was typical in the construction period proposed.[18] It would be expected that other selected boards would be at least of similar quality and width, and multiples would be used to form the section (Figure 3). The support, now cut to "frame" the pictorial layers and iconographical image, must have been much larger, incorporating perhaps two or three additional lateral scenes of similar size. Although the original support of the second panel, *St. John the Baptist*, is no longer in existence, the preparatory and decorative layers present damage that suggests similar placement of a vertical joint and cross-grain battens, making it likely that boards of identical width were also used to construct this support. Additionally, the presence of the joint in an asymmetrical noncentral position indicates that this support also extended to the side.

This evidence points to the placement of both paintings in a lateral *calle* of a larger altarpiece. The central panel, together with the *ático,* was typically constructed independently of the *calles*. Typically the *calles* consisted of one piece from top to bottom or several smaller "tiers," depending upon the overall size of the retablo. The wood grain of the larger individual elements would run either vertically or horizontally, contingent on the overall size of the retablo, as the board orientation would be efficiently used by the carpenters to achieve the maximum size, using the minimum about of timber.[19] Here in the Suermondt-Ludwig panels, the grain direction runs vertically in both supports, which suggests that these panels come from a vertical *calle*.

The proportions of the images also suggest a vertical orientation and lateral placement of the panels. The image size of both panels is consistent, measuring ~92 × 48 cm, giving a proportional relationship of almost 2:1. The design of Spanish altarpieces was typically based on harmonious proportional symmetry. The central section, based on the golden ratio, would be twice as wide and as high as the individual elements of the *calle*.[20] However, without more sections of the missing retablo, the existing evidence is insufficient to support further conjecture or even to speculate on the size of the entire original retablo; however, it must have been large, measuring meters in height and width. Existing floor-to-ceiling fifteenth-century retablos are still in situ in the Cathedral of Barcelona and other churches in the region. Dismantled contemporary examples from the entire region are on display in the Museum of Fine Arts in Valencia and the National Museum of Catalan Art in Barcelona. These contemporary examples provide a visual context of how the Suermondt-Ludwig panels would have appeared in their original surroundings. An attempt to establish a connection between other dispersed panels based on stylistic grounds has recently been made.[21] Further material-technical study of all proposed sections will be necessary to confirm this hypothesis.

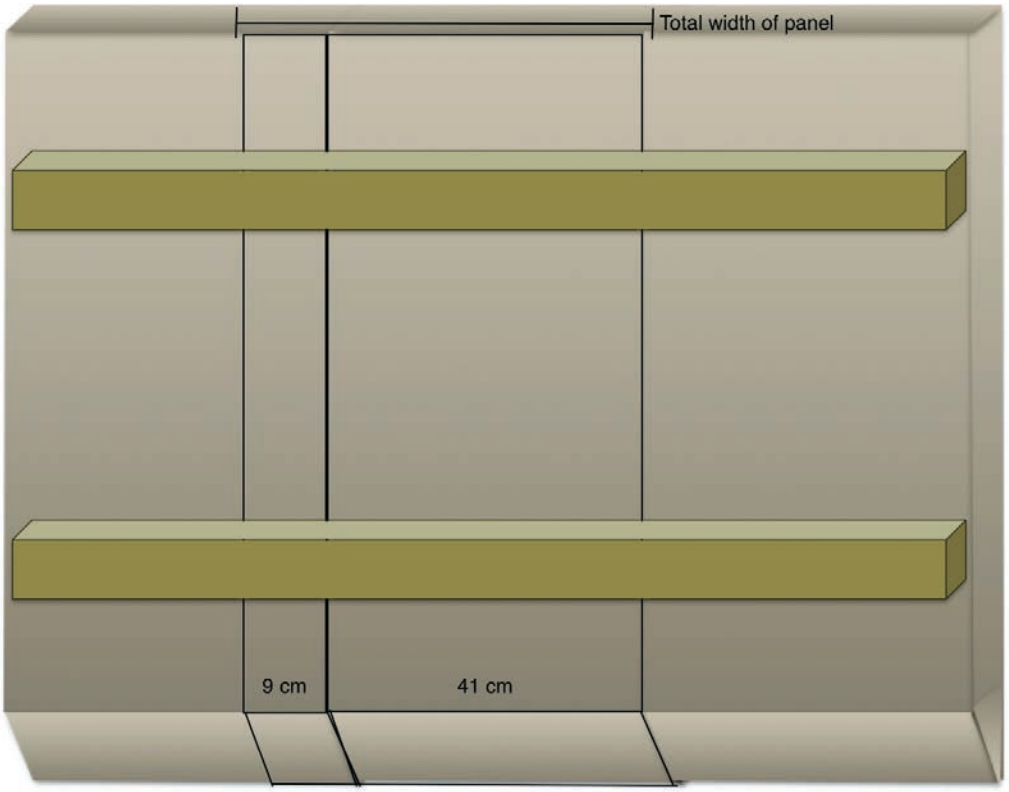

FIGURE 3. Diagram showing the possible construction of the panel support. Three or more boards of even width are joined together using crossbeams. The panel of *St. John the Evangelist* has been cut out of a section like this and consists of two boards 9 and 41 cm in width.

Assembly Technique

Studying the traces of original construction elements provided further evidence for the geographical origin of the panels. Construction and assembly of Spanish retablos were customarily done by specialist craftsmen in a workshop separate from where the painting and gilding were carried out. Typically, fifteenth-century Spanish panels were assembled using locally sourced wood, most commonly pinewood in Castile and Aragon.[22] After seasoning of the timber, the supports were constructed by joining several boards together using wooden or metal dowels, or pegs, to achieve the correct alignment. Glue was used to adhere the boards together. How the joint was constructed is indicative of workshop practice. However, in the case of the Suermondt-Ludwig panel no trace of glue was found in the joint, and only one large, round wooden dowel was placed centrally in the joint. Although the former can be explained as a regional or workshop practice, the latter again points to a resizing of the panel.[23]

Carpenters working in the northwestern region of medieval Spain often used less seasoned wood, combined with cross battens, dowels, and no adhesive in the joints, to construct panel supports, tabernacles, altar fronts, and other large wooden objects. These joints are called *uniones vivas*. Roughly hewn, wide, and thick boards of considerable length were used to make wooden constructions quickly.[24] Boards of these dimensions and thickness would have exerted considerable tension as the moisture content diminished and would have had a tendency to twist or warp on drying. This proclivity to warp would be inhibited by the cross battens, but the boards would shrink in a lateral direction, producing gaps between them. If glue were present during this process, fractures would ensue in the boards themselves. Therefore, the absence of fractures relating to drying (and thus evidence that glue had been used in the joint) and the absence of the remains of any glue in the joint suggest a regional construction technique specific to contemporary provinces of Aragon, Catalonia, and Valencia.

Once the retablo support was constructed, it was left in the chapel or church to await the next step. The application of decorative layers often occurred in situ because of the large scale of these retablos even if the larger altarpieces were constructed in sections. This phase in the decoration process could vary from months to years and also served to illustrate how the material behaved in situ. The first step in the process of painting and gilding

FIGURE 4. Detail of the reverse of *St. John the Evangelist* showing the wooden wedges, *chuletas*, one of which was temporarily taken out of the joint. Image: SRAL.

would have been cleaning the wooden supports and correcting imperfections that occurred during the waiting period.[25] This step involved filling the narrow gaps between the boards that appeared as the wood lost moisture content. Gaps were filled in a number of ways. Again, the manner in which this occurred would likely be indicative of the practice of a particular workshop. Examples have been documented in which strips of parchment cover the gap on the front face and/or on the reverse or the gap is filled with a paste of plant fibers or even rope.[26] Applying caulk in the gap also seems to have been standard practice and is mentioned in ordinances. A typical feature in the construction of Valencian altarpieces seems to have been to fill up these narrow gaps with narrow wedges or fillets of wood called *chuletas*.[27] The joint of the Suermondt-Ludwig panel, *St. John the Evangelist*, is filled with these wedges, although the exteriors are missing, each measuring ~4 cm in length and a~0.4 cm in width (Figure 4). The wedges were usually hammered in from the front, with the narrowest part ending up at the reverse of the panel. The excess would be planed down at the front face prior to the application of the preparatory layers. Thus, this key piece of evidence made it possible to narrow down the origin of the panels to the northeastern coastal provinces of Spain.

Indications of cross-board support also offer further insight into the original construction of the Suermondt-Ludwig retablo. Holes, placed in horizontal lines, are present in both panels, at roughly similar heights. Although these are clearly visible when observing the reverse of the *St. John the Evangelist* panel, X-radiography was required to determine the presence and positions of holes on the transferred panel.[28] Damage in the paint and preparatory layers can clearly be distinguished. These holes result from nails, now removed, used to attach cross battens to the reverse of the panels. The *travesaños* (cross battens) were part of the original construction technique and are now missing. The position of the cross battens may also be indicative of a workshop or regional practice; however, with only traces that bear witness to these, it is not possible to draw further conclusions from this evidence.

Often these battens were fastened, as is the case in these panels, with hand-forged iron nails inserted from the front and clinched at the reverse.[29, 30] Remnants of an iron nail were found in one hole on the *St. John the Evangelist* panel; the others have been forcibly removed. The front of the support would have been planed smooth prior to the attachment of the cross battens, and the heads of the nails would have been countersunk into the flat surface. Larger constructions often had multiple battens distributed over the reverse. In Valencia, one pair of cross battens was typically placed diagonally in the shape of a St. Andrew's cross (X), covering almost the entire height of the retablo. Furthermore, a series of additional horizontal cross battens was added, usually three or four. In Castile, a solely cross-grain, horizontal placement of the battens was more typical. Although the remnants in the original supports in this case point to a horizontal placement, a Valencian origin cannot be excluded on the basis of this factor alone since this one panel probably represents only a small fragment of a larger retablo and cruciform cross battens might have been present in other areas.[31] Cross battens were attached to the reverse not only to reinforce the construction but also to aid in fixing the retablo to the wall of the church or chapel. Again, here, no evidence remains in the Suermondt-Ludwig panels to indicate how this was established.

TECHNICAL INVESTIGATION: NONINVASIVE AND MICROINVASIVE TECHNIQUES

Methods of Analysis

An investigation of the materials and techniques used to paint the panels focused on providing evidence to support or refute the hypothetical origin of the works as concluded from the structural examination described above. The budget for this phase of the investigation was limited. Thus, a select number of noninvasive and microinvasive methods for analysis were used that were available at SRAL or could be achieved under existing collaboration projects.[32] Pigment analysis was carried out using cross-section samples using an analytical microscope and scanning electron microscopy-energy dispersive X-ray spectroscopy (SEM-EDS) linked with backscattered electrons (BSE) to identify the inorganic content. Where necessary, results were strengthened or corroborated using portable X-ray fluorescence (pXRF) in situ analysis.[33] Fourier transform infrared spectroscopy–attenuated total reflectance (FTIR-ATR), in combination with microchemical spot tests, was used to characterize the components of the ground material.[34] Identification of the various binding media present in the decorative layers was not carried out because of the surface contamination by later additions, which included (oleoresinous) varnishes, waxes, and dirt. Analytical

equipment to identify trace amounts of binding media was also not available. However, the use of multiple analytical techniques allowed a thorough examination and corroboration of results, determining the range of pigments used and confirming painting technique. Conclusions were drawn by combining the information gained from all these techniques.

RESULTS AND DISCUSSION

Preparatory Layers: Preliminary Layers and Ground

The layer buildup used was confirmed by examination of the surface using an optical light microscope and samples prepared as paint cross sections. The first phase in preparing the panel for decoration could not be identified in the samples; however, the researchers assume that this step was taken as it was standard practice. First, a layer of *cola fuerte* (hot animal glue) priming was applied to reduce the absorbency of the wood and provide good adherence for the subsequent layers. Often, the extract from boiled cloves of garlic was added to this glue. In this case the treatises call the glue a *gíscola*. The addition of garlic to this size layer was not investigated in the case of the Suermondt-Ludwig panels. Because it was well known that wooden supports "moved" after losing moisture content, the second step involved applying additional support over joints and knots to mitigate cracking in the layers applied subsequently. Materials included hemp fibers and parchment scraps; in the case of the Suermondt-Ludwig panels the entire front face of the panel was covered with a fine (linen) canvas soaked in carpenter's glue. The superimposed elements such as the carved wooden tracery present in both paintings examined here were added at this stage.[35]

The buildup of the subsequent decorative layers in the two panels studied is similar to the standard practice described by Francisco Pacheco (1564–1644).[36, 37] Two ground layers consisting of gypsum bound in animal glue were applied over the entire surface of the panel previously covered by the linen canvas and superimposed tracery. Initial microchemical analysis, using an acidic solution of HCl, of scraping samples from the ground layers indicated that the ground contained gypsum ($CaSO_4$) rather than chalk ($CaCO_3$).[38] The exact chemical nature of these samples was confirmed using FTIR-ATR analysis and by EDS spot analysis on cross sections, described below. The FTIR-ATR spectra also showed peaks that indicated the presence of animal glue as a binder.[39] Analytical techniques that would provide confirmation of the binding media, such as gas chromatography mass spectrometry or high-performance liquid chromatography, were not carried out because of access and financial restrictions. Cross sections examined with a light microscope showed that no pigments were added to the ground. This lack of colorant or pigments was confirmed by the SEM-EDS analysis of a cross section taken from the blue cloak of St. John the Evangelist.[40] This sample, when studied using the SEM-BSE mode, showed the particle morphology of each layer and revealed a remarkable difference in consistency between upper and lower ground layers (Figure 5). This difference of particle morphology confirmed the application of two types of ground, the coarse *yeso grueso* and the finer *yeso mate*.[41] The SEM-EDS analysis provided confirmation of the presence of calcium and sulfur in the ground layer (see below). These materials and techniques are not exclusive to the coastal provinces of the Kingdom of Aragon or even the Iberian Peninsula, but they are typical of this region and period. The use of calcium sulfate as the constituent material for ground layers was commonplace in Valencia and Andalusia.[42, 43]

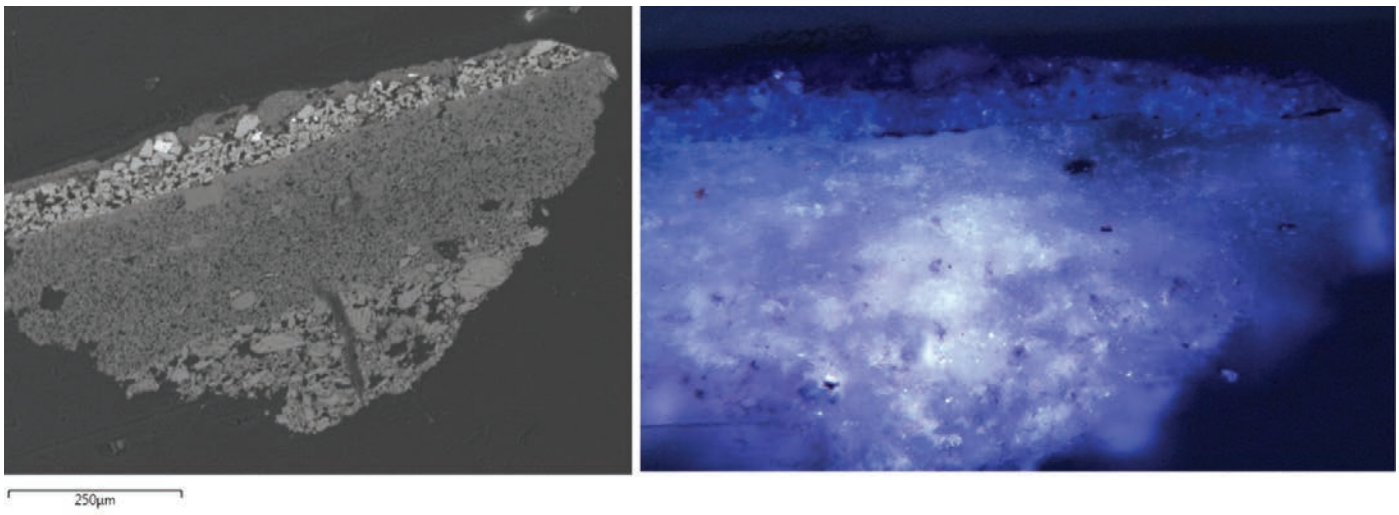

FIGURE 5. A SEM-BSE image showing the layer buildup of the sample taken from the blue cloak of St. John the Evangelist. The ground is applied in two layers whose particle morphologies are clearly different. Image: SRAL.

Underdrawing and Incised Lines

The methods used for the decorative painting process also follow standard practice for this period and region as described in the sources previously referenced. In the case of the Suermondt-Ludwig panels, the composition was laid out on the smooth surface of the ground layer using two different techniques, ink and incision lines. The presence of an underdrawing in both paintings, made by the same hand, was confirmed using both IR digital photography and IR reflectography (IRR).[44] A detailed plan of the composition was applied with brushes and possibly a stiffer (reed) pen using a dilute black medium. Application brushstrokes of varying widths and emphasis made by different drawing materials are visible in losses to the upper decorative layers, especially in the face of King Herod in the *St. John the Baptist* panel, and in the IRR reflectograms. The underdrawing delineates outlines of figures and architectural elements. Hatching was used to indicate shadows or modeling. The underdrawing is carried out meticulously by a skilled, confident draftsman. Although straight edges were used for the lines creating the architecture, the underdrawing of the figures and drapery is freehand. The underdrawing material was present in a number of cross sections removed from both paintings. Microscopic analysis of these cross sections identified a carbon-containing material. No color notations were found in the underdrawing phase as has been seen in other contemporary examples.[45]

The second method used in the initial outlay of the decorative scheme employed incised lines to delineate specific decorative elements. These lines can be seen clearly in raking light and in the X-radiographs. The incisions follow the outlines of areas designated for gilding (application of the bole) and the application of blue color.[46] The incision channels were used to prevent the fluid medium (bole or pigment bound with animal glue) from flowing outside the designated area. Changes (*arrepentimientos*) in the initial decorative design become apparent when studying closely the overlay of paint application with the incision lines. Some areas, for instance, the windows in the background of *St. John the Evangelist*, were neither gilded nor painted blue. These *arrepentimientos* are few.

Again, here, the evidence gathered does not relate to a specific regional location but clearly correlates to artistic practice employed in the fifteenth century that is mentioned in contemporary Spanish sources. A study comparing the underdrawing style to those present in other contemporary panels could prove beneficial for the identification of a specific studio practice.

Dorado (Gilding)

Metal leaf decorations were applied over a red bole layer, and gilded areas are delineated by incision lines. The bole and subsequent gilding were completed before painting. Different metals were used, depending upon the type of material depicted or spiritual significance of the image. Gold was used for the halos of the saints and the armor of one of the soldiers, whereas silver was found in the (steel/iron) helmets and weapons of the guards. The metal leaf application was subsequently painted or glazed to enhance the illusion of the metal depicted. Punch marks are present in the halos, armor, and background decorations—these were applied after the gilding. The metal was identified by elemental analysis using in situ pXRF spot analysis and on relevant cross sections using SEM-EDS. The metal leaf is also clearly visible in the cross sections from selected areas.

As mentioned, most of the gilded areas were decorated using pigment bound in a sticky but fluid (oleoresinous) medium. The handling properties of this semitranslucent glaze are clearly visible at higher magnification. The edges of the colored glaze application are rounded, indicating a fluid application well past the no-flow point. The binding medium has not yet been identified, but its oleoresinous nature was concluded on the basis of visual appearance, UV fluorescence, and solubility characteristics. Again, here, the use of these colored glazes follows standard artistic practice for this period, not only for panel painting but also for the decoration of polychrome sculpture.[47] These sgraffito and *estofado* techniques are applied to the surfaces of the gilded areas after the surrounding areas are painted. The effect creates a rich display of a variety of textiles and surfaces (Figure 6). However, many of these final decorative coatings on the Suermondt-Ludwig panels are reconstructions, although islands of original surface remain. These were deemed to be too sparse to use for sampling. Furthermore, later applications of varnish and other coatings, applied during previous restoration campaigns, have contaminated the original surface. It was felt that the later additions would confuse the interpretation of the results of any analysis carried out and thus did not justify sampling the scarce original material.

Binding Media and Surface Appearance

Materials added over the centuries have altered the surface appearance of the panels. These additions also limited the opportunity for sampling the binding media used for the original paint. However, a study of the surface and the accompanying stylistic analysis was facilitated by conservation treatment that included the removal of varnish and overpaint layers. Observations were compared with standard painting practice as described by Pacheco and contemporaries.

It was common fifteenth-century Spanish painting practice to combine tempera underpaints with oil glazes and pigmented oleoresinous coatings applied to gilded areas. The amalgamation of these surface finishes creates an interplay of painterly effects. The fine brushwork and application technique, especially in the faces, indicates the use of egg tempera, whereas the surface of the gilded draperies appears to have been created by glazing underpaint using an oil binding medium. Combining earlier paint technology with newer developments points toward a Hispano-Flemish influence within the workshop constructing the Suermondt-Ludwig panels.

Contemporaneous treatises suggest a proteinaceous binding medium would have been used for the azurite draperies, as

FIGURE 6. Detailed images showing different *dorado* techniques. Photograph taken during treatment after removal of upper varnish layer. Image: SRAL.

this pigment did not perform well bound in oil, giving these a matte appearance.[48] Unless these matte blue azurite applications were glazed with an oil-bound paint, it is likely that the matte effect was intentional, as was the silky glossy effect of the glazed gilding. Today, it is common knowledge that medieval tempera paintings were left unvarnished. That may have been the case for the surface of the Suermondt-Ludwig panels. The resulting surface would have been full of contrasts: partly brilliant and glittering, partly opaque and matte. The variation in surface effects is now lost because of past interventions and applications, including varnishes and other surface coatings.[49]

The combined use of egg tempera medium and oil glazing points to a Hispano-Flemish link. Strong links existed between the Low Countries and the Iberian Peninsula, sealed with a royal marriage between Philip the Good and Isabella of Portugal in 1430. Northern artists flocked to the south, bringing with them innovations in painting practice from the Low Countries. The binding medium used prior to the introduction of northern European techniques was predominantly egg tempera, utilized in a manner similar to that in the Italian peninsula. However, Flemish influence became dominant in Spain in the fifteenth century, and the introduction of oil-containing paints can be seen as a result of these cultural exchanges brought by artists arriving from the north. The combination of binding media is key to placing the Suermondt-Ludwig panels in a temporal context—late fifteenth century.

Paint Layers

Pigment analysis with pXRF was undertaken at several locations per color. Sites, where appropriate, were selected to correspond to cross-section sampling. Almost all the elements identified in the pXRF spectra can be linked to historic pigments that were used in the fifteenth century in Spain.[50, 51] Table 1 provides an overview of the elements found in the panel of *St. John the Evangelist* and the pigments they are associated with. Anomalies were found relating to elements typical for modern pigments, such as zinc. These clearly related to overpaints, and

TABLE 1. Overview of pXRF measurements carried out on *St. John the Evangelist*. Similar measurements were also found for *St. John the Baptist*. The condition of the original paint layers is much worse than on *St. John the Evangelist* (photograph taken during treatment). Much of this surface has been heavily repainted with paints containing zinc. The measurements here are thus not conclusive.

No.	Color	Elements detected	Pigment used
1	White	Pb, Ca	Lead white
2		Pb, Ca	Lead white
3	Black	Pb, Ca, Sr, Fe, P	Bone black
4	Blue	Cu, Ca, Sr, Fe, Pb	Azurite
5	Blue	Cu, Ca, Ba, S, Zn, Sr, Pb, Al, Si	(Modern) azurite with zinc oxide and barium sulfide fillers
6	Blue	Cu, Zn, Ba, Fe, Ca, Al, Si, S, Pb	(Modern) azurite with zinc oxide and barium sulfide fillers
7	Blue	Cu, Zn, Ba, Fe, Ca, Al, Si, S, Pb	(Modern) azurite with aluminum silicate and barium sulfide fillers
8	Green	Zn, Pb, Fe, Ca, P, Al, Si	(Modern) green paint with copper-based pigment and aluminum silicate extender
9	Red	Pb, Sr, Ca, Al	Red lake pigment
10	Red	Pb, Ca, Sr, Hg	Vermillion
11	Metal leaf	Ag, Pb, Ca, Sr, P	Silver leaf with earth pigments applied on top
12	Metal leaf	Au, Fe, Ca, Sr, Pb	Gold leaf, possibly glazed with ochres
13	Metal leaf	Ag, Pb, Ca, Sr, Fe, Cu	Silver leaf with earth pigments applied on top
14	Gray	Pb, Fe, Ca, Sr, P	Lead white with very little bone black (weak phosphorous peak)
15	Flesh tone	Pb, Hg, Ca, Sr, Fe	Lead white mixed with vermillion
16	Brown	Pb, Fe, Ca, Sr, Zn	Lead white, earth pigments, and zinc-containing overpaint
17	Flesh tone	Pb, Ca, Sr, Hg	Lead white mixed with vermillion
18	Green	Cu, Pb, Ca, Sr, Fe	Copper-based green such as malachite, verdigris, or copper resinate
19	Yellow	Pb, Ca, Sr, Fe,	Lead white and earth pigments
20	Purple	Pb, Ca, Sr	Possibly lake pigment
21	Brown	Pb, Fe, Ca, Sr, Zn	Lead white, earth pigments, and zinc-containing overpaint
22	Yellow	Pb, Fe, Ca, Sr	Ochre
23	Red brocade	Au, Hg, Ca, Sr	Vermillion on gold leaf

this evidence was discarded as this pigment use is anachronistic to the period in question. Other elements that can be linked to the use of modern paints were barium and sulfur (barium sulfide) and aluminum and silica (aluminum silicate), compounds often used as fillers in modern paints. Paints containing these materials clearly covered damaged original material. These areas were identified and confirmed with a close observation of the surface under magnification and in the corresponding cross sections.

The outline, folds, and shadows of blue drapery have been demarcated with incised lines. In the Santa Marina retablo from Mayorga, investigated and treated in the late 1990s at the Hamilton Kerr Institute (HKI), something similar was observed.[52] In this artwork, the blue draperies were also painted using an aqueous, proteinaceous medium. The pigment used was a very coarse azurite, and the color was applied in an even, flat layer. The folds and shading were indicated later, by painting hatching over the first flat layer of blue. Another remarkable find in the retablo treated at HKI was that there was a layer of black paint underneath the azurite layer. This layer gave the drapery a dark blue color when the azurite paint (with a low covering power due to the coarseness of the pigment particles) was applied over it. This technique made it possible to reduce the amount of azurite needed to create a rich blue paint and was thus an economical use of an expensive pigment. The black underpaint covered

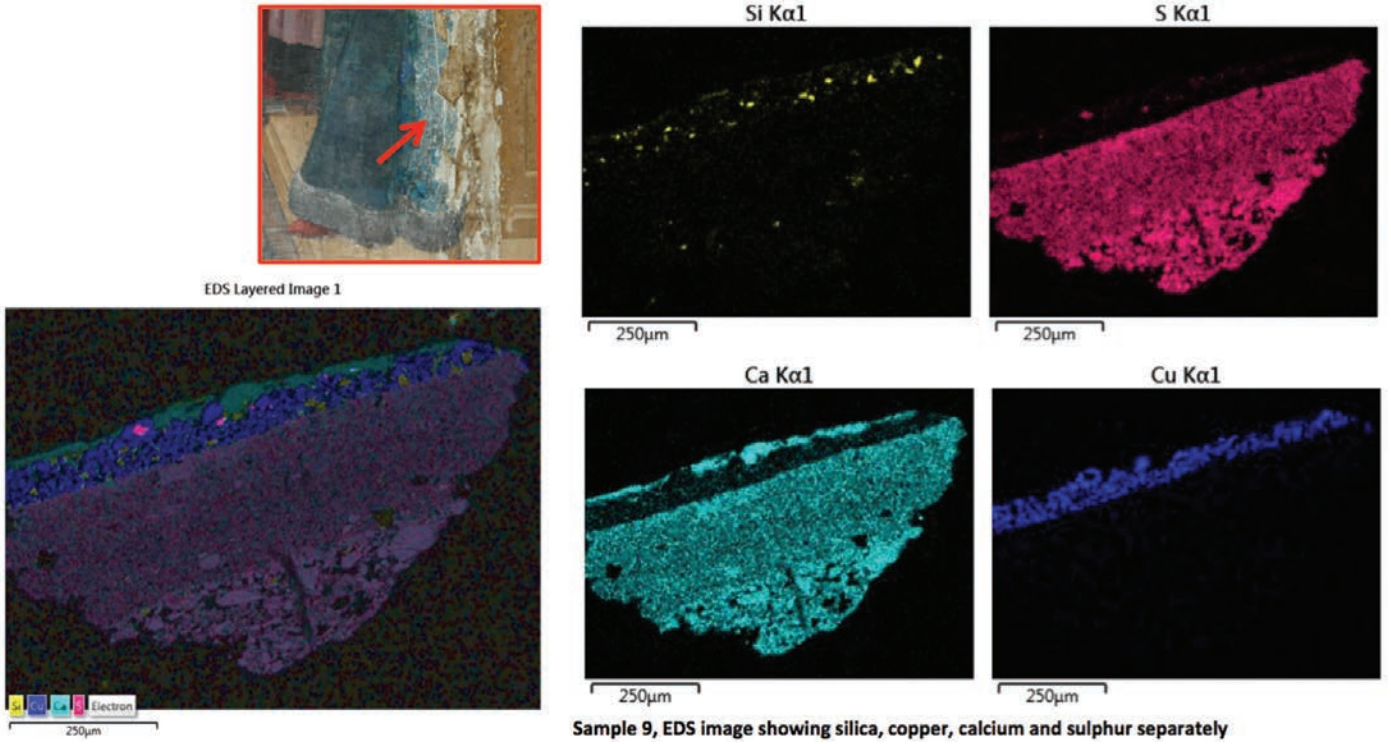

FIGURE 7. Composite showing sample site. Combined false-color SEM-EDS backscatter image with superimposed elemental mapping (left) and SEM-EDS elemental maps for silicon, sulfur, calcium, and copper. Image: SRAL.

the underdrawing, necessitating the use of incised lines to indicate shapes and folds.[53] However, no such black underlayer was found in the Suermondt-Ludwig panels.

A cross section from the blue drapery of the seated priest in the panel of *St. John the Evangelist* shows a ground applied in two layers, a thin black layer (directly related to the ink underdrawing) and an upper layer of coarse azurite. Remnants of additional layers containing ultramarine are present (likely from an early overpaint application). They are difficult to observe in the cross section using the analytical microscope but can be clearly observed on the surface.

To gain further understanding of the abovementioned cross-section sample, elemental mapping and false-color imaging were carried out using SEM-EDS (Figure 7). Results showed the presence of the element copper in the undermost paint layer, imaged in blue. The element silicon (colored yellow) is present in the same layer as the copper. Silicon is indicative of silica and/or quartz; both minerals are associated with natural copper mineral compounds such as azurite and lapis lazuli. However, the morphology of the particles containing copper indicates azurite ($2CuCO{\cdot}Cu(OH)_2$) as opposed to ultramarine ($(Na,Ca)_8(AlSiO_4)_6(S,SO_4,Cl)_{1-2}$). Elemental calcium is mapped in light blue in this cross section, whereas the element sulfur is mapped in pink. Both elements are present in both ground layers. This result is suggestive of the use of calcium sulfate ($CaSO_4$), confirming the findings of the previously mentioned microchemical tests. Calcium is also mapped above the azurite-containing layer, which may be associated with the filling material applied to repair damage adjacent to the sampled area. The absence of sulfur in the mapping of this layer suggests the use of calcium carbonate for the fill, which was confirmed by a microchemical analysis of the filling material. The remnants of an ultramarine glaze (possibly in an oil medium) applied over the azurite layer were visible using light microscopy of the area where the sample was taken. However, elements associated with this mineral pigment, such as sodium and aluminum were not mapped in this cross section. It is possible that the sample was removed from an area that did not contain this pigment. No intermediate varnish layers were observed in this sample. The authors hypothesize that the blue drapery was painted using a copper-containing pigment, probably azurite, that was later covered with a paint containing ultramarine. Different binding media were used for the different layers.

The cross-section analysis did not help the authors in determining the originality of the upper, now damaged, ultramarine oil paint. This paint has been applied over all of the blue draperies covering the azurite paint on both panels. The binding medium of this layer is unconfirmed, but it has the appearance under magnification of an oil paint as opposed to tempera.[54] One

hypothesis is that the original matte blue azurite paint was glazed with an oil-bound ultramarine paint as part of the original painting technique. However, this would negate the supposition that the overall surface appearance was intended to use contrasting textures of matte and gloss. The opposing, perhaps more likely, argument would be that the ultramarine layers were an early restoration applied to cover damage to the water-sensitive proteinous bound azurite layers. These layers are severely damaged and only partially preserved. Interpretations of the layer buildup and originality of materials are complicated as the ultramarine-containing layers are also severely damaged. Furthermore, many of these areas were also covered by additional overpaints before the current conservation treatment. Undercutting resulting from later cleaning campaigns of all layers has also been identified. The authors are aware that additional research is necessary to confirm the hypotheses proposed here but feel that it is appropriate to discuss this tentative technological finding with a wider audience.

STYLISTIC ATTRIBUTION

It is not the intention of this paper to provide an attribution of the Suermondt-Ludwig panels to a particular artist or workshop. However, there is a close stylistic resemblance between the Suermondt-Ludwig paintings and that of Jaume Huguet (1412–1492), who was recorded as working in Barcelona. The similarities are striking, in particular in relation to the different hats worn by the figures. Also working in similar style was Juan Reixach (active 1431–1482), active in Valencia and Catalonia. Further comparisons could be made with other works in the 2006 exhibition catalog *Greco, Velázquez, Goya* from the Museum of Fine Arts Budapest that could substantiate the hypothesis here.[55, 56]

CONCLUSION

Contemporary Spanish painting techniques are clearly described elsewhere, most famously by Pacheco, and although writing around 150 years later, many of the practices he describes can be applied to fifteenth-century artworks. Medieval artists-craftsmen were working in a controlled mass production market; each phase of the construction and decoration process was carefully regulated by ordinances, statutes, and contracts. The Suermondt-Ludwig panels conform to these norms.

The systematic study of the artworks, using both nondestructive and microdestructive analytical techniques, provided conservators with sufficient information to facilitate the decision-making process for treatment options. The poor condition of the works was evident on initial examination, which initiated the material-technical study. The investigation aimed to provide information to inform strategies for treatment that are reported elsewhere.[57] Evidence of the materials and construction techniques used in the panels has highlighted the rarity of similar artworks in German collections and has thus placed a greater emphasis on the current investigation and conservation treatment. Preserving the original materials without altering their nature has become paramount. The insect-damaged support will be maintained and stabilized. Future aesthetic treatment will involve the removal of nonoriginal paint layers, identified in this study.

This study provided considerable information about the original materials used to construct the panels and their physical history. Combining the hard facts resulting from the material-technical study with more theoretical discussions regarding the iconography and fifteenth-century Spanish painting practice specific to Catalonia or the province of Valencia allowed the authors to contextualize the results of both studies. Uniting conjectural hypotheses with factual data has enabled conclusions to be drawn. It can be concluded that both panels were once part of a much larger whole. The presence of wooden *chuletas* means that a more specific origin can be pinpointed. This construction technique is typical of Catalonia or Valencia, regions that were part of the Crown of Aragon in the fifteenth century. Establishing a clearer provenance for the panels would perhaps reveal the location of other sections of the altarpiece and even the exact church for which this retablo was constructed. This investigation still needs to be carried out. However, taking into consideration local historical events, it is possible that the panels were removed from their original setting in the church and dismembered for sale on the art market prior to or in the early nineteenth century. That would explain the change in dimension and partially elucidate their current condition. It should be stressed that there is, to date, no archival evidence supporting this assumption.

Acknowledgments

The authors thank Luis Bertomeu Contreras (Universitat Politècnica de València), Luuk Hoogstede (SRAL), Arnold Truyen (SRAL), and Paul van Kan (consultant SRAL and Van Kan & Willems). The authors give special thanks to Britta New (The National Gallery, London) for her strategizing and advice with regard to decision making for treatment. Additional thanks go to all experts who have contributed in expanding the understanding of Spanish painting techniques of the authors, in particular Guillermo Torres Llopis (Esconres, Huesca, Aragon) and Ana Calvo (Universidad Complutense de Madrid).

The conservation team has included Marya Albrecht, Melissa Daugherty, Lieve d'Hont, Femke van Gurp, Jazzy de Groot, and Diana de Man—all participating in various stages during their yearlong residency at SRAL, under the supervision of Kate Seymour, as part of their postgraduate training at the University of Amsterdam. Ray Marchant (HKI) has consulted on the structural treatment of the St. John the Evangelist panel, and his knowledge of fifteenth-century Spanish construction techniques was key to interpreting the complexities of this project. The project is ongoing at the time of press. The project has been facilitated by Michael Rief and the team at the Suermondt-Ludwig-Museum in Aachen. The National Science Foundation

is gratefully acknowledged for two grants for nondestructive instrumentation at Washington and Lee University (W&L; NSF MRI CHE-0959625 and CHE-1337481). The Lenfest Summer Grant program at W&L is gratefully acknowledged for funding Erich S. Uffelman's travels to The Netherlands with the pXRF. The team is most grateful for these contributions.

NOTES

1. This paper was originally presented at the International Council of Museums–Committee for Conservation interim meeting "The Non-Invasive Analysis of Painted Surfaces: Scientific Impact and Conservation Practice" held at the Lunder Conservation Center in February 2014 under the title "CSI Aachen: Unraveling the History of Two Fifteenth Century Spanish Panels Using Forensic Methodologies."
2. The two panel paintings are registered under the titles *St. John the Evangelist Drinking from the Poisoned Chalice* (GK84a) and *The Beheading of St. John the Baptist and the Feast of Herod* (GK84b), Suermondt-Ludwig-Museum, Aachen. Throughout this paper they will be referred to as *St. John the Evangelist* and *St. John the Baptist*.
3. Little information has come to light regarding Louis (Ludwig) Beissel. His father, also called Ludwig, was a founding member of the Firmierung Draht-Fabrik-Compagnie in Aachen, along with Johann Friedrich Thyssen (1804–1877). Thyssen is an ancestor of Baron Hans Heinrich Thyssen-Bornemisza, who bequeathed his art collection to the Spanish government in 1993; the collection is now on display at the Thyssen-Bornemisza Museum in Madrid. This link needs further investigation.
4. Archival documentation folders associated with GK84a+b of the Suermondt-Ludwig-Museum, Aachen, Germany, accessed June 2012.
5. The 1914 documentation folder from the Suermondt-Ludwig-Museum Archives states, "zwei altarflügel in einen Rahmen. Szenes aus dem Leben der beiden Johannes. Burgundisch (?) XV. Jahrhundert."
6. E. Nyerges, *El Greco, Velázquez, Goya: Five Centuries of Spanish Masterpieces* (Budapest: Museum of Fine Arts, 2006), 42–43.
7. Matthew 14:1–12, consulted at Biblia.com, http://biblia.com/bible/esv/Mt%2014.1-12 (accessed 2 June 2015).
8. The Acts of John is an early second-century Christian collection of Johannine narratives and traditions, long known in fragmentary form. The traditional author was said to be Leucius Charinus, a companion and disciple of John. M. R. Jones, trans., *The Apocryphal New Testament* (Oxford: Clarendon Press, 1924), sections 94–96, http://gnosis.org/library/actjohn.htm (accessed 2 June 2015).
9. The frame is no longer in existence and is probably a nineteenth-century faithful stylistic copy. The intact condition of the pinnacles is discordant with the age, some 500 years, and the damaged condition of the panel paintings.
10. J. Hall, *Dictionary of Subjects and Symbols in Art*, rev. ed. (New York: Harper & Row, 1979).
11. From the beginning of the twelfth until the early eighteenth century, the Crown of Aragon was a thalassocratic Mediterranean state, consisting of the modern-day Spanish provinces of Aragon, Catalonia, and Valencia, as well as territories held in Italy and Greece, including the Balearic Islands, Corsica, Sardinia, and Sicily. Zaragoza was the political center in the fourteenth and fifteenth centuries. Cultural exchange and influence from these territories dominated artistic development in Spain prior to the later medieval Flemish connections.
12. J. Berg-Sobre, "Two Fifteenth-Century Aragonese Retables and Painters of the Calatayud Group," *Metropolitan Museum Journal* 15 (1980): 91–118.
13. Bernat Martorell, *Retaule dels sants Joans*, inventory no. 064045-CJT, Museu Nacional d'Art de Catalunya, http://www.museunacional.cat/ca/colleccio/retaule-dels-sants-joans/bernat-martorell/064045-cjt (accessed 2 June 15); Bernat Martorell, *St. John the Evangelist Drinking from the Poisoned Chalice*, Musee Rolin, Autun, France. Dated ca. 1435–1445. Dimensions 344 × 261.5 × 10.5 cm.
14. The terminology of Spanish altarpieces is described in F. Descamps, *Methodology for the Conservation of Polychromed Wooden Altarpieces* (Seville, Spain: Consejería de Cultura, 2002), and the resulting online resource, Getty Conservation Institute and Instituto Andaluz del Patrimonio Histórico, "Altarpieces: Illustrated Basic Terminology," http://www.gciresources.org/retablo/index2.php?id=2 (accessed 2 June 2015). The central section of the altarpiece (retablo) is termed *banco*, the lateral columns are called *calles*, the upper portion is called ático, and the lower section is termed *sotto banco*. The definitions for other terms are given in the text.
15. There is no documentation relating to this treatment. The only existing reference is an article from the local newspaper *Aachener Nachrichten* (no. 293, 23 December 1978), a photocopy of which is kept in the documentation folder for GK84a+b in the Suermondt-Ludwig-Museum SLM archives. The article describes the work of restorer Helmut Weirich (now deceased); the photograph accompanying the article shows the restorer retouching the panel of *St. John the Evangelist*. By comparing this photograph with the current state of the panel it became clear that the panel was already transferred to a new support at that time. Helmut Weirich most probably carried out the treatment shortly before the photograph was taken.
16. Wood species analysis was carried out by Peter Klein (then University of Hamburg, Germany) in 1995 and was identified as pinewood. Archival documentation folder for GK84a+b of the Suermondt-Ludwig-Museum, accessed June 2012.
17. Wood samples, frass, and insect remains were examined by Jos Creemers from SHR (http://www.SHR.nl). He identified the presence of two xylophagous species of insects: a beetle deriving from the Anobiidae family, given the diameter of the galleries and the shape of the fecal pellets, and a beetle from the *Nicobium* genus, based on the presence of a cocoon.
18. Construction of churches and similar edifices was rampant in fifteenth-century Spain. As the Moors were pushed out of the country, the reassertion of the Christian faith led to the mass construction of new churches and decorations for these interiors.
19. A. Calvo Manuel, "Retablos Medievales del Norte Valencia," in *Retablos: Técnicas, materiales y procedimientos* (Madrid: Grupo Español IIC, 2004), 6, http://ge-iic.com/files/RetablosValencia/anacalvoRetablosnortevalenciano.pdf (accessed 2 June 2015).
20. Guilermo Torres Llopis, Escuela Superior de Conservación y Restauración de Bienes Bulturales de Aragon, personal communication with the authors, 16 February 2014.
21. C. Fava Monllau, "El Calvario cuatrocentista catalán del Museo de Bellas Artes de Bilbao," *Boletín del Museo de Bellas Artes de Bilbao* 8 (2014): 47–83.
22. R. Bruquetas Galan, "Los gremios, las ordenanzas, los obradores," in *Retablos: Técnicas, materiales y procedimientos* (Madrid: Grupo Español IIC, 2004), 7, http://ge-iic.com/files/RetablosValencia/R_Bruquetas.pdf (accessed 2 June 2015).
23. At least two dowels are required along the length of a joint to achieve correct alignment.
24. A. Nualart i Torroja, M. Mascarella Vilageliu, and I. Bautista Morenilla, "Frontals d'altar medievals: Marques d'eines a la fusta i tecnologia de construcció del support," In *La Recerca en Conservació des de la Visió del Conservador-Restaurador II. Setmana de la Ciència, Barcelona, 20 i 21 de novembre de 2014* (Barcelona: Secció de Conservació-Restauració, Facultat de Belles Arts, Universitat de Barcelona, 2014), 29–36, http://diposit.ub.edu/dspace/bitstream/2445/60507/1/3RCRII_Nualart%20et%20al.pdf (accessed 2 June 2015).
25. A. Carrassón López de Letona, "Construcción y ensamblaje de los retablos en madera," in *Retablos: Técnicas, materiales y procedimientos* (Valencia: Grupo Español IIC, 2004), 3–4, http://www.ge-iic.com/files/RetablosValencia/AnaC_Construccion_ensamblaje.pdf (accessed February 2015).
26. Bruquetas Galan, "Los gremios, las ordenanzas, los obradores," 8; S. Hodge, M. Spring, and R. Marchant, "The Santa Marina Retable from Mayorga, Attributed to the Master of Palanquinos, c.1490's," *Hamilton Kerr Institute Bulletin* 3 (2000): 7–40.
27. Calvo Manuel, "Retablos medievales del Norte Valencia," 6–7.
28. X-radiographies were carried out by Arnold Truyen (SRAL) using ERESCO 160 MFR2 industrial X-ray equipment. The range of the tube is 200 kV, but energies over 99.99 kV are blocked. Settings used to acquire optimum contrast are available on request.
29. V. Vivancos Ramón, "Aspectos técnicos y estructurales de la retablística Valenciana," in *Retablos: Técnicas, materiales y procedimientos* (Madrid: Grupo Español IIC, 2004), 6, http://ge-iic.com/files/RetablosValencia/V_Vivancos_ATyEstructurales.pdf (accessed 2 June 2015).
30. An undecorated fifteenth-century panel support using the described technique can be found in the Conservation Studio of the Museo Nacional del Prado, Madrid.
31. Calvo Manuel, "Retablos medievales del Norte Valencia," 6.
32. A fruitful collaboration for technical analysis exists between SRAL (Maastricht, Netherlands) and Washington and Lee University (Lexington, Virginia, USA). This ongoing collaboration brings coauthor Erich S. Uffelman, along

with a range of portable analytical equipment, to The Netherlands on an almost yearly basis. Details of the techniques and equipment used under the auspices of this collaboration are given throughout the rest of this paper.

33. All measurements were carried out by Erich S. Uffelman (Washington and Lee University) using a Bruker Tracer III-SD, Rh anode X-ray tube at 40 kV and 11 μA, 20 Torr interior pressure inside the instrument, 180 s spectrum accumulation time, 2,048 channels. The spot size analyzed consisted of a 4 × 6 mm oval. The front of the instrument was carefully placed parallel to the picture plane. Great care was used to position the instrument safely (using a tripod with a manually controlled, geared instrument mount) within approximately 1 mm of the painting surface. The element assignments were made using the Bruker Artax 7.2.1.1 software, but comprehensive tables of XRF lines are readily available in common sources.
34. Cross-section samples were embedded in Polypol (polyester resin). The embedded samples were sanded wet and dry polished using Micromesh. The samples were carbon coated for SEM-EDX analysis. Scraping samples were used for FTIR-ATR and microchemical tests.
35. Vivancos Ramón, "Aspectos técnicos," 7.
36. F. Pacheco, *Arte de la pintura* (1641), 2nd ed. (Madrid: Manuel Galiano, 1866), https://books.google.nl/books?id=IitPAAAAYAAJ&printsec=frontcover&hl=nl&source=gbs_ge_summary_r&cad=0#v=onepage&q&f=false (accessed 2 June 2015).
37. Z. Véliz, "Pacheco's Comments on Painting in Oil," *Studies in Conservation* 27, no. 2 (1982): 49–57.
38. A microchemical spot test was carried out to determine whether chalk ($CaCO_3$) or gypsum ($CaSO_4$) was used in the ground and for the filling previously inserted along the open joint. A scraping sample was taken of both ground and filling. When a carbonate (CO_3^{2-}) comes into contact with an acid, CO_2 is released, which can be seen under magnification as small bubbles appearing in the liquid. This technique is not precise but provided a first step in the analytical protocol used to investigate these panels. Both scrapings were mounted on a glass microscope slide, and a few drops of HCl were added while the slides were examined under the microscope. The sample from the ground did not react, which indicates the presence of gypsum. The sample from the fillings did show the formation of bubbles, indicating the presence of a carbonate. The exact nature of the gypsum mineral and its related water content were not confirmed with this method, nor was the exact nature of the carbonate. The white fill is radio-opaque and thus is likely to contain a lead white pigment component.
39. The FTIR analysis was carried out on a Bio-Rad FTS-6000 equipped with a Pike Gladi ATR setup. Spectra were controlled by WinIR Pro software and compared to standards in the Infrared Users Group (IRUG) database. The spectrum of the analyzed sample shows stretching vibration bands at 1,200–1,050 and 680–600 cm^{-1}. The analysis was carried out by Paul van Kan (a consultant for SRAL).
40. The SEM-EDS analysis was carried out on a JEOL JSM-5800 equipped with an Oxford INCA X-act EDS system with a Solid State Data (SSD) detector controlled by Oxford AZTEC software. The analysis was carried out by Paul van Kan (a consultant for SRAL).
41. Véliz, "Pacheco's Comments on Painting in Oil," 50.
42. Z. Véliz, "Wooden Panels and Their Preparation for Painting from the Middle Ages to the Seventeenth Century in Spain," in *The Structural Conservation of Panel Paintings: Proceedings of the Symposium at the J. Paul Getty Museum 1995* (Los Angeles: J. Paul Getty Museum, 1995), 136–148.
43. A. Rodríguez-López, N. Khandekar, G. Gates, and R. Newman, "Materials and Techniques of a Spanish Renaissance Panel Painting," *Studies in Conservation* 52 (2007): 81–100.
44. Infrared digital imaging was performed with an XNite Lumix LX5 UV+VIS+IR camera obtained from MaxMax that had the IR blocking filter removed. A filter adapter was attached to the front of the camera, and images were taken using either a filter that blocked ultraviolet-visible (UV-VIS) and IR electromagnetic radiation up to 715 nm or a filter that blocked UV-VIS and IR electromagnetic radiation up to 1,000 nm. Both filters were also obtained from MaxMax. Given that the camera's silicon-based detector cuts off around 1,050 nm, the imaging windows were thus about 715–1,050 nm or 1,000–1,050 nm. The camera was part of the equipment brought to SRAL by Erich S. Uffelman (Washington and Lee University, Virginia, USA). The IRR reflectography was carried out with the Hamamatsu Vidicon camera present at SRAL. Vidicon has a PbS photoconductive detector and has a resolution of 768 × 576 pixels for Pal or 640 × 480 pixels for NTSC. Vidicon cameras are sensitive from ~800 to 2,200 nm, with a maximum (optimal) response at around 1,900 nm. The UV-VIS radiation was eliminated using appropriate filters. Images were snatched from the live feed and stitched together by hand using Adobe Photoshop software.
45. C. Barry, "Observations on Workshop Practice in 15th Century Castile: The Altarpiece from the Cathedral at Ciudad Rodrigo by Fernando Gallego and His Workshop," in *Studying Old Master Paintings: Technology and Practice,* ed. M. Spring (London: Archetype, 2011), 295–301.
46. The incised lines would prevent the more fluid bole and blue paint from bleeding into adjacent areas that would receive other colors, thus preventing any chromatic interference with any overlying color.
47. It should be remarked that the artisans painting the panel paintings were the same as those applying the decorative layers on polychrome sculptures in this historical period.
48. The binding medium of the blue paint applications has yet to be confirmed by any instrumental analysis but follows standard medieval practice discussed. All blue areas on the panels have suffered severe damage in past cleaning campaigns, underlining the use of a proteinaceous binding medium. The majority of these areas are heavily overpainted, which makes the interpretation of original layers difficult.
49. The authors are aware that this hypothesis is unconfirmed through analysis. This type of connoisseurship, when taken in context with other evidence, can provide reliable conclusions that are far more than assumptions.
50. A. Križnar, V. Munoz, F. De la Paz, M. Respaldiza, and M. Vega, "Portable XRF Study of Pigments Applied in Juan Hispalense's 15th Century Panel Painting," *X-ray Spectrometry* 40 (2011): 96–100, http://dx.doi.org/10.1002/xrs.1314.
51. Rodríguez-López et al., "Materials and Techniques," 81–100.
52. Hodge et al., "The Santa Marina Retable," 7–40.
53. M. Spring, "The Technique and Materials of the Blue Draperies," *Hamilton Kerr Institute Bulletin* 3 (2000): 24–25.
54. The saturation of the layer and the handling of the paint indicate oil rather than a protein layer.
55. Nyerges, *El Greco, Velázquez, Goya,* 42–43.
56. Fava Monllau, "El Calvario cuatrocentista," 47–83.
57. K. Seymour, M. Albrecht, M. Daugherty, S. Van Oudheusden, L. d'Hont, M. Rief, and R. Marchant, "The Thin End of the Wedge: Stabilisation of a Damaged Panel Painting Support Using Tapered Wooden Sections," In *ICOM-CC 17th Triennial Conference Preprints, Melbourne, 15–19 September 2014,* ed. J. Bridgland (Paris: International Council of Museums Art, 2014), article 1312.

BIBLIOGRAPHY

Barry, C. "Observations on Workshop Practice in 15th Century Castile: The Altarpiece from the Cathedral at Ciudad Rodrigo by Fernando Gallego and His Workshop." In *Studying Old Master Paintings: Technology and Practice*, ed. M. Spring, pp. 295–301. London: Archetype, 2011.

Berg-Sobre, J. "Two Fifteenth-Century Aragonese Retables and Painters of the Calatayud Group." *Metropolitan Museum Journal* 15 (1980): 91–118.

Bruquetas Galan, R. "Los gremios, las ordenanzas, los obradores." In *Retablos: Técnicas, materiales y procedimientos*. Madrid: Grupo Español IIC, 2004. http://ge-iic.com/files/RetablosValencia/R_Bruquetas.pdf (accessed 2 June 2015).

Calvo Manuel, A. "Retablos Medievales del Norte Valencia." In *Retablos: Técnicas, materiales y procedimientos*. Madrid: Grupo Español IIC, 2004. http://ge-iic.com/files/RetablosValencia/anacalvoRetablosnortevalenciano.pdf (accessed 2 June 2015).

Carrassón López de Letona, A. "Construcción y ensamblaje de los retablos en madera." In *Retablos: Técnicas, materiales y procedimientos*. Valencia: Grupo Español IIC, 2004. http://www.ge-iic.com/files/RetablosValencia/AnaC_Construccion_ensamblaje.pdf (accessed 2 June 2015).

Descamps, F. *Methodology for the Conservation of Polychromed Wooden Altarpieces*. Seville, Spain: Consejería de Cultura, 2002.

Fava Monllau, C. "El Calvario cuatrocentista catalán del Museo de Bellas Artes de Bilbao." *Boletín del Museo de Bellas Artes de Bilbao* 8 (2014): 47–83.

Getty Conservation Institute and Instituto Andaluz del Patrimonio Histórico. "Altarpieces: Illustrated Basic Terminology." http://www.gciresources.org/retablo/index2.php?id=2 (accessed 2 June 2015).

Hall, J. *Dictionary of Subjects and Symbols in Art*. Rev. ed. New York: Harper & Row, 1979.

Hodge, S., M. Spring, and R. Marchant. "The Santa Marina Retable from Mayorga, Attributed to the Master of Palanquinos, c.1490's." *Hamilton Kerr Institute Bulletin* 3 (2000): 7–40.

Jones, M. R., trans. *The Apocryphal New Testament*. Oxford: Clarendon Press, 1924. http://gnosis.org/library/actjohn.htm (accessed 2 June 2015).

Križnar, A., V. Munoz, F. De la Paz, M. Respaldiza, and M. Vega. "Portable XRF Study of Pigments Applied in Juan Hispalense's 15th Century Panel Painting." *X-ray Spectrometry* 40 (2011): 96–100. http://dx.doi.org/10.1002/xrs.1314.

Nualart i Torroja, A., M. Mascarella Vilageliu, and I. Bautista Morenilla. "Frontals d'altar medievals: Marques d'eines a la fusta i tecnologia de construcció del support." In *La Recerca en Conservació des de la Visió del Conservador-Restaurador II. Setmana de la Ciència, Barcelona, 20 i 21 de novembre de 2014*, pp. 29–36. Barcelona: Secció de Conservació-Restauració, Facultat de Belles Arts, Universitat de Barcelona, 2014. http://diposit.ub.edu/dspace/bitstream/2445/60507/1/3RCRII_Nualart%20et%20al.pdf (accessed 2 June 2015).

Nyerges, E. *Greco, Velázquez, Goya: Five Centuries of Spanish Masterpieces*. Budapest: Museum of Fine Arts, 2006.

Pacheco, F. *Arte de la pintura*. 1641. 2nd ed. Madrid: Manuel Galiano, 1866. https://books.google.nl/books?id=IitPAAAAYAAJ&printsec=frontcover&hl=nl&source=gbs_ge_summary_r&cad=0#v=onepage&q&f=false (accessed 2 June 2015).

Rodríguez-López, A., N. Khandekar, G. Gates, and R. Newman. "Materials and Techniques of a Spanish Renaissance Panel Painting." *Studies in Conservation* 52 (2007): 81–100. http://dx.doi.org/10.1179/sic.2007.52.2.81.

Seymour, K., M. Albrecht, M. Daugherty, S. Van Oudheusden, L. d'Hont, M. Rief, and R. Marchant. "The Thin End of the Wedge: Stabilisation of a Damaged Panel Painting Support Using Tapered Wooden Sections." In *ICOM-CC 17th Triennial Conference Preprints, Melbourne, 15–19 September 2014*, ed. J. Bridgland, article 1312. Paris: International Council of Museums Art, 2014.

Spring, M. "The Technique and Materials of the Blue Draperies." *Hamilton Kerr Institute Bulletin* 3 (2000): 24–25.

Suermondt-Ludwig-Museum. Archival documentation folder pertaining to GK84a+b Suermondt-Ludwig-Museum, Aachen, Germany.

Véliz, Z. "Pacheco's Comments on Painting in Oil." *Studies in Conservation* 27, no. 2 (1982): 49–57.

———. "Wooden Panels and Their Preparation for Painting from the Middle Ages to the Seventeenth Century in Spain." In *The Structural Conservation of Panel Paintings: Proceedings of the Symposium at the J. Paul Getty Museum 1995*, ed. K. Dardes and A. Rothe, pp. 136–148. Los Angeles: J. Paul Getty Museum, 1995.

Vivancos Ramón, V. "Aspectos técnicos y estructurales de la retablística Valenciana." In *Retablos: Técnicas, materiales y procedimientos*. Madrid: Grupo Español IIC, 2004. http://ge-iic.com/files/RetablosValencia/V_Vivancos_ATyEstructurales.pdf (accessed 2 June 2015).

Portable X-ray Fluorescence and Infrared Fluorescence Imaging Studies of Cadmium Yellow Alteration in Paintings by Edvard Munch and Henri Matisse in Oslo, Copenhagen, and San Francisco

Jennifer Mass,[1] Erich Uffelman,[2] Barbara Buckley,[3] Inger Grimstad,[4] Anna Vila,[5] John Delaney,[7] Jorgen Wadum,[5] Victoria Andrews,[2] Lindsay Burns,[2] Samuel Florescu,[2] and Alyssa Hull[6]*

[1] University of Delaware, Department of Chemistry and Biochemistry, 5105 Kennett Pike, Winterthur, Delaware 19735, USA.

[2] Department of Chemistry, Science Addition A427, Washington and Lee University, Lexington, Virginia 24450, USA.

[3] Barnes Foundation, 2025 Benjamin Franklin Parkway, Philadelphia, Pennsylvania 19130, USA.

[4] Munch Museum, Tøyengata 53, 0578 Oslo, Norway.

[5] CATS and Statens Museum for Kunst, Sølvgade 48-50, 1307, Copenhagen, Denmark.

[6] Department of Chemistry and Biochemistry University of Delaware, Newark, Delaware 19716, USA.

[7] Conservation Division, National Gallery of Art, 2000B South Club Drive, Landover, Maryland 20785, USA.

* Correspondence: J. Mass, jmass@udel.edu

Manuscript received 21 February 2015; accepted 22 February 2016.

ABSTRACT. The identification of altered cadmium yellow paints in early modernist works is critical to their stabilization and to the long-term preservation of the paintings in which they occur. The identification of incipient photoalteration of these pigments, before there is visual evidence of their chemical degradation, is of particular concern. The alteration of these pigments causes chalking, flaking, fading, and darkening of the yellow paints, leading to irreversible changes in the physical and chemical structure of the paint layer and dramatically altering the appearance of the work. Standoff methods for the identification of this phenomenon are desired to rapidly and efficiently survey the condition of the pigment across an entire work and also to minimize invasive and destructive analyses wherever possible. Such methods are a particular need for collections with large holdings of Impressionist and early modernist works from the 1880s to the 1920s, for which these cadmium yellow alterations are particularly problematic and a rapid surveying method for the collection is needed. To address this challenge, four standoff methods were attempted (both alone and in concert): ultraviolet-induced visible fluorescence, ultraviolet-induced infrared fluorescence, multispectral imaging, and X-ray fluorescence. Questions addressed included the following: Is the imaging method being tested comprehensive? Is it efficient at surveying an entire painting? Does it reveal the state of preservation of the pigment? Does it reliably discriminate among intact versus altered cadmium yellow pigments? To answer these questions, the methods were tested on Henri Matisse's *Le Bonheur de vivre* (1905–1906, the Barnes Foundation, Philadelphia) and oil sketches for this work in the San Francisco Museum of Modern Art and the Statens Museum for Kunst, Copenhagen. They were also tested on Edvard Munch's *The Scream* (ca. 1910?, Munch Museum, Oslo). It was found that ultraviolet-induced visible fluorescence has the best ability to discriminate between altered and unaltered cadmium yellow paints (even before alteration is visible to the unaided eye), whereas multispectral imaging allows for the most efficient and comprehensive localization of the cadmium pigments in a work.

INTRODUCTION

Cadmium Yellow Alteration in Works of the Early Modernists

The synthetic inorganic pigments of the early modernist paintings from the turn of the twentieth century are undergoing chemical and physical degradation phenomena ranging from fading and color shifts to flaking and spalling (the breaking off of larger fragments). These phenomena have been particularly notable in the yellow pigments popular in this time period, with discoloration of zinc yellow ($K_2O{\cdot}4ZnCrO_4{\cdot}3H_2O$), chrome yellow ($PbCrO_4$), and cadmium yellow (CdS) paints being observed in the works of Georges Seurat (zinc yellow and cadmium yellow), Vincent van Gogh (chrome yellow and cadmium yellow), and Pablo Picasso (cadmium yellow; Casadio et al., 2011; Leone et al., 2005; Van der Snickt et al., 2012). Since the late nineteenth century cadmium yellow paints (in particular, the paler shades) have been observed to undergo disfiguring fading and discoloration (Church, 1890), and the phenomenon has been noted in the art conservation literature since 1986 (Fiedler and Bayard, 1986). At the time, this deterioration was attributed to either adulterants in the paint formulation or to the smaller particle sizes (and hence higher surface areas) of the paler shades. In conjunction with the fading and discoloration that one often observes, an irreversible degradation of the oil paint binder results in a chalky, crumbling, flaking, and, ultimately, spalling paint layer—this degradation proceeds from the exterior to the interior of the paint layer (Mass et al., 2013a). Leone et al. (2005) performed the first systematic study of the alteration of cadmium yellow pigments, including the characterization of 12 works from 1887 to 1923, encompassing those by Vincent van Gogh, Pablo Picasso, Georges Seurat, and Fernand Leger. Notably, amorphous or nanocrystalline CdS was identified in 7 of the 12 paintings (based upon the absence of X-ray diffraction patterns). Potential CdS photodegradation products identified in the paintings included cadmium carbonate ($CdCO_3$), cadmium oxide hydroxide, cadmium carbonate oxide, and cadmium sulfate ($CdSO_4$). It is important to note that $CdCO_3$ and $CdSO_4$ are both reagents for the wet process syntheses of CdS, so their identification alone does not constitute conclusive proof of photooxidation (Mass et al., 2013b; Plahter and Topalova-Casadiego, 2011). However, the identification of these phases at the paint's surface as discolored degradation crusts can suggest that they were produced by a photooxidation mechanism. Artificial aging experiments on period cadmium yellow paints were also carried out by Leone et al. (2005) at 45% relative humidity (RH) and 85% RH. The samples aged under high-RH conditions were noted to have a matte or etched appearance, and time-of-flight secondary ion mass spectrometry analysis revealed a lower concentration of fatty acids at the degraded surface, suggesting that the paint binding medium is being attacked during the degradation process (Leone et al., 2005). This led the researchers to propose a mechanism in which amorphous or nanocrystalline (and thus reactive) CdS pigment was photooxidized to produce CdO, $CdSO_4$, and SO_2 gas. Van der Snickt et al. (2009) have observed the formation of $CdSO_4{\cdot}2H_2O$ and $[NH_4]2Cd(SO_4)_2$ on the surface of faded cadmium yellow paints in the works of James Ensor (1860–1949). μ-X-ray absorption near edge spectroscopy was used in the Ensor study to demonstrate that the sulfur in the CdS was oxidized to SO_4^{2-}, and it was hypothesized that the soluble cadmium sulfate was reprecipitating at the surface of the painting to form the observed white globules on the yellow paint layer. The ammonium phase was ascribed to a potential reaction with a previous cleaning treatment. This study also notes that a characteristic ultraviolet-induced orange fluorescence for the CdS is observed only in regions of the painting not blocked by the frame, so the authors associate this fluorescence with the photodegradation process, noting that the CdS yellow blocked by the frame appears brown under UV illumination.

Cadmium Yellow Alteration in Works by Henri Matisse and Edvard Munch

Le Bonheur de vivre (Figure 1) is considered to be one of the icons of modern art, responsible for cementing Matisse's reputation as an innovative Fauvist and breaking with traditional academic modes of representation. Several regions of alteration in the yellow paints have been identified in *Le Bonheur de vivre,* most notably the yellow foliage in the upper left corner of the work, the yellow foreground beneath the central reclining figures, and the yellow fruits in the tree in the upper right quadrant. A 1990 conservation assessment of the work first reported that regions of the yellow paint had turned light brown and that other areas of the yellow paint had "disintegrated into a fragile powder" (Samet, 1990). The problem is most pronounced in the medium impasto brushstrokes of yellow paint under the central reclining figures.

Matisse painted three other works related to this final version (*Le Bonheur de vivre*, 1905–1906, The Barnes Foundation BF719): *Sketch for Le Bonheur de vivre* (The Barnes Foundation, BF35), *Esquisse pour "Le Bonheur de vivre"* (San Francisco Museum of Modern Art [SFMOMA], 91.160), and *Landscape near Collioure: Study for The Joy of Life* (Statens Museum fur Kunst [SMK], Copenhagen). An understanding of the changes that the Barnes painting has undergone can be obtained by visually comparing the Barnes work to these related works, especially the oil sketch for *Le Bonheur de vivre* at the San Francisco Museum of Modern Art. The San Francisco painting has warm yellow foliage in its upper left corner and a pure bright yellow foreground under the central reclining figures. The ocher-hued foliage of the upper left corner of the Barnes painting was therefore likely a warm yellow color originally, and the mottled ivory hue of the paint beneath the central reclining figures would have originally

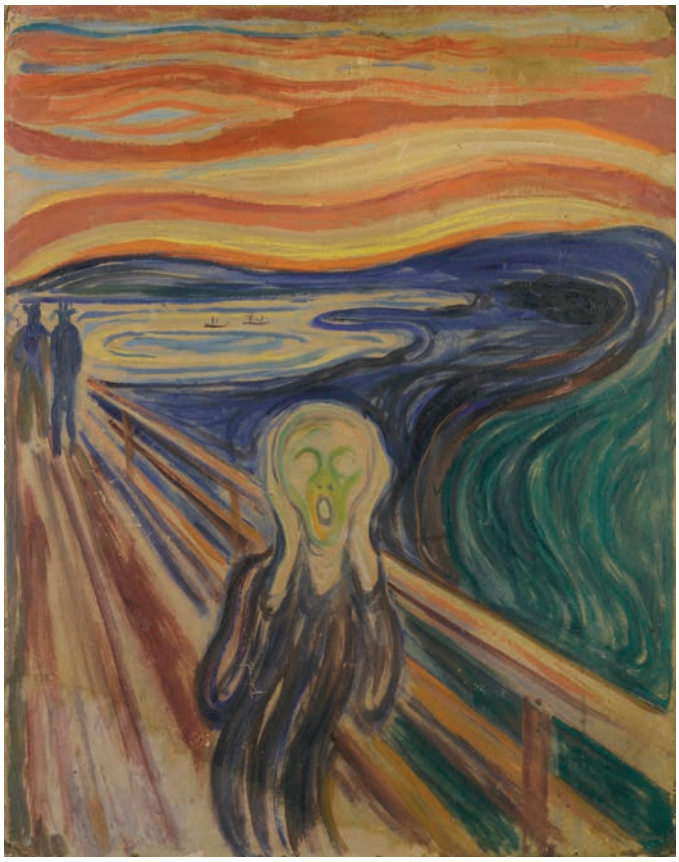

FIGURE 1. Paintings examined for this study. Henri Matisse's (top right) *Le Bonheur de vivre*, also called *The Joy of Life* (between October 1905 and March 1906, 69½ × 94¾ inches [176.5 × 240.7 cm], The Barnes Foundation, Philadelphia, BF719), (bottom right) *Esquisse pour "Le Bonheur de vivre"* (*The Joy of Life*, 40.64 × 54.61 cm, 1905–1906, SFMOMA, San Francisco, 91.160), and (bottom left) *Landscape near Collioure: Study for The Joy of Life*, 1905, Statens Museum for Kunst, Copenhagen, © 2016 Succession H. Matisse/Artists Rights Society (ARS), New York. (top left) Edvard Munch: *The Scream* 1910(?), Munch Museum, Oslo; Photo © Munch Museum.

been bright yellow. The dirty white alteration crust of the fruits in the tree in the upper right, by this same logic, hides a warm yellow color.

A great deal of elemental, molecular, and microscopic characterization of these altered regions has been carried out by our group, and the fading has been attributed to photooxidation (Mass et al., 2013a, 2013b). In particular, the off-white alteration crusts are composed predominately of the white cadmium compounds cadmium carbonate ($CdCO_3$) and cadmium sulfate ($CdSO_4 \cdot nH_2O$; Mass et al., 2013a). Other alteration products observed on the painting include lead sulfate ($PbSO_4$) and cadmium oxalate (CdC_2O_4).

The SFMOMA and SMK paintings appear to be unaltered by photodegradation, with the pigment hues unchanged from Matisse's original intent. This lack of change may result from Matisse having used different paints for his work in Collioure versus Paris. However, from a preservation perspective, it is critical to know if Matisse did, in fact, use cadmium yellow paints in these closely related paintings and, if so, what the current condition of these paints is.

The cadmium yellow pigments on Edvard Munch's painting *The Scream* (ca. 1910?, the Munch Museum) are recently reported to have altered to an off-white color (Plahter and Topalova-Casadiego, 2011) and have also been studied by a number of elemental and molecular analysis methods (Plahter and Topalova-Casadiego, 2011). The authors concluded that $CdCO_3$ was not a photooxidation product in this case, but rather a synthesis-starting reagent from the indirect wet process synthesis of CdS. Cadmium carbonate is documented to have been used as a starting material for both the dry process and indirect wet process syntheses of CdS yellow paints (Fiedler and Bayard, 1986; Plahter and Topalova-Casadiego, 2011). In considering the presence of $CdCO_3$ in *The Scream*, it is important to note that $CdCO_3$ and cadmium oxalate were also thought to have been intentionally added to CdS paints as paint extenders during this period (Fiedler and Bayard, 1986). However, this seems like an unlikely process in light of the high costs of these materials.

Edvard Munch's *The Scream* overall exhibits alteration phenomena similar to those of Matisse's *Le Bonheur de vivre*. A cadmium yellow brushstroke in the sky in the upper right has faded to an ivory color, as well as two brushstrokes in the central figure's neck. Spalling has also been observed in yellow brushstrokes in the water to the right of the bridge.

Ultraviolet-Induced Luminescence of Cadmium Yellow Pigments

The characteristic ultraviolet-induced visible fluorescence of CdS (cadmium yellow pigment) was first investigated in the context of artists' pigments by de la Rie (1982). Fluorescence occurs when a compound absorbs electromagnetic radiation at a short wavelength, promoting electrons to higher electronic energy levels. These electrons then undergo a nonradiative relaxation before returning to the ground electronic state, emitting light at a longer wavelength (lower energy) than was absorbed as they do so. Since fluorescence results from the electronic structure of the molecule, it occurs at a fixed wavelength (or wavelengths) regardless of the exact wavelengths of the incident radiation. This phenomenon rarely occurs for inorganic artists' pigments and is observed primarily for zinc white and cadmium-based pigments (e.g., cadmium yellows, oranges, and reds; de la Rie, 1982). Cadmium pigments fluoresce in the red/orange through the infrared as a result of this semiconductor pigment having trace impurities in its crystal lattice. These impurities are generally below the minimum detection limits of minor element analysis techniques used at museums such as X-ray fluorescence (XRF) or scanning electron microscopy energy-dispersive X-ray spectroscopy (SEM-EDS; de la Rie, 1982). The fluorescence maximum for cadmium yellow shifts slightly depending on the pigment's exact composition (cadmium red has a fluorescence maximum at a longer wavelength than cadmium orange, which fluoresces at a longer wavelength than cadmium yellow); however, the CdS maximum occurs at ~750 nm, tailing off into the near infrared at ~850 nm. By contrast, cadmium orange, $CdS_{1-x}Se_x$, has a fluorescence maximum at ~800 nm.

It has been suggested that pure CdS will not fluoresce, nor will CdS yellow from all manufacturers. However, it must also be noted that cadmium yellow paints fluoresce orange not only because of the presence of trace impurities causing deep trap states (intermediate energy levels between the semiconductor's valence band and conduction band) but also because of the formation of deep trap states that can be a result of surface or internal crystal defects in the pigment particles (Thoury et al., 2011). As a result, the orange fluorescence can, in theory, be observed in pure cadmium yellow paints. In addition, as noted above there have been observations suggesting that although altered cadmium yellow paints have a bright orange fluorescence, unaltered cadmium yellow paints can appear brown under ultraviolet illumination (Van der Snickt et al., 2009).

EXPERIMENTAL METHOD

Locating cadmium-based pigments in the paintings was first attempted using longwave ultraviolet illumination to excite the characteristic visible fluorescence (brilliant reddish orange) for the cadmium paints. To block the visible fluorescence interference from zinc white and purpurin, this same illumination was used again, but this time the fluorescence was collected with a camera filter that blocked fluorescence below 715 nm. See Table 1 for a summary of the imaging and analysis techniques employed for each painting in this study.

Ultraviolet-Induced Visible Fluorescence

At the Munch Museum and at the Statens Museum for Kunst a shortwave handheld UV source (a Reskolux UV 365) was kept approximately 2 to 4 inches (5.08 to 10.16 cm) away from the surface of the paintings to excite the fluorescence of the zinc- and cadmium-containing pigments present, as well as any fluorescent organic pigments such as purpurin. The visible component of this fluorescence, as well as the visible fluorescence of all other paintings studied, was collected using a commercial handheld digital camera. The Munch Museum also supplied UV-induced visible fluorescence images of *The Scream* (ca. 1910?). These images were collected using a PHILIPS TLD 36w/08, Holland longwave UV source. This is a low-pressure mercury vapor discharge lamp that has an inner envelope coated with a fluorescent powder. The dark blue glass envelope transmits UV-A radiation but only minimum visible radiation. The Barnes Foundation

TABLE 1. Analysis techniques employed for the paintings studied.

Technique	The Barnes Foundation, *Le Bonheur de Vivre* (1905–1906)	Statens Museum for Kunst, *Landscape near Collioure. Study for 'The Joy of Life'* (1905)	SFMOMA, *Esquisse pour "Le Bonheur de vivre"* (1905–1906)	Munch Museum, *The Scream* (ca. 1910?)
UV-induced visible fluorescence	X	X	X	X
UV-induced IR fluorescence	X	X	X	X
Portable X-ray fluorescence	X	X	X	X
Multispectral imaging	X			

ultraviolet illumination source used for the *Le Bonheur de vivre* images was a Spectroline lamp with a Spectronics BLE-220B Wavelength 365nm (longwave) 4W bulb.

Ultraviolet-Induced Infrared Fluorescence

A Panasonic Lumix DMC-LX5 camera modified by removing the IR-blocking filter was used to image *The Scream*, *Le Bonheur de vivre*, *Esquisse pour "Le Bonheur de vivre,"* and *Landscape near Collioure* by employing a visible-light-blocking filter that transmitted IR above 715 nm. Ultraviolet illumination (described above) was then used to excite both visible and infrared fluorescence of the paintings' pigments. The 715-nm filter blocks the visible light fluorescence of competing pigments such as zinc oxide white, allowing only the infrared fluorescence of pigments such as cadmium yellow to be detected.

Portable XRF and XRF

A Bruker Tracer III-SD was used to collect portable XRF (pXRF) spectra (rhodium anode, 40 keV, 11 μA, no filter, operating under vacuum [10–35 torr]). Spectra were collected (180-s acquisition time) and analyzed using Bruker Artax software. This spectrometer was employed for the Barnes Foundation and Munch Museum paintings. A Bruker Artax XRF with a Rh tube and a He flow was used at the SMK's Centre for Art Technological Studies and Conservation laboratory for elemental analysis of the paints in *Landscape near Collioure*. Analysis times of 200 s were used along with a tube voltage of 50 kV and a tube current of 600 or 700 μA.

Multispectral Imaging

Multispectral imaging for visualization of cadmium red, yellow, and orange pigments in *Le Bonheur de vivre* was performed using blue-green excitation (380–520 nm) obtained with two filtered slide projectors set up at ~45° from the normal at 12 feet (3.66 m) from the painting. Multispectral images were collected with a silicon CCD camera with 50-nm-spaced filters (40 nm full width half maximum). False-color emission maps were generated for the emissions at 650, 700, and 850 nm in order to maximize the signals generated from CdS and $CdS_{(1-x)}Se_x$ pigments.

RESULTS

Cadmium Yellow Localization Using Ultraviolet-Induced Visible Fluorescence Imaging, Ultraviolet-Induced Infrared Fluorescence Imaging, Multispectral Imaging, and X-ray Fluorescence

Locating the cadmium-based pigments in *Le Bonheur de vivre*, the two oil sketches related to this work, and *The Scream* (ca. 1910?) was the first step in ultimately imaging the cadmium yellow degradation in these works. Ultraviolet-induced infrared fluorescence imaging allowed us to view the paintings' fluorescence in a region where impure cadmium yellow paints and cadmium sulfoselenides are known to have a characteristic emission (de la Rie, 1982; Thoury et al., 2011). As mentioned above, this method has the advantage of blocking out the fluorescence from surrounding pigments and fillers such as zinc oxide white that can interfere with imaging the orange fluorescence of the cadmium yellow. The results of these measurements were then compared to pXRF measurements that were used to map the presence of cadmium-based pigments in the paintings. In the case of *Le Bonheur de vivre* (1905–1906, The Barnes Foundation) multispectral imaging was also carried out to assess the efficacy and comprehensive nature of the imaging and analysis methods listed above.

Ultraviolet-induced visible fluorescence of *Le Bonheur de vivre* (1905–1906, The Barnes Foundation) did not provide comprehensive imaging of the cadmium yellow pigments (Figure 2). For example, when this technique is used on the region beneath the central reclining figures (which is painted entirely with cadmium yellow according to pXRF analysis), it only reveals the

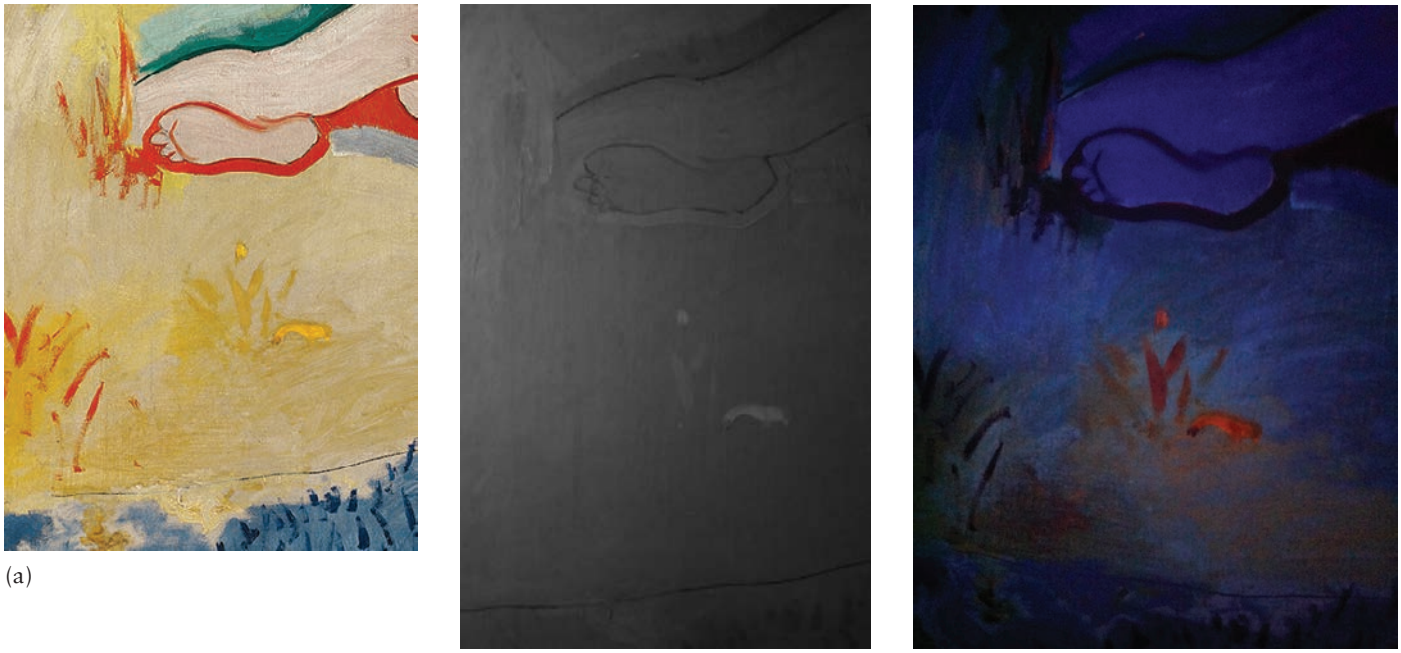

(a) (b) (c)

FIGURE 2. Detail from *Le Bonheur de vivre* (Barnes Foundation 719, © 2016 Succession H. Matisse/Artists Rights Society (ARS), New York): (a) visible light image, (b) ultraviolet-induced infrared fluorescence, and (c) ultraviolet-induced visible fluorescence of the region under central reclining figures.

locations where the cadmium carbonate–rich alteration crust has flaked away to reveal the intact CdS yellow paint underneath. So it is observed that only the (relatively) unaltered cadmium yellow paint is imaged by this method. Ultraviolet-induced infrared fluorescence (Figure 2b) produced similar results, imaging the visibly intact cadmium yellow paint but not revealing the location of the altered cadmium yellow. The altered, photooxidized cadmium yellow paints in *Le Bonheur de vivre* thus do not all have the characteristic orange fluorescence expected for cadmium yellow, likely because of major changes in the electronic structure of the pigment as it alters and photooxidizes and the possible quenching of the fluorescence by photooxidation by-products. The ivory background surrounding the thickly painted blades of grass in the image below is altered cadmium yellow, but it has minimal orange fluorescence (see Figure 2c) and no fluorescence in the infrared. This result is consistent with the thick cadmium carbonate and sulfate alteration crusts known to be present in this region (according to cross-section photomicroscopy), fully removing the CdS semiconductor structure that is required for the characteristic fluorescence.

Even with this limitation, ultraviolet-induced visible fluorescence proved more efficient in this large-scale work for identifying cadmium-based pigments than pXRF analysis. See, for example, the yellow centers of the daisies between the pink figures at the lower right of the painting (Figure 1). These flowers, which were found to have a bright orange fluorescence when studied by ultraviolet-induced visible luminescence, had been overlooked as possibly containing cadmium yellow during the first round of pXRF analysis. As a result, pXRF and ultraviolet-induced visible fluorescence proved to be valuable and complementary, but neither of them was comprehensive on its own.

The off-white region behind the green embracing figures was identified as cadmium yellow using pXRF, but only a small area of this discolored region fluoresces, suggesting that the alteration crust in this small area is thin enough to allow the fluorescence from the intact cadmium yellow to be revealed (see Figure 3). Intact cadmium yellow may not be extant in the regions that do not fluoresce, or it may be too deeply buried beneath alteration crusts. In either case, this phenomenon highlights a need for further molecular analysis in this region of the painting. Note that in this area of the painting there are regions of altered CdS that have a brownish fluorescence color, thought to be indicative of intact cadmium yellow paints. This reveals that a dark appearance of cadmium yellow paint (visible fluorescence) in the ultraviolet does not always indicate a lack of photodegradation.

Multispectral imaging results of *Le Bonheur de vivre* demonstrate that this is the most comprehensive method for imaging cadmium pigments in easel paintings. The results of this technique (Figure 4), using blue-green excitation (380–520 nm), reveal Matisse's extensive use of cadmium-based yellow, orange, and possibly red pigments in *Le Bonheur de vivre*. These false-color emission maps suggest again that the electronic structure

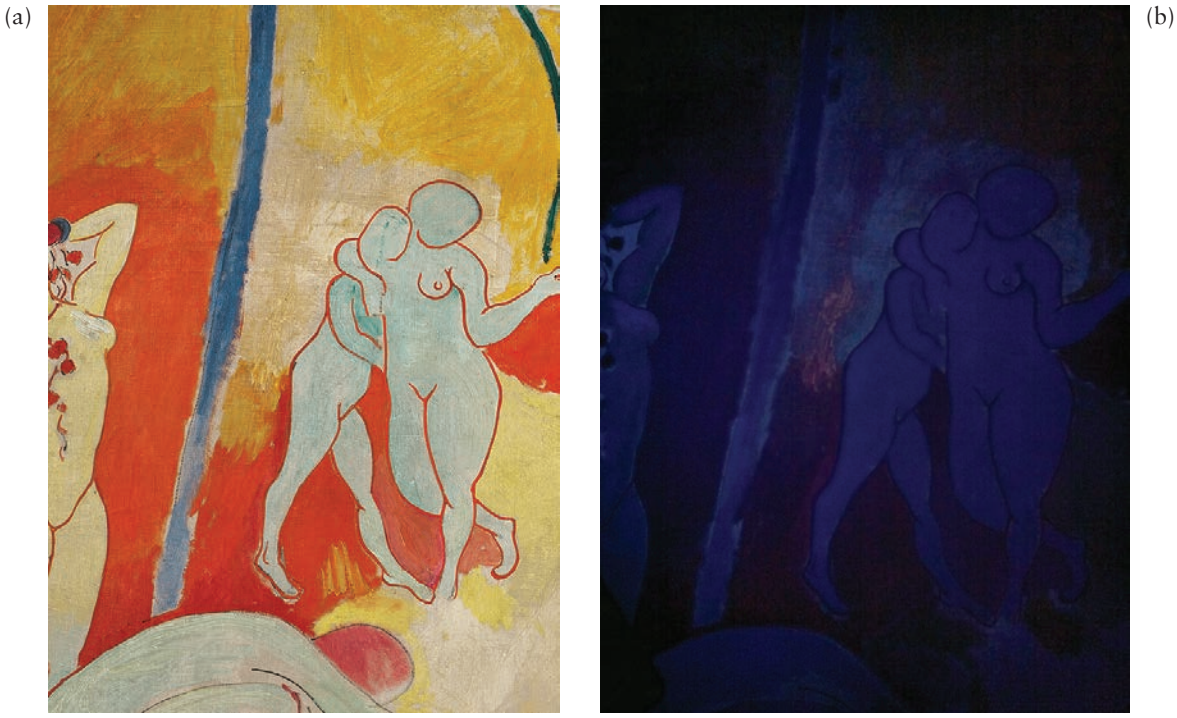

FIGURE 3. Altered cadmium yellow region behind embracing green figures viewed in (a) visible illumination and (b) long-wave ultraviolet illumination, *Le Bonheur de vivre* (The Barnes Foundation, 1905–1906, © 2016 Succession H. Matisse/Artists Rights Society (ARS), New York).

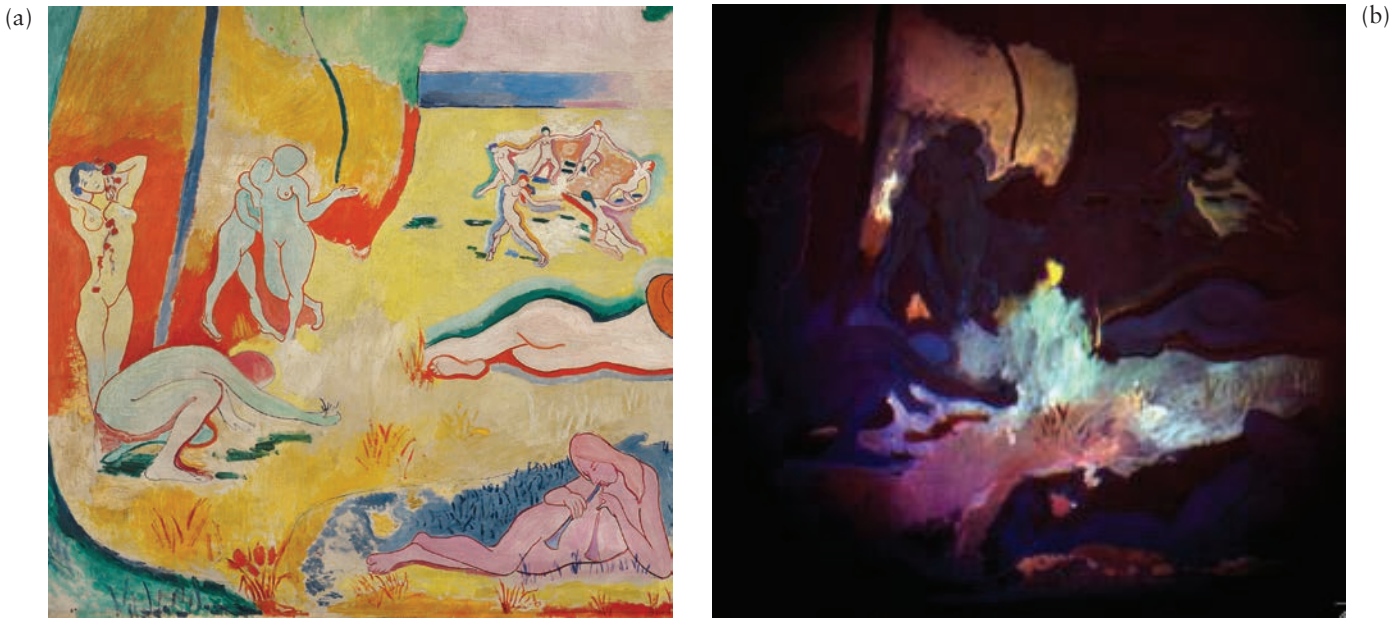

FIGURE 4. (a) Visible light image and (b) false-color emission map of *Le Bonheur de vivre* (Barnes Foundation 719, © 2016 Succession H. Matisse/Artists Rights Society (ARS), New York), excited at 380–520 nm (blue-green excitation) and emission/fluorescence recorded for 650, 700, and 850 nm.

of the CdS changes with its state of preservation. Furthermore, the fluorescence of other cadmium-containing compounds such as cadmium sulfate cannot be excluded. Images (Figure 4) starkly reveal the variable nature of the fluorescence of altered cadmium yellow paint. Consider, for example, the lightened cadmium yellow to the left of the embracing green figures. In visible light the cadmium yellow has faded to a single dirty and mottled ivory hue, but the fluorescence phenomena of the species in this region vary dramatically. This inhomogeneity of fluorescence reflects variability in the alteration products formed on the painting's surface and of the electronic structure of the remaining CdS. Alteration products identified thus far on *Le Bonheur de vivre* include cadmium sulfate, cadmium carbonate, and cadmium oxalate (Mass et al., 2013a, 2013b). Another cadmium-containing species identified in the cadmium yellow paint in *Le Bonheur de vivre*, cadmium chloride, is thought to be present as a residual starting reagent (Mass et al., 2013a). Note that multispectral imaging, although comprehensive, is not selective. We cannot now use the false-color images to discern which cadmium paints are intact versus the altered paints; instead, the image reveals all of the cadmium-containing paints present.

The relatively intact cadmium yellow paint above the embracing green figures demonstrates more fluorescence overall than the faded region behind these figures and a more uniform fluorescence broken up mostly by patterns of brushstrokes. This result appears to confirm the hypothesis that intact CdS is required at the paint layer's surface for the characteristic fluorescence to be observed. Also note in Figure 4 that the characteristic fluorescence of the cadmium yellow paint is visible through overlying paint layers when blue-green excitation is used. This phenomenon is observed in the outline of the central reclining figure, which, although it appears to be three shades of green in the visible light image, is revealed to have a cadmium yellow brushstroke above the woman's calf that is now covered by green paint. The region beneath and to the left of the central reclining figures has faded to a dirty ivory hue. Unlike the region behind the embracing green figures, however, this area strongly fluoresces. Importantly, the observation of substantial fluorescence throughout this region, not observed for ultraviolet excitation, suggests that the use of a longer (blue-green) excitation wavelength penetrates deeper into the painting and excites fluorescence from the buried intact cadmium yellow.

In sum, although both pXRF and multispectral imaging are totally nondestructive, the efficiency and comprehensive nature of the latter are demonstrated here.

Unaided visible light examination for the Statens Museum for Kunst's *Landscape Near Collioure* (1905) has revealed none of the visible evidence of photoalteration observable in the Philadelphia painting (see Figure 1). Like the other colors in Matisse's palette for this work, the yellow paints are vibrant and glossy, with no evidence of fading, discoloration, chalking, or other alteration phenomena. This difference may be due to Matisse having used a cadmium yellow deep mixed with a zinc white base in order to achieve a cadmium yellow light (this mixture is visible upon close examination of the Copenhagen painting), rather than using a cadmium yellow light that is formulated with cadmium-based filler (or residual starting reagent) such as cadmium carbonate or oxalate, as cadmium yellow lights are known to be less stable. This change in practice may simply be a result of Matisse having different paint suppliers in the south of France versus Paris. Although cadmium yellow was not used in exactly the same locations as it was used in the Barnes Foundation work, XRF was used to confirm that it was employed in the foliage in the upper left, in the fruits in the trees at the upper right, and in the foreground where the central reclining figures appear in the Barnes work.

As might be predicted from the visual examination of the piece, longwave ultraviolet examination revealed no evidence of the orange fluorescence associated with altered cadmium yellow (data not shown). It is notable that although cadmium sulfide particles with surface defects can fluoresce even in the absence of photoalteration, this phenomenon is not observed here, suggesting that something about the manufacturing process used to produce this pigment batch creates impurities that quench this fluorescence or that this "native" fluorescence is too weak to be observed under the illumination conditions employed. Similarly, no ultraviolet-induced infrared fluorescence is observed for the cadmium yellow pigments in this painting. Since both visible and infrared fluorescence of cadmium yellow paints can serve as indicators of photoalteration, even before the phenomenon is visible to the naked eye, it can be concluded that the cadmium-based paints of the SMK work are in excellent condition and that no incipient photoalteration is occurring.

The 1905 oil study for *Le Bonheur de vivre* at SFMOMA was also examined using pXRF, ultraviolet-induced visible fluorescence, and ultraviolet-induced infrared fluorescence. As with the Copenhagen work, an overall visual examination of the surface suggests that the painting is in excellent condition in terms of the brightness of the cadmium yellow colors and their surface condition.

However, a more detailed examination of the work reveals individual brushstrokes that may be starting to show physical and chemical alteration due to photooxidative degradation. For example, the detail above (see Figure 5a, from the central foreground, below the reclining figures) shows a brushstroke that is starting to develop a brownish crust and also appears to have faded to an off-white color. However, the brown material may be surface soil or residue from a varnish removal, and upon close inspection the region was painted with yellow and white paints mixed together to create a pale yellow, so a determination of fading is challenging to make. Figure 5c (yellow region above the embracing green figures) also shows a single brushstroke that appears to be developing an ivory alteration crust. However, this subtle discoloration is subject to interpretation, and overall, the work appears in excellent condition.

Under longwave ultraviolet illumination, however, both of the brushstrokes in question have the characteristic orange fluorescence associated with photooxidized cadmium yellow pigments. This finding reveals that ultraviolet-induced visible fluorescence has the potential to be a rapid, inexpensive, portable,

FIGURE 5. Visible light and longwave ultraviolet-induced visible fluorescence images from regions of SFMOMA's *Esquisse pour "Le Bonheur de vivre,"* 1905–1906, 91.160, © 2016 Succession H. Matisse/Artists Rights Society (ARS), New York. (a) Visible light detail of yellow paint in central foreground, below the reclining figures. (b) Detail of yellow paint in central foreground under longwave UV illumination showing the same brushstroke fluoresces orange. (c) Detail of yellow foliage from the painting's upper left corner (above the embracing green figures) showing a single brushstroke that appears to have a white alteration crust developing. (d) Detail of yellow foliage from the painting's upper left corner, under longwave UV illumination, showing the same brushstroke from (c) fluoresces orange in the ultraviolet.

FIGURE 6. (a) Ultraviolet-illuminated infrared fluorescence image of *The Scream* (1910(?), Munch Museum, Oslo; Photo © Munch Museum). (b) Visible light image, (c) ultraviolet-illuminated infrared fluorescence image, and (d) visible light fluorescence image showing cadmium yellow paint brushstrokes in the sky. (e) Visible light image, (f) ultraviolet-illuminated infrared fluorescence image, and (g) visible light fluorescence image showing cadmium yellow paint brushstrokes in the central figure's neck and hand.

and accessible imaging technique that can be used to screen for the photoalteration of cadmium pigments in its earliest stages, when it is difficult or impossible to perceive using the unaided eye. Note that all of the paint surrounding the altered brushstrokes shown above is also cadmium yellow and that it does not have this characteristic fluorescence, which is unlikely to be due to Matisse changing paint sources over such a small area on a single work. Instead, this difference among brushstrokes suggests that the orange fluorescence does indeed reveal incipient photooxidation. These findings were confirmed by ultraviolet-induced infrared fluorescence, which was strongest in these two brushstrokes with the dirty appearance (data not shown).

The ultraviolet-induced visible fluorescence image for *The Scream* (ca. 1910?, Munch Museum) shows the orange fluorescence characteristic of defect-containing cadmium yellow pigments in three prominent brushstrokes in the sky, in the water to the right of the central figure, in the railing, and in the clothing of the central figure (see Figure 6a). However, only a weak orange fluorescence was observed in the swirling water to the right of the pair of figures on the bridge, and only one potential brushstroke of characteristic fluorescence for cadmium was observed in the central figure's face or neck. Crucially, pXRF studies of the central figure's face and neck indicate the use of cadmium-containing pigments, so ultraviolet-induced visible fluorescence is once again not a comprehensive method for identifying cadmium pigments.

The cadmium-yellow-containing paint suspected in the sky on the basis of the ultraviolet-induced visible fluorescence was clearly imaged using the ultraviolet-induced infrared fluorescence technique (Figure 6c). However, some cadmium-yellow-containing paints that could not be observed in the sky with visible fluorescence could be observed with infrared fluorescence (Figure 6b–d). Conversely, note that the bottommost brushstroke in the sky that fluoresces orange (Figure 6b,c) and so is clearly observable in the visible fluorescence image cannot be definitively identified as cadmium yellow using the infrared fluorescence image (Figure 6b,d). Portable XRF of this brushstroke confirmed the presence of cadmium yellow and vermilion, the yellow and red pigments mixed to prepare the orange hue observed. The brown fluorescence of much of the cadmium yellow paints in this work does not appear to correlate with the condition of these paints. Also, unlike the cadmium yellow paint with the brown fluorescence observed by Van der Snickt et al. (2009), this paint has not been protected from the light, so this fluorescence may be due to a lack of photodegradation that more likely results from the paint's formulation than for environmental reasons.

Competition from other pigments that fluoresce in the visible, such as zinc white, prevents the ultraviolet-induced visible fluorescence method from being comprehensive, as does the orange fluorescence of cadmium yellow paints being impacted by their states of preservation (discussed above for the Matisse paintings).

As seen in the Matisse works, many of the altered and photooxidized cadmium yellow paints in *The Scream* (ca. 1910?) do have the characteristic orange fluorescence, but not all of them (for example, the two yellow brushstrokes altered to an ivory color in the central figure's neck; see Figure 6d–f; cadmium content confirmed by pXRF). This finding may suggest a thick cadmium carbonate and/or sulfate alteration crust (or, in the case of such thin brushstrokes, a complete conversion to a mixture of alteration phases throughout the paint layer), fully removing the CdS semiconductor structure that may be required for the characteristic fluorescence.

This comparison demonstrates that visible fluorescence images alone are insufficient to completely map the cadmium pigments on a work experiencing cadmium yellow photodegradation and alteration.

The origin of the orange and near-IR fluorescence of cadmium sulfide pigments has been ascribed to emission from deep trap states in the compound's crystal structure ("native fluorescence") and also to impurities in the crystal lattice that occur during the photodegradation of the compound. In theory, crystal defects at the surface of the compound could represent a second source of native fluorescence, but this phenomenon was not observed here—unaltered cadmium yellow paint did not fluoresce. Much systematic study remains to be done to determine if the fluorescence of cadmium sulfide yellow pigments is a reliable indicator of their state of photodegradation, which this work suggests, particularly for the SFMOMA painting *Esquisse pour "Le Bonheur de vivre."* However, the different synthesis procedures used by different paint manufacturers must be taken into account in these studies since that has been shown to greatly affect the purity of the resulting cadmium sulfide pigments formed, particularly at the turn of the twentieth century when the photodegradation of these pigments is found to be prevalent.

CONCLUSIONS

The photodegradation of cadmium yellow paints can cause substantial and irreversible changes in early modernist paintings, and it is critical that art conservators and cultural heritage scientists have the tools to identify these changes at their inception. It is also critical that they be able to monitor any changes in affected paintings. The four stand-alone imaging and analysis techniques used here were found to be complementary, and each was important (in fact, irreplaceable) for identifying cadmium-based paints and surveying and understanding their states of preservation. Only pXRF can provide the conclusive identification of cadmium paints on the basis of their X-ray emission lines, free from interference of pigments that also fluoresce when excited in the ultraviolet such as purpurin. Ultraviolet-induced visible fluorescence was found not to comprehensively identify cadmium paints on altered works such as *The Scream* (ca. 1910?) or *Le Bonheur de vivre* (1905–1906). Instead, cadmium yellow paints that were severely altered did not have the characteristic orange fluorescence expected for CdS, likely because of alteration crusts rich in other compounds such as $CdCO_3$ and $CdSO_4$ that have different electronic structures. Ultraviolet-induced visible

fluorescence was useful for imaging the cadmium pigments at the beginnings of alteration process, when impurities forming in the crystal lattice cause the deep trap states responsible for the semiconductor pigment's characteristic fluorescence. As a result, this imaging technique will prove critical for identifying paintings right at the start of a pressing preventive conservation need.

Ultraviolet-induced infrared fluorescence was found to be a useful confirmatory technique for the visible fluorescence technique and also critical for identifying altered cadmium yellow brushstrokes in the neck of the central figure in *The Scream* (Munch Museum, ca. 1910?). Further work is needed to determine why certain altered cadmium paints exhibit fluorescence in the infrared and not the visible. Finally, multispectral imaging has great promise for comprehensively imaging cadmium pigments using their near-infrared luminescence. The excitation wavelengths used here (380–520 nm) excited fluorescence in all of the cadmium pigments, altered and unaltered, in *Le Bonheur de vivre* (1905–1906).

Acknowledgments

We gratefully acknowledge the National Science Foundation for funding W&L's portable cultural heritage instrumentation (NSF MRI grants CHE-0959625 and CHE-1337481).

REFERENCES

Casadio, F., S. Xie, S. C. Rukes, B. Myers, K. A. Gray, R. Warta, and I. Fiedler. 2011. Electron Energy Loss Spectroscopy Elucidates the Elusive Darkening of Zinc Potassium Chromate in Georges Seurat's *A Sunday on La Grande Jatte—1884*. *Analytical and Bioanalytical Chemistry*, 399(9):2909–2920. http://dx.doi.org/10.1007/s00216-010-4264-9.

Church, A. H. 1890. *The Chemistry of Paints and Painting*. London: Seeley.

de la Rie, R. 1982. Fluorescence of Paint and Varnish Layers. *Studies in Conservation*, 27(1):1–7.

Fiedler, I., and M. A. Bayard. 1986. "Cadmium Yellows, Oranges, and Red." in *Artists' Pigments: A Handbook of Their History and Characteristics*, ed. R. L. Feller, pp. 65–108. New York: Oxford University Press.

Leone, B., A. Burnstock, C. Jones, P. Hallebeek, K. Keune, and J. Boon. 2005. "The Deterioration of Cadmium Sulphide Yellow Artists' Pigments." In *ICOM Committee for Conservation 14th Triennial Meeting*, pp. 803–813. The Hague: James and James.

Mass, J. L., R. Opila, B. Buckley, M. Cotte, J. Church, and A. Mehta. 2013a. The Photodegradation of Cadmium Yellow Paints in Henri Matisse's *Le Bonheur de vivre* (1905–1906). *Applied Physics A: Materials Science and Processing*, 111:59–68. http://dx.doi.org/10.1007/s00339-012-7418-0.

Mass, J. L., J. Sedlmair, C. Schmidt Patterson, D. Carson, B. Buckley, and C. Hirschmugl. 2013b. SR-FTIR Imaging of the Altered Cadmium Sulfide Yellow Paints in Henri Matisse's *Le Bonheur de vivre* (1905–6)—Examination of Visually Distinct Degradation Regions. *Analyst*, 138(20):6032–6043. http://dx.doi.org/10.1039/C3AN00892D.

Samet, W. 1990. Condition Report. Philadelphia: The Barnes Foundation.

Thoury, M., J. K. Delaney, E. R. de la Rie, M. Palmer, K. Morales, and J. Krueger. 2011. Near-Infrared Luminescence of Cadmium Pigments: In Situ Identification and Mapping in Pigments. *Applied Spectroscopy*, 65(8):939–951. http://dx.doi.org/10.1366/11-06230.

Topalova-Casadiego, B. and U. Plahter. 2011. "Cadmium Yellow in 'The Scream' painted by Edward Munch." In *The National Gallery Technical Bulletin 30th Anniversary Conference*, pp. 61. London: Archetype.

Van der Snickt, G., J. Dik, M. Cotte, K. Janssens, J. Jaroszewicz, W. De Nolf, J. Groenewegen, and L. Van der Loeff. 2009. Characterization of a Degraded Cadmium Yellow (CdS) Pigment in an Oil Painting by Means of Synchrotron Radiation Based X-Ray Techniques. *Analytical Chemistry*, 81(7):2600–2610. http://dx.doi.org/10.1021/ac802518z.

Van der Snickt, G., K. Janssens, J. Dik, W. De Nolf, F. Vanmeert, J. Jaroszewicz, M. Cotte, G. Falkenberg, and L. Van der Loeff. 2012. Combined Use of Synchrotron Radiation Based Micro-X-ray Fluorescence, Micro-X-ray Diffraction, Micro-X-ray Absorption Near-Edge, and Micro-Fourier Transform Infrared Spectroscopies for Revealing an Alternative Degradation Pathway of the Pigment Cadmium Yellow in a Painting by Van Gogh. *Analytical Chemistry*, 84(23):10221–10228. http://dx.doi.org/10.1021/ac3015627.

Materials and Meanings: Analyzing Kazimir Malevich's *Painterly Realism of a Football Player—Color Masses in the 4th Dimension*

Maria Kokkori, Stephanie D'Alessandro, Kristin Lister, and Francesca Casadio*

ABSTRACT. This paper examines Kazimir Malevich's (1878–1935) materials and methods for his *Painterly Realism of a Football Player—Color Masses in the 4th Dimension* painted in 1915. *Football Player* is an impressive painting constructed of colored geometric forms, representative of Kazimir Malevich's Suprematist period. This painting is from a remarkable group of works the artist produced for *0.10 (Zero–Ten): The Last Futurist Exhibition of Painting* held in Petrograd in 1915 where Malevich's Suprematist works debuted. The pristine condition of *Football Player* allows for the accurate interpretation of Malevich's artistic vision and makes this painting an excellent candidate for a technical study using noninvasive techniques. Methods used included X-ray, infrared reflectography, and ultraviolet visible fluorescence imaging, microscopic examination, and analysis of pigments and binding media using X-ray fluorescence spectroscopy (XRF) and reflectance Fourier transform infrared spectroscopy (FTIR). Results from XRF analysis showed a closely similar palette to other Suprematist paintings by Malevich and highlighted the presence of paints in limited use such as cobalt violet, whereas reflectance FTIR results provided new insights into the binding media used, the condition of the oil paint, and the presence of extenders, organic additives, and degradation products.

INTRODUCTION

Kazimir Malevich (1878–1935) is one of the most significant and rigorous pioneers of abstraction. He led the way to total nonobjective abstraction with his own variant, which he named Suprematism, in 1915. For a few years before this, he had been working in a Cubo-Futurist style, translating images of figures and everyday objects into complex compositions influenced by the speed of modern life. His particular experiments in 1914 with *zaum* (literally, beyond the mind) or "transrational" painting—a term adopted from the Russian poets Velimir Khlebnikov (1885–1922) and Aleksei Kruchenykh (1886–1968) to mean language beyond logic or acquired meaning—further challenged the conventions of representational art.[1]

Over the summer and fall of 1915 Malevich worked in absolute secrecy in his studio making works of art that would demonstrate his new and revolutionary approach. His goal was to contribute a significant number of paintings for the exhibition *0.10 (Zero–Ten): The Last Futurist Exhibition of Painting*, organized in Petrograd by the artist Ivan Puni (1892–1956) and his wife, Ksenia Boguslavskaia (1892–1972), which aimed to present the 10 artists included as those seeking to find the most elemental, irreducible base (the "zero") of painting.[2] As Malevich wrote in June of that momentous year,

The Art Institute of Chicago, 111 S. Michigan Ave., Chicago, Illinois 60603, USA.

* Correspondence: M. Kokkori, mkokkori@artic.edu

Manuscript received 7 July 2014; accepted 22 February 2016.

> All previous and contemporary painting before Suprematism—sculpture, the word, music—were enslaved by the form of nature, and they await their liberation in order to speak in their own tongue and not depend upon intellect, sense, logic, philosophy, psychology, the various laws of causality and technical changes in life. . . . The striving of the artistic powers to direct art along the path of intellect produced a zero of creativity . . . but I have transformed myself into a zero of form and gone beyond "0" to "1" . . . I cross over to Suprematism, to the new realism in painting, to objectless creation.[3]

In preparation for this exhibition, Malevich produced a series of over 40 paintings that completely eradicated all references to the recognizable world and focused instead on the inherent relationships of strictly geometric shapes of various colors that float on top of white backgrounds. The powerful icon-like presence of these works was emphasized by their presentation in the exhibition: arranged in three rows across the walls of a room dedicated to the artist and crowned by Malevich's *Black Square* (1915; State Tretyakov Gallery, Moscow), which hung high above in a corner. The works in this exhibition set the course for much of the development of abstract art thereafter and are recognized today as objects of great aesthetic as well as historic merit. One of those is the work discussed here, *Painterly Realism of a Football Player—Color Masses in the 4th Dimension*, a remarkably bold and dynamic canvas that significantly augmented the Art Institute of Chicago's holdings of modern art upon its acquisition in 2011 (Figure 1).

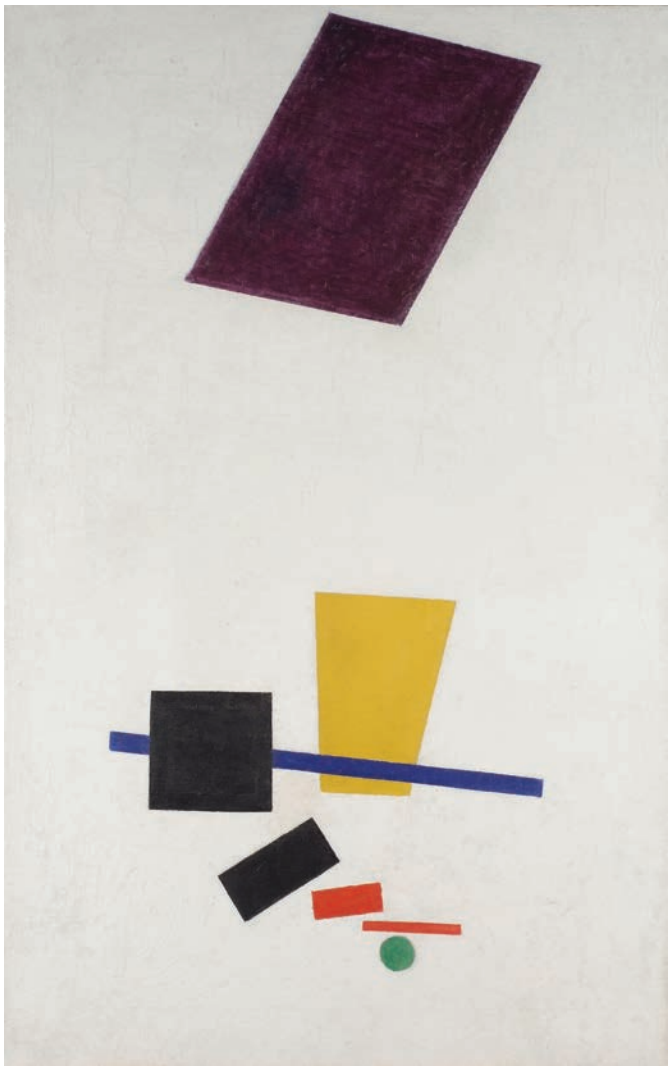

FIGURE 1. Kazimir Malevich, 1915. *Painterly Realism of a Football Player—Color Masses in the 4th Dimension,* oil on canvas, 27 × 17 1/2 in. (71 × 44.5 cm). ©The Art Institute of Chicago.

PROVENANCE

Painterly Realism of a Football Player—Color Masses in the 4th Dimension was in Malevich's possession when he was invited in 1927 to present a retrospective of his work in Warsaw, Poland, and at the *Grosse Berliner Kunstausstellung* (Great Art Exhibition) in Berlin, Germany. Within the larger presentation of at least 70 paintings, Malevich also showed about 22 research tables that introduced his investigations of modern art, the "science of painting" (*zhivopisnaia nauka*) as he described it, carried out at the State Institute for Artistic Culture in Petrograd (GINKhUK) between 1923 and 1926, and 27 Suprematist works, including *Football Player*.[4] Malevich was obliged to return to the Soviet Union before the exhibition's end and left his works in the care of architect Hugo Häring (1882–1958). At Malevich's request, none of the works were to be returned to him in Moscow since he had hoped to return to Europe the following year to exhibit his work in Paris and other west European cities and possibly even remain in the West.[5] Following Malevich's death in 1935, the collection remained with Häring until 1957, when he was convinced through the advice of artist Naum Gabo (1890–1977) and architect Mies van der Rohe (1886–1969) to transfer all the remaining 84 works to the Stedelijk Museum in Amsterdam. *Football Player* stayed in the collection of the Stedelijk until 2008, when it was returned, along with four others, as part of a settlement with Malevich's heirs.[6]

HISTORICAL CONTEXT

The painting is executed in oil paint on a canvas support and titled by Malevich "Football Player" as inscribed on the verso and dated 1915 (Figure 1). The first part of the title, *Painterly Realism of a Football Player*, may have been a reference to Albert Gleizes (1881–1953) and Jean Metzinger's (1883–1956)

discussion on "realism" in their treatise *Du "Cubisme"* published in 1912[7] and Umberto Boccioni's (1882–1916) futurist painting *Dynamism of a Soccer Player* (oil on canvas, 193.2 × 201 cm, The Museum of Modern Art, New York), painted in 1913, which was well known among Russian avant-garde artists as it was reproduced in contemporary art journals. The second part of the painting's title, *Color Masses in the 4th Dimension*, refers to the mathematical theory of fourth-dimensional space, a concept appropriated by many early twentieth-century avant-garde artists to justify their work beyond immediate sensory perception. For Malevich, Suprematism was intimately linked with a transforming and modern, mystical experience associated with concepts of space-time physics and the notion of the fourth dimension. These ideas had been introduced in the 1880s by the British mathematician Howard Hinton (1853–1907) and Russian philosopher Peter Uspenskii (1878–1947) and centered on the concept of a space outside sensory perception that made the present world illusory.[8] The title of the painting reflects this concept: although it references the natural world, it also breaks with it, moving far beyond description to depict its subject in lines and planes freed from the weight of the third dimension. As Malevich explained, "in naming some of the paintings I do not wish to point out what form to seek in them, but I wish to indicate that real forms were approached in many cases as the ground for formless painterly masses from which a painterly picture was created, quite unrelated to nature."[9] Indeed, recent scholarship has proven just how distanced from depiction Malevich had become, as evidenced by the deep geometric interconnectedness of all the works he produced for *0.10*, which can even be traced to their exact placement and interaction on the walls. Furthermore, Malevich would soon give up the last vestige of the art of representation—the notion of a proper "top" and "bottom" for his canvases—in favor of a "new logic of a non-referential space."[10] Malevich's paintings achieved the look of modern-day icons, and he specifically envisioned their place in a new, modern world. He believed Suprematism to be "the beginning of a new culture . . . a new form [that would] announce that man has gained his equilibrium."[11] Paintings like *Painterly Realism of a Football Player* were metaphysical and spiritual tools meant to raise human consciousness. This utopian view had even greater urgency with the October revolution of 1917, and his Suprematist paintings' appearance—simple, pure, modern—became, for a time, part of the visual idiom of the new society. But for all their look of being preordained absolute signs, under close examination the works reveal the extreme care, complexity of execution, and thinking of the artist.

TECHNICAL EXAMINATION AND SCIENTIFIC ANALYSIS

Kazimir Malevich was an avid writer, aspiring constantly to express and explain his artistic beliefs and methods, especially as they related to his Suprematist system. In spite of the very large art historical literature devoted to the painter, there is surprisingly little on his methods and materials.[12] This dearth of technical literature is perhaps due to the mistaken assumption that the works of art may be technically simplistic, especially in regard to his Suprematist paintings.

The combination of exacting abstract forms rendered in pure colors and the remarkable condition of this painting made it the perfect candidate for a noninvasive investigation of his materials and techniques. For this examination a combination of complementary noninvasive techniques was used, including X-ray, infrared reflectography, ultraviolet imaging, and microscope examination. The analysis of pigments and binding media was achieved with X-ray fluorescence spectroscopy (XRF) and reflectance Fourier transform infrared spectroscopy (FTIR; Table 1).

TABLE 1. Results of the paint analyses using X-ray fluorescence spectroscopy and reflectance Fourier transform infrared spectroscopy.

Paint	Pigments	Extenders	Additional components
White	Lead white (ground layer), zinc white (paint layers)	Barium sulfate (and/or lithopone), manganese and silica compounds	Zinc stearates, zinc oxalates, manganese palmitate
Black	Ivory black		Wax
Yellow	Lead chromate	Hydrated magnesite	
Red	Vermilion	Hydrated magnesite and silica compounds	
Green	Emerald green	Barium sulfate, magnesium carbonate	Dammar
Blue	Ultramarine blue	Hydrated magnesite	Zinc stearate
Violet	Cobalt violet, cobalt blue, ultramarine blue	Barium sulfate	Zinc stearate, dammar

RESULTS AND DISCUSSION

Painting Techniques and Materials

In Malevich's Suprematist paintings he sought to position geometric forms in space and to intuitively suggest their directional movement by implying forces, such as attraction and repulsion, that would lead to their alignment, concentration, or dispersal. Malevich maintained order in his painting process and control of subtleties in order to achieve this vision. Variations in the mass, position, and shape of his forms were critical to intended forces and effects and often required adjustments at different stages of the painting process. X-ray images revealed changes in composition, especially in the black geometric shapes in the lower part of the painting (Figure 2). Evidence from infrared reflectography (IRR) also showed many reworked lines, reconsidered placements, and revised sizes of forms, as the artist altered the composition. (Figure 3). In this work, the forms occupy two separate ends of the picture plane. The paint quality and brushwork of the two halves also vary slightly, corresponding to the difference in forms depicted. Malevich painted with two sets of complementary colors—the purple/yellow contrast of larger forms over a wider range at one end and the red/green contrast of smaller forms over a shorter span at the other end. This palette of contrasting colors is augmented by the curve of the dark rectangles, from purple to black to red in a tonal continuum across the picture plane. Thus, the entire canvas represents a rectangular form—a playing field whose borders concentrate the energy and exert a force on the purple parallelogram—effectively transforming it into a more dynamic shape.

For *Football Player*, Malevich used a medium-sized fine-weight plain-weave linen canvas stretched over a nonstandard size wooden stretcher and began his composition on a lead white–chalk ground that he applied thinly so that the texture of the canvas remained prominent, sketching in charcoal the forms he would later paint following his preliminary outlines. The paint layers followed around the sketched forms along with a second slightly different layer of white. Under ultraviolet illumination,

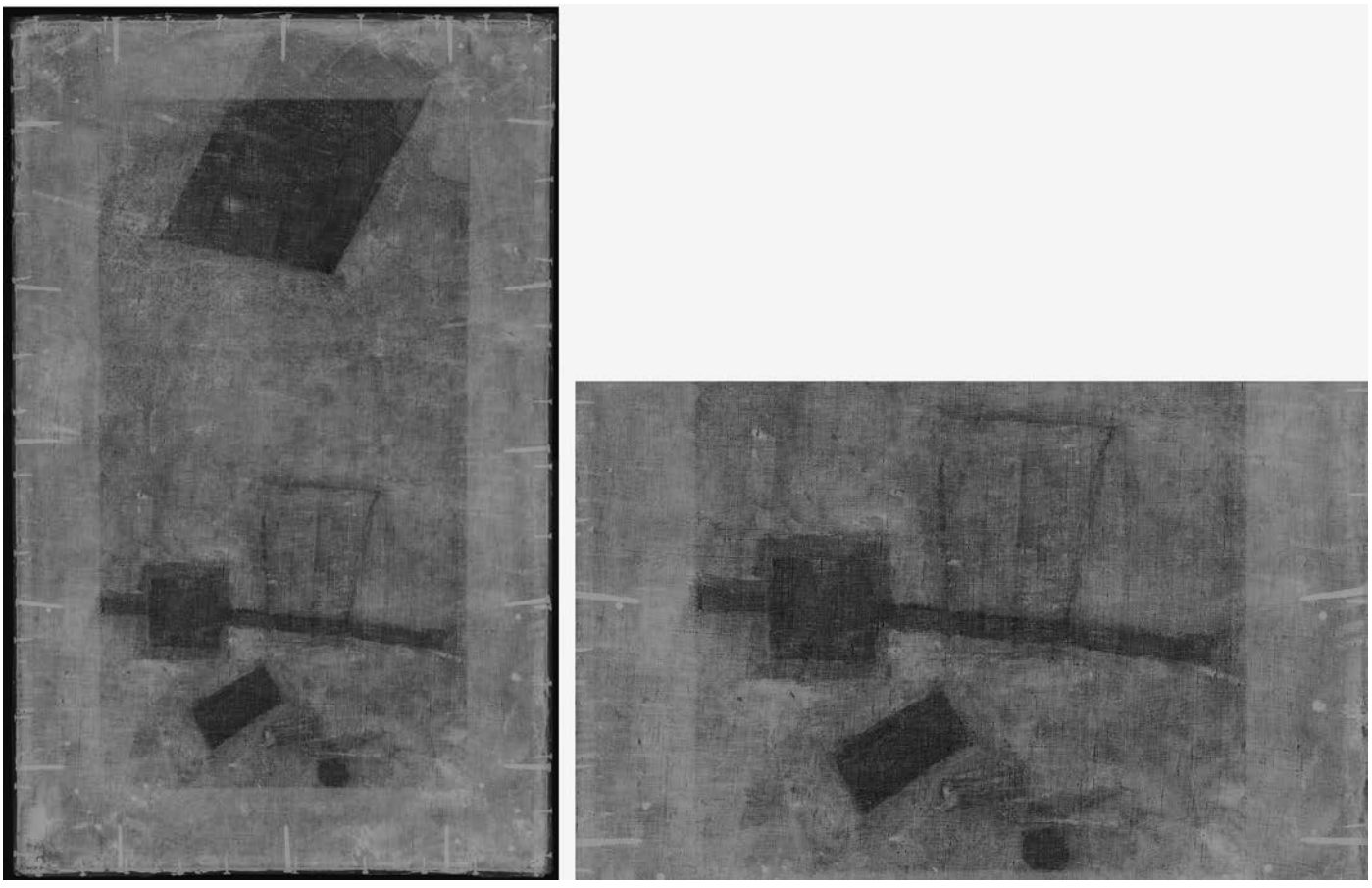

FIGURE 2. X-ray image showing changes in composition, especially in the black geometric forms in the lower part of the painting. Left: overall. Right: detail of lower half. ©The Art Institute of Chicago, Conservation department.

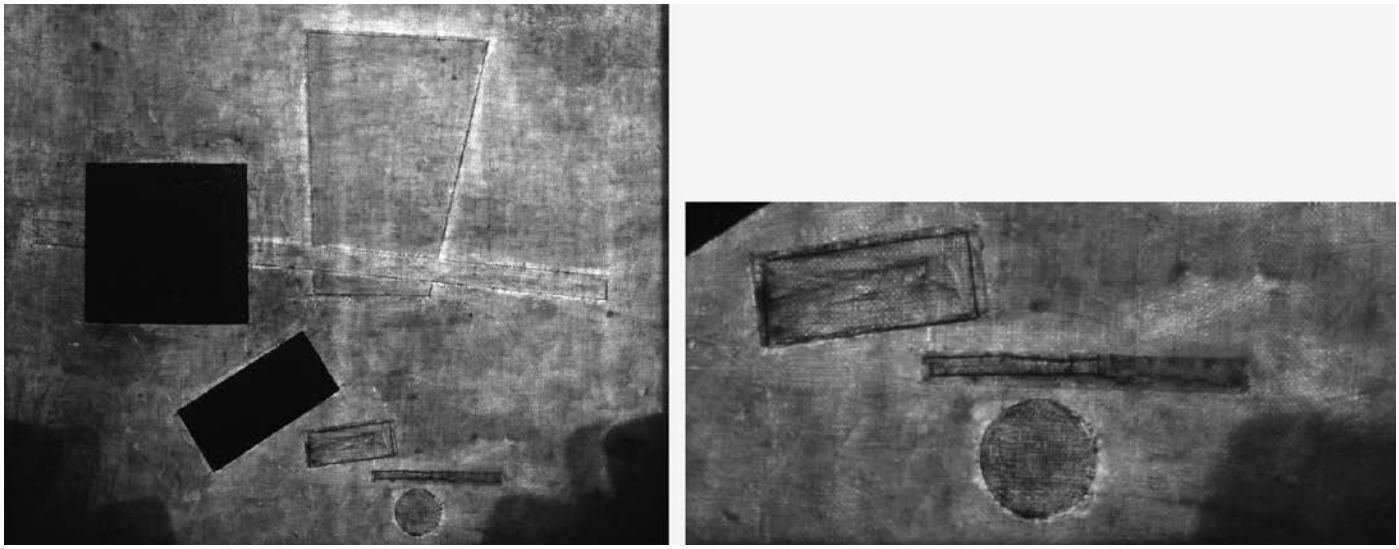

FIGURE 3. Details of the IRR image showing reworked lines and revised sizes of geometric forms visible in the lower half of the painting. Left: bottom half of the painting. Right: detail from the lower right quadrant. ©The Art Institute of Chicago, Conservation department.

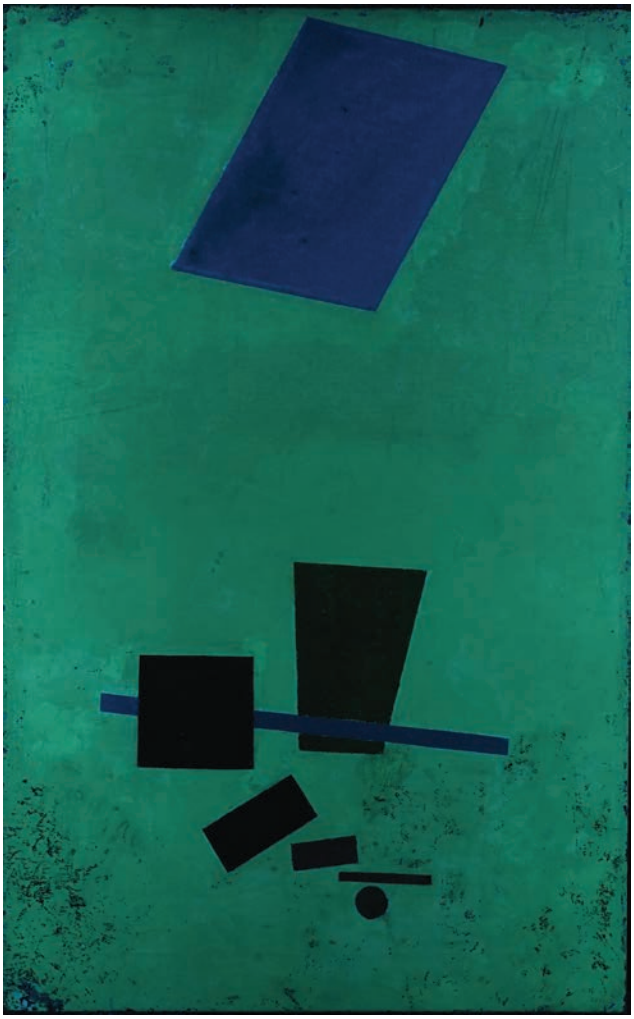

FIGURE 4. Ultraviolet image showing a bright yellowish white autofluorescence, characteristic of zinc oxide. ©The Art Institute of Chicago, Conservation department.

the top white layer exhibits the bright yellowish white autofluorescence, characteristic of zinc oxide (Figure 4).

The XRF analysis confirmed the presence of lead white (basic lead carbonate) found to be present throughout and to originate from the ground layer,[13] whereas zinc white (zinc oxide) has been identified as used for the white background and in admixtures with the paints.

Forms were delineated using a card as a guide to create a straight-edged colored border. Forms were then painted with green, black, red, blue, yellow, or purple. Malevich may have applied some of the colors while the white paint layer was still partially wet, as evidenced by impressions left by the card edge. Once the forms were established on the canvas, Malevich painted the space surrounding the forms in zinc white paint: at the bottom of the composition he worked the paint straight out of the tube for more control in short energetic strokes; on the top, he painted with fluid brushstrokes across the open field of the canvas. The traces of his working methods—the raised impressions in the still-wet paint the cards made as they were removed from the painting's surface, the flattened high spots on the white paint, the imprint of the cards' outer edges revealing their sizes, even Malevich's own fingerprints in the white paint above the black square—can be seen across the paint surface, suggesting a far

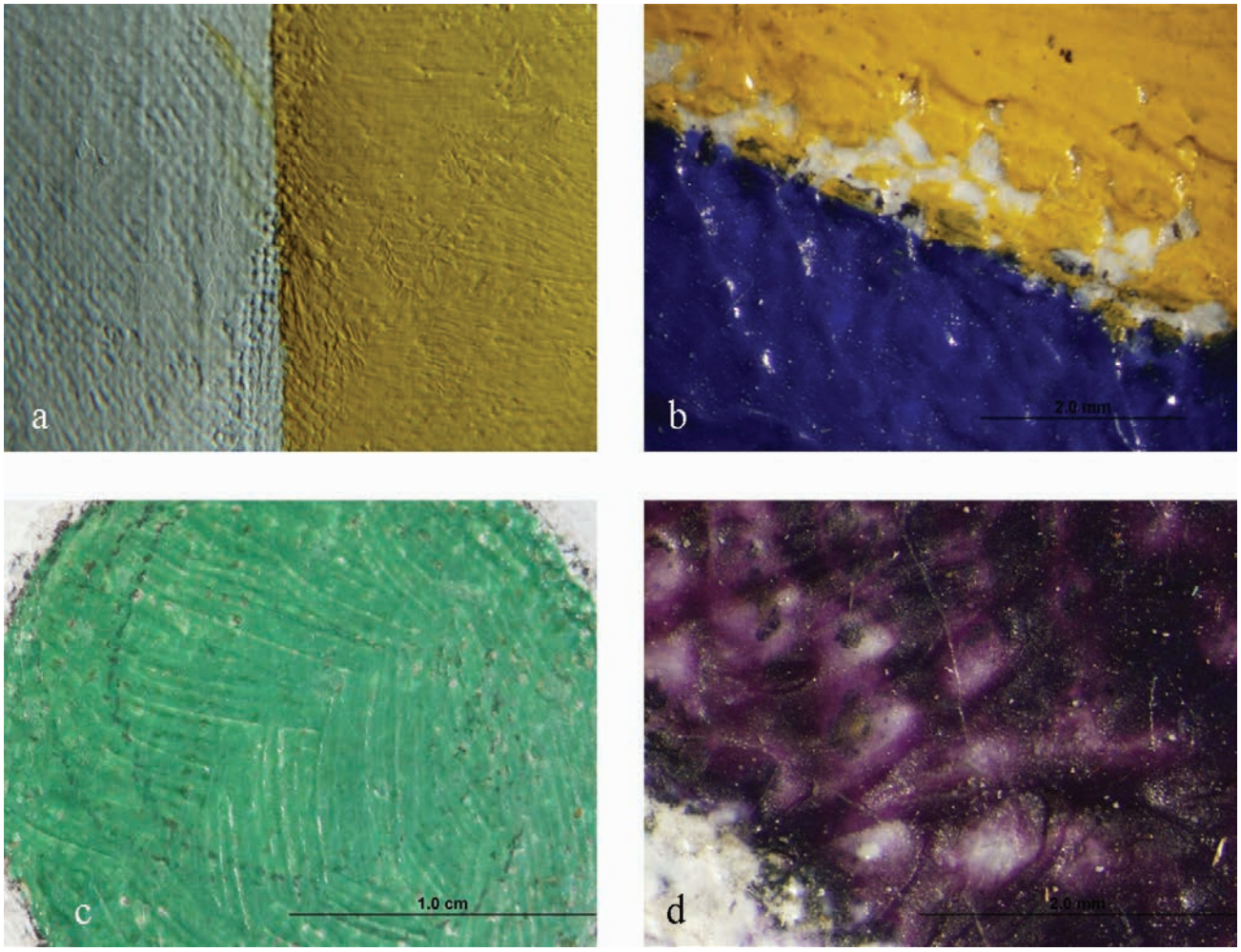

FIGURE 5. Details of *Football Player* showing the paint application. (a) Lower half of yellow form showing evidence of use of a card as a guide to create straight lines; the different textures of the two white paints are also evident. (b) Detail of the trapezoidal yellow form crossed by a blue bar showing small areas of exposed white underlayer. (c) Detail of the green circle showing the artist's underdrawing. (d) Detail of the purple trapezoid showing the paint texture. ©The Art Institute of Chicago, Conservation department.

more organic and intuitive process than might be inferred from the spare abstract composition (Figure 5).

Ground Layer and White Paint Composition

To characterize the ground, six spots spanning various areas of the white painted ground in the painting were analyzed with reflectance FTIR spectroscopy. All spectra were fairly similar, with minor variations in the drying oil binder. The presence of zinc oxide was also confirmed (Figure 6).[14]

The XRF analysis also detected the presence of varying amounts of barium in white passages, likely indicating the use of barium sulfate as an extender in the tube paint formulation used by Malevich. A more significant amount of barium was found in the ground layer than the upper paint layers. Because the analysis detected both barium and zinc in the white paint, the presence of lithopone cannot be completely excluded.[15] These results require confirmation by a complementary technique such as UV/visible fiber-optic reflectance spectroscopy (FORS; in the range 300–800) or Raman in situ, which were unavailable at the time of this study.

Yellow Paint

The trapezoidal yellow form crossed by a blue bar was painted in two sections. All yellow areas examined with reflectance FTIR showed lead chromate (with bands centered at 860–880 cm^{-1}) confirmed by XRF detection of chromium and lead.

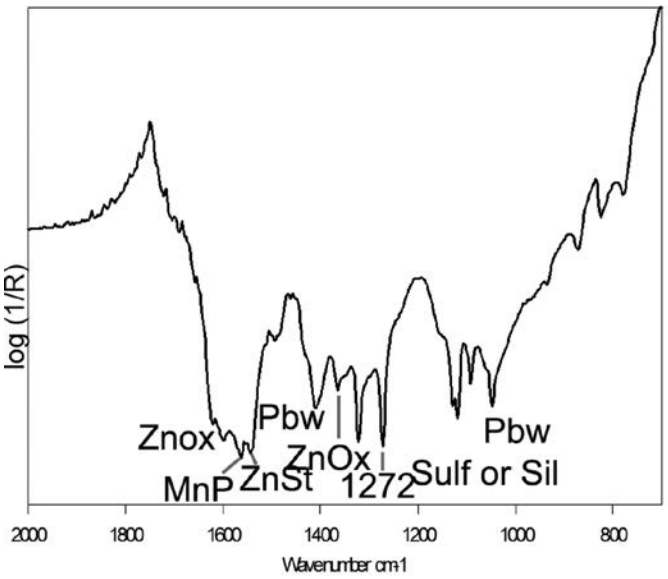

FIGURE 6. The FTIR reflection spectrum of the white painted area (Znox: zinc oxalates; ZnSt: zinc stearates; MnP: manganese palmitate; Pbw: lead white; Sulf or Sil: sulfates and/or silicates).

The presence of paint extender based on hydrated magnesite was confirmed with reflectance FTIR.[16] Around the form the texture of the thin ground over the canvas is visible (Figure 5a), whereas the surrounding areas of the background are covered to different degrees with the glossy top layer, which appears smooth or shows traces of brushwork when thicker or, when thin, exposes the color and texture of the ground. The layer structure of the yellow paint varies above and below where it is intersected by the blue bar, as evident in the IRR image (Figure 3), as well as from XRF analysis, which detected chromium above and below but not underneath the blue bar; hence, we can assume there is no yellow under the blue. Comparison of the XRF spectra of the upper and lower parts of the yellow trapezoid form bisected by the blue bar showed that the lower part had greater intensity for Zn, suggesting that Malevich first painted the yellow shape up to the border area with the blue bar but not extending below it; he then added more zinc white paint around it and, finally, painted on top of the zinc white layer the lower part of the yellow form.

Black Paint

It is evident that Malevich made several subtle changes to the forms as he drew the composition on the canvas. Although infrared reflectography is not effective for revealing underdrawing beneath a black paint layer, it revealed charcoal lines extending beyond the edges that indicated a narrower form was originally planned for the black rectangle. Malevich also enlarged the black square slightly over a centimeter in each direction, bringing the forms into a tighter grouping, as evident from the X-radiograph. Reflectance FTIR analysis of the black forms identified bone black.[17] In the XRF analysis, the lower part of the square shows higher-intensity peaks for Zn, suggesting reworking in the area after the artist had applied the second white background layer around the forms. Under high magnification it is evident that Malevich also repainted the adjacent ends of the blue bar so that they align with the edges of black square.

Red and Blue Paint

In other changes during the coloring stage, Malevich extended the red rectangle several centimeters farther toward the right edge of the painting. The XRF detection of mercury in red areas is an indication of the use of vermilion extended with hydrated magnesite and containing trace silicates as confirmed by reflectance FTIR.

Reflectance FTIR analysis of the blue bar confirmed the presence of ultramarine blue.[18] This is in line with both historical and artistic documentation, and scientific analysis of Malevich artworks revealed his extensive use of French ultramarine.[19]

Green Paint

On the green area, XRF analysis identified a strong correlation between copper and arsenic, suggesting the use of a copper arsenite pigment, such as emerald green.[20] This is consistent with Malevich's practice as it has been reported that emerald green was one of the most commonly found pigments on Malevich's oil paintings. Scheele's green[21] cannot be completely excluded; Malevich's use of Scheele's green is less likely since it was no longer in use at the end of the nineteenth century because of its tendency to blacken. The FTIR analyses also indicated the presence of chrome yellow, barium sulfate, and dammar varnish. Interestingly, XRF results showed that zinc was absent in the green area, whereas it was present in all other colored areas analyzed, suggesting that the green ball is painted directly on the ground layer, as the first colored geometric form Malevich positioned on the canvas.

Violet Paint

Malevich expanded the violet form on three sides, so that instead of painting within an area of reserve, he painted over the wet zinc white paint. Because the artist painted the purple over the edge of the surrounding white background, although he did so very precisely, the two colors do mix slightly in some strokes. In the purple parallelogram, Malevich painted with cobalt violet, a pigment known for its transparency. He carefully controlled the brushwork, applying thin, parallel strokes to extend the paint. He also went back with the brush and texturized some of the thicker deposits of purple. In the examined purple areas, reflectance FTIR also indicated the presence of zinc stearates, barium sulfate, zinc white from the white under layers, and dammar resin—possibly

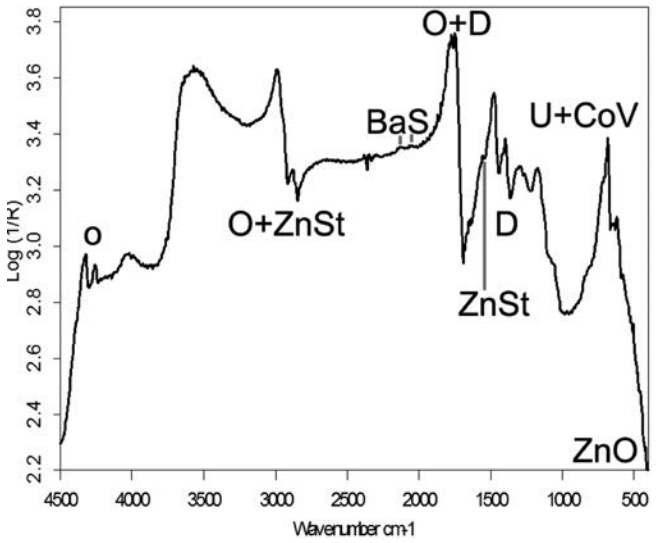

FIGURE 7. The FTIR reflection spectrum of the purple painted area (ZnSt: zinc stearates; ZnO: zinc white; U: ultramarine blue; CoV: cobalt violet; BaS: barium sulfate; D: dammar).

added by Malevich to increase the sense of depth, transparency, and gloss of the painted form (Figure 7).[22, 23]

Cobalt violet was an expensive color to buy in early twentieth-century Russia, and it was specifically mentioned in the technical literature, including manuals written by Malevich's teacher, Fedor Rerberg (1865–1938), as being a pigment for use in exceptional cases such as exhibitions and similar events. Its visual and handling properties and its transparency allowed it to be used in painting to create rich enamel-like effects.[24] It was extensively discussed by Russian avant-garde artists within the context of *faktura*, translated in English as "texture," "facture," or "structure," and materiality in art and also provided inspiration to poets. Cobalt violet pigment had literary, political, and social connotations; it became synonymous with European modernism and was often described in Russian literature as a "French" or "bourgeois" pigment. In avant-garde poetry, colors were essential, for they conveyed mystical intimations of things beyond human experience. In 1904, Aleksandr Blok (1880–1921), for example, wrote the famous poem "Such a violet west is oppressive" (fioletovyi zapad gnetet),[25] and Vladimir Mayakovsky (1893–1930), in his *Verlaine and Cézanne* (Verlen i Sezan), stated that the color of "Paris is violet."[26] After the October revolution of 1917 the availability of cobalt violet became scarce since the trade with western European countries was cut off.

Condition of the Painting

Considering the fate of avant-garde art in Russia and Germany, the cataclysmic destruction of Berlin in World War II, and the general wear and tear that can ravage any artwork that is exposed to adverse conditions, it is remarkable that *Painterly Realism of a Football Player* survived in such good state, unlike many other paintings from the Russian avant-garde.[27]

In the present study, a number of carboxylate soaps were detected, such as zinc stearates and oxalates, manganese palmitate, and possibly copper oxalates. Although some of these compounds may be deliberate additions by the paint manufacturer as paint driers and dispersants, many should be considered deterioration products and may have an impact on future conservation choices.

Surface and Facture

In Cubo-Futurist works preceding *Football Player* Malevich made use of differences in texture and gloss and applied local varnishes for subtle distinctions in surface appearance. *Football Player* is consistent with this practice since an aged natural resin varnish, locally applied, can be detected on the purple and green form and may well be original. Malevich would have deliberately applied varnish to the purple/violet form to enhance its transparency. Elsewhere in the composition, the yellow form painted with lead chromate is very opaque and in contrast to the purple form positioned above.

As previously indicated, the study of color and *faktura* were fundamental in the development of Suprematism, "the essence of painting," as Malevich wrote.[28] *Faktura* was a basic principle of avant-garde art—the specific combination of materials and painting techniques used within the creative process that lead to the sensation experienced when viewing the work of art, denoted the material quality of a work of art: the way of making it, the materials used, the paint layers, and their opacity and transparency. The term used extensively by Cubo-Futurist and Suprematist artists and then by Futurist poets and Formalist theorists was quickly adopted by the Constructivists to express a materialist ideology and utilitarian orientation in artistic production.[29] *Faktura* was explored by Malevich and his students as an idea, a formless phenomenon, a technological or scientific development, and a focus for future discoveries.

CONCLUSIONS

Malevich's *Football Player* is a work of incredible delicacy and subtle, dimensional painting; its surface is full of contrasting texture, color, opacity, and finish. The powerful and dynamic composition, which at first may seem technically simplistic, exhibits a complexity of brushwork and revisions that are the hallmarks of Malevich's preoccupation with color, form, and texture.

This study has been made possible by new developments in noninvasive analytical methods that yield significant information about the artist's methods and materials and allow detailed and critical analysis and imaging of an artwork's entire structure.[30–36] The study of this painting integrating X-ray fluorescence with

infrared spectroscopy confirmed Malevich's palette included lead white, zinc white, vermilion, lead chromate yellow, bone black, emerald green, ultramarine blue, and cobalt violet with some cobalt blue. Although, overall, the binding medium of the paint was confirmed as oil, local application of dammar resin varnish was detected on the purple form, an example of Malevich's expert paint handling and careful attention to *faktura* in his Suprematist oeuvre.

Acknowledgments

The authors thank Frank Zuccari, Kim Muir, Allison Langley, Kelly Keegan, and the staff of Ryerson & Burnham Libraries at the Art Institute of Chicago and John Delaney and Kate Dooley, National Gallery of Art, Washington, D.C., for preliminary, confirmatory FORS measurements. The financial support of the Stockman Family Foundation, the Andrew W. Mellon Foundation, and the Grainger Foundation is also gratefully acknowledged.

APPENDIX

X-ray Fluorescence Spectroscopy

Analysis was performed using a Bruker TRACeR III energy dispersive X-ray fluorescence analyzer, with a Peltier cooled Silver-free SiPIN detector with a 13-μm Be window and a resolution of approximately 175 eV for the full width at half maximum of the Mn Kα line. The system is equipped with a rhodium transmission target. Analysis was conducted at 45 kV and a beam current of 2.0 μA pulling a vacuum at the tip of the instrument to enhance light element detection. Acquisition time was 120 s. The size of the analyzed spot may vary, but it is approximately 6–8 mm in diameter.

Reflectance Fourier Transform Infrared Spectroscopy

A portable Bruker-Alpha FTIR spectrometer equipped with a deuterated triglycine sulfate (DTGS) detector was used. Spectra were collected as the sum of 256 scans at 4 cm^{-1} resolution.

NOTES

1. For more on the concept of *zaum*, see Charlotte Douglas, *Swans of Other Worlds: Kazimir Malevich and the Origins of Abstraction in Russia* (Ann Arbor, MI: UMI Research Press, 1980); Gerald Janecek, *Zaum: The Transrational Poetry of Russian Futurism* (San Diego: San Diego State University Press, 1996).
2. Linda S. Boersma, *0.10: The Last Futurist Exhibition of Painting* (Rotterdam: 010 Publishers, 1994).
3. Kazimir Malevich, *Ot kubizma i futurizma k suprematizmu: novyi zhivopisnyi realizm* (Moscow: tip. Obshchestvennaia Pol'za, 1916), 11–27.
4. Troels Andersen, *Malevich: Catalogue Raisonné of the Berlin Exhibition 1927* (Amsterdam: Stedelijk Museum, 1970); Maria Kokkori and Alexander Bouras, "Charting Modernism: Kazimir Malevich's Research Tables," in *Malevich*, ed. Achim Borchardt Hume. (London: Tate, 2014), 164–195.
5. J. M. Joostens, "Malevich in the Stedelijk," in *Kazimir Malevich 1878–1935*, ed. W. A. L. Beeren (Amsterdam: Stedelijk Museum, 1988), 44–54.
6. Leonard Malewicz et al., Plaintiffs, v. City of Amsterdam, Defendant. United States District Court, District of Columbia. 517 F. Supp.2d 322. D.D.C. 2007.
7. Albert Gleizes and Jean Metzinger, "Du 'Cubism' [27 December 1912]," in *A Cubism Reader: Documents and Criticism 1906–1914*, ed. M. Antliff and P. Leighten (Chicago: University of Chicago Press, 2008), 435.
8. For more on Malevich's interest in the fourth dimension, see Linda Dalrymple Henderson, *The Fourth Dimension and Non-Euclidean Geometry in Modern Art* (Princeton, NJ: Princeton University Press, 1983), 274–294; John Golding, "Malevich and the Ascent into Ether," in *Paths to the Absolute: Mondrian, Malevich, Kandinsky, Pollock, Newman, Rothko, and Still*, A. W. Mellon Lectures in the Fine Arts, 1997 (Princeton, NJ: Princeton University Press, 2000), 47–80.
9. Henderson, *The Fourth Dimension*, 287, n. 185.
10. This decision, in combination with photographs of his 1915, 1920, and 1927 exhibitions, which record the changing orientation of certain paintings, has led to differing interpretations about whether Malevich reconsidered the orientation of his Suprematist compositions. *Painterly Realism of a Football Player* was shown twice with the purple form at the top (1915 in Petrograd and 1927 in Berlin) and twice with the form at the bottom (1920 in Moscow and 1927 in Warsaw).
11. Malevich, *Ot kubizma i futurizma k suprematizmu*, 27.
12. Milda Vikturina and Alla Lukanova, "A Study of Technique: Ten Paintings by Malevich in The Tretiakov Gallery," in *Kazimir Malevich, 1878–1935* (Los Angeles: Armand Hammer Museum of Art and Cultural Center, 1990), 187–197; Ann Hoenigswald, "Kazimir Malevich's Paintings: Surface and Intended Appearance," in *Conservation Research, 1996/1997*, Studies in the History of Art 57, Monograph Series II (Washington, D.C.: National Gallery of Art, 1997), 109–125; Yulian Khalturin, "Kazimir Malevich's Artistic Method and Evolution of His Painting Technique" (Ph.D. diss., Lomonosov Moscow State University, 2006); Maria Kokkori, "Russian Avant-Garde Art: A Historical Contextualization of Selected Paintings by Kazimir Malevich, Ivan Kliun, and Liubov Popova c.1905–1925" (Ph.D. diss., Courtauld Institute of Art, 2008); Maria Kokkori and Alexander Bouras, "The Painting Techniques of Kazimir Malevich: 1900–1910," in *Painting Techniques, History, Materials and Studio Practice* (Amsterdam: Rijksmuseum, 2015, in press).
13. It can be deduced that lead white is confirmed because of the inversion of the intensity of the Pb La and Lb lines when the XRF analysis was conducted in the recto and also because a stronger signal from Pb was observed when acquiring the XRF spectra from the verso of the painting/canvas.
14. The drying oil binder was characterized by the doublet at 4,340–4,250 cm^{-1} ascribed to the $\nu + \Delta(CH)$ mode of aliphatic chains and the first overtone of $\nu(CH)$ at about 5,800–5,680 cm^{-1}, as well as the $\nu(CO)$ band centered at 1,740 cm^{-1}. The $\nu(CH)$ bands of the oil medium are obscured by strong and sharp absorption bands inverted by the *reststrahlen* effect centered at 2,916 and 2,848 cm^{-1}, which, in association with the sharp negative peak at 1,540 cm^{-1} assigned to $\nu(COO^-)$, clearly identify the presence of zinc stearates. Other carboxylate soaps were also identified, namely, zinc oxalates indicated by the inverted bands at 1,630, 1,364, 1,320, and 824 cm^{-1} as well as manganese palmitate (1,569, 1,544, 1,451, 1,429, 1,420, and 1,404 cm^{-1}). Zinc oxide was confirmed in all examined areas because of the broad *reststrahlen* inverted band with inception at 700 cm^{-1}. The sharp inverted peak at 1,272 cm^{-1} could possibly be associated with cellulose nitrate or a plasticizer containing phthalate attributed to previous conservation treatments. For more on noninvasive analysis using reflected FTIR, see M. Vagnini, C. Miliani, L. Cartechini, P. Rocchi, B. G. Brunetti, and A. Sgamellotti, "FT-NIR Spectroscopy for Non-invasive Identification of Natural Polymers and Resins in Easel Paintings," *Analytical and Bioanalytical Chemistry* 395, no. 7 (2009): 2107–2118, http://dx.doi.org/10.1007/s00216-009-3145-6; R. Mazzeo, S. Prati, M. Quaranta, E. Joseph, E. Kendix, and M. Galeotti, "Attenuated Total Reflection Micro FTIR Characterisation of Pigment-Binder Interaction in Reconstructed Paint Films," *Analytical and Bioanalytical Chemistry* 392, nos. 1–2 (2008): 65–76, http://dx.doi.org/10.1007/s00216-008-2126-5; B. Doherty, M. Pamplona, R. Selvaggi, C. Miliani, M. Matteini, A. Sgamellotti, and B. Brunetti, "Efficiency and Resistance of the Artificial Oxalate Protection Treatment on Marble against Chemical Weathering," *Applied Surface Science* 253, no. 10 (2007): 4477–4484, http://dx.doi.org/10.1016/j.apsusc.2006.09.056.
15. Although occasionally used for artists' paints, lithopone extenders were extensively used in the house paint industry.

16. The examined areas were characterized by bands at 433, 598, 851, 880, 1,428, 1,480 3,449, and 3,514 cm^{-1} and a particularly diagnostic sharp –OH stretching band at 3,647 cm^{-1}.
17. A diagnostic sharp positive peak at 2,014 cm^{-1} is combined with peaks between 1,600 and 1,320 cm^{-1} and bands ascribed to vibrations of the phosphate group with *reststrahlen* inverted bands with a minimum at 1,024 cm^{-1} and positive peaks at 964 and 876 cm^{-1}. The ν(CH) area showed sharp negative peaks at 2,915 and 2,843 cm^{-1} associated with weak peaks at 717–730 cm^{-1}, likely related to the presence of wax, possibly connected with the wax lining treatment of the canvas. For more on spectral distortions in reflected FTIR, see C. Miliani, F. Rosi, A. Daveri, and B. G. Brunetti, "Reflection Infrared Spectroscopy for the Non-invasive in Situ Study of Artists' Pigments," *Applied Physics A* 106, no. 2 (2012): 295–307, http://dx.doi.org/10.1007/s00339-011-6708-2.
18. The reflectance FTIR spectra showed characteristic bands for ultramarine blue with negative peaks centered at 577 and 640 cm^{-1} and a *reststrahlen* inverted peak for the ν(Si-O) with a minimum around 950 cm^{-1}. The blue bar also contains barite with characteristic overtones at 2,063, 2,136, and 1,965 cm^{-1}; traces of zinc stearates; and hydrated magnesite.
19 See note 12.
20. $3Cu(AsO_2)2Cu(CH3COO)_2$.
21. General formula $CuHAsO_3$.
22. The XRF detection of Co and P and a complex convolution of bands between 710 and 1,171 cm^{-1} shown by reflectance FTIR are consistent with cobalt phosphates mixed with an ultramarine underlayer. Point areas analyzed with FORS by John Delaney and Kate Dooley (National Gallery of Art, Washington D.C.) highlighted the presence of cobalt blue, possibly used to darken the hue or present in adulteration with ultramarine blue. Cobalt blue was described in the Russian technical literature on paints as an excellent permanent blue pigment, an important pigment to be included in the modern palette; however, because of its cost, colormen often adulterated cobalt pigments with ultramarine blue. See Fedor Rerberg, *Palitra sovremennogo khudozhnika* (Moscow: Gosizdat, 1921), 43.
23. The detection of ultramarine blue by reflectance FTIR and cobalt blue by FORS led to the creation of mockups demonstrating that a layered system with ultramarine blue below and cobalt violet above would give spectra consistent with the ones recorded in situ on the painting. Technical analysis of Malevich's other Suprematist works ca. 1915–1917 has also revealed that the artist often used a multilayering technique to achieve certain colors and textures. See Kokkori, "Russian Avant-Garde Art."
24. Fedor Rerberg, *Kraski i drugie khudozhestvennye sovremennye materialy* (Moscow: Izd. Moskovskago tovarishchestva khudozhnikov′, 1905), 19–20.
25. Aleksandr Blok, *Polnoe sobranie stikhotvorenii v trekh tomakh* (Moscow: Progress-Pleiada, 2009–2011).
26. Vladimir Mayakovsky, *Parizh* (Moscow: Moskovskii rabochii, 1925).
27. During the 1950s, while on deposit at the Stedelijk Museum, all of Malevich's paintings were wax lined and varnished, as was common practice at the time. The synthetic varnish has since been removed from the surface. For more about Malevich surface appearances, see Louise Wijnberg, "Do We See What We Know or Do We Know What We See? Conservation of Oil Paintings in the Stedelijk Museum Amsterdam," in *Issues in Contemporary Oil Paint*, ed. Klaas Jan van den Berg, Aviva Burnstock, Matthijs de Keijzer, Jay Krueger, Tom Learner, Alberto de Tagle, and Gunnar Heydenreich (Cham, Switzerland: Springer, 2014), 21–23.
28. Malevich, *Ot kubizma i futurizma k suprematizmu*, 11.
29. For further discussion on *faktura,* see Vladimir Markov, *Printsipy tvorchestva v plasticheskikh iskusstvakh: faktura* (Petrograd: Izdanie Obshchestva Khudozhnikov 'Soiuz Molodezhi', 1914); Aage Hanse-Löve, "Faktura, Fakturnost," *Russian Literature* 17, no. 1 (1985): 29–38; Benjamin H. D. Buchloh, "From Faktura to Factography," *October* 30 (Autumn1984): 82–119, http://dx.doi.org/10.2307/778300; Maria Gough, "Faktura: The Making of the Russian Avant-Garde," *RES: Anthropology and Aesthetics* 36 (Autumn 1999): 32–59; Alexander Bouras, "Faktura utopii," in "Khudozhestvennaia tekhnika i materialyv teorii i praktike russkogo avangarda" (Ph.D. thesis, Moscow Architectural Institute, 2016).
30. F. Rosi, C. Miliani, C. Clementi, K. Kahrim, F. Presciutti, M. Vagnini, V. Manuali, A. Daveri, L. Cartechini, B. G. Brunetti, and A. Sgamellotti, "An Integrated Spectroscopic Approach for the Non-invasive Study of Modern Art Materials and Techniques," *Applied Physics A* 100, no. 3 (2010): 613–624, http://dx.doi.org/10.1007/s00339-010-5744-7.
31. F. Rosi, A. Burnstock, K. J. Van den Berg, C. Miliani, B. G. Brunetti, and A. Sgamelotti, "A Non-invasive XRF Study Supported by Multivariate Statistical Analysis and Reflectance FTIR to Assess the Composition of Modern Painting Materials," *Spectrochimica Acta A* 71, no. 5 (2009): 1655–1662, http://dx.doi.org/10.1016/j.saa.2008.06.011.
32. C. Miliani, K. Kahrim, B.G. Brunetti, A. Sgamellotti, A. Aldrovandi, M. R. van Bommel, K. J. van den Berg, and H. Janssen, "MOLAB, a Mobile Facility Suitable for Non-invasive in-Situ Investigations of Early and Contemporary Paintings: The Case-Study of *Victory Boogie Woogie* (1942–1944) by Piet Mondrian," in *ICOM Committee for Conservation 15th Triennial Meeting, New Delhi, 22–26 September 2008,* ed. Janet Bridgland (New Delhi: Allied Publishers, 2008), 857–864.
33. C. Miliani, F. Rosi, A. Burnstock, B. G. Brunetti, and A. Sgamelotti, "Non-invasive in-Situ Investigations Versus Micro-sampling: A Comparative Study on a Renoirs Painting," *Applied Physics A* 89, no. 4 (2007): 849–856.
34. L. Monico, F. Rosi, C. Miliani, A. Daveri, and B. Brunetti, "Non-invasive Identification of Metal-Oxalate Complexes on Polychrome Artwork Surfaces by Reflection Mid-infrared Spectroscopy," *Spectrochimica Acta Part A: Molecular and Biomolecular Spectroscopy* 116 (December 2013): 270–280, http://dx.doi.org/10.1016/j.saa.2013.06.084.
35. M. Alfeld, J. V. Pedroso, M. V. Hommes, G. Van der Snickt, G. Tauber, J. Blaas, M. Haschke, K. Erler, J. Dik, and K. Janssens, "A Mobile Instrument for in Situ Scanning Macro-XRF Investigation of Historical Paintings," *Journal of Analytical Atomic Spectrometry* 28, no. 5 (2013): 760–767, http://dx.doi.org/10.1039/c3ja30341a.
36. J. K. Delaney, J. G. Zeibel, M. Thoury, R. Littleton, M. Palmer, K. M. Morales, E. R. de la Rie, and A. Hoenigswald, "Visible and Infrared Imaging Spectroscopy of Picasso's *Harlequin Musician*: Mapping and Identification of Artist Materials *in Situ*," *Applied Spectroscopy* 64 (2010): 584–594, http://dx.doi.org/10.1366/000370210791414443.

BIBLIOGRAPHY

Alfeld, M., J. V. Pedroso, M. V. Hommes, G. Van der Snickt, G. Tauber, J. Blaas, M. Haschke, K. Erler, J. Dik, and K. Janssens. "A Mobile Instrument for in Situ Scanning Macro-XRF Investigation of Historical Paintings." *Journal of Analytical Atomic Spectrometry* 28, no. 5 (2013): 760–767. http://dx.doi.org/10.1039/c3ja30341a.

Andersen, Troels. *Malevich: Catalogue Raisonné of the Berlin Exhibition 1927.* Amsterdam: Stedelijk Museum, 1970.

Blok, Aleksandr. *Polnoe sobranie stikhotvorenii v trekh tomakh.* Moscow: Progress-Pleiada, 2009–2011.

Boersma, Linda S. *0.10: The Last Futurist Exhibition of Painting.* Rotterdam: 010 Publishers, 1994.

Bouras, Alexander. "Faktura utopii." In "Khudozhestvennaia tekhnika i materialyv teorii i praktike russkogo avangarda." Ph.D. diss., Moscow Architectural Institute, 2016.

Buchloh, Benjamin H. D. "From Faktura to Factography." *October* 30 (Autumn 1984): 82–119. http://dx.doi.org/10.2307/778300.

Delaney, J. K., J. G. Zeibel, M. Thoury, R. Littleton, M. Palmer, K. M. Morales, E. R. de la Rie, and A. Hoenigswald. "Visible and Infrared Imaging Spectroscopy of Picasso's *Harlequin Musician*: Mapping and Identification of Artist Materials *in Situ*." *Applied Spectroscopy,* 64, no. 6 (2010): 584–594. http://dx.doi.org/10.1366/000370210791414443.

Doherty, B., M. Pamplona, R. Selvaggi, C. Miliani, M. Matteini, A. Sgamellotti, and B. Brunetti. "Efficiency and Resistance of the Artificial Oxalate Protection Treatment on Marble against Chemical Weathering." *Applied Surface Science* 253, no. 10 (2007): 4477–4484. http://dx.doi.org/10.1016/j.apsusc.2006.09.056.

Douglas, Charlotte. *Swans of Other Worlds: Kazimir Malevich and the Origins of Abstraction in Russia.* Ann Arbor, MI: UMI Research Press, 1980.

Gleizes, Albert, and Jean Metzinger. "Du 'Cubism' [27 December 1912]." In *A Cubism Reader: Documents and Criticism 1906–1914*, ed. M. Antliff and P. Leighten, p. 418–437. Chicago: University of Chicago Press, 2008.

Golding, John. "Malevich and the Ascent into Ether." In *Paths to the Absolute: Mondrian, Malevich, Kandinsky, Pollock, Newman, Rothko, and Still,* pp. 47–80. A. W. Mellon Lectures in the Fine Arts, 1997. Princeton, NJ: Princeton University Press, 2000.

Gough, Maria. "Faktura: The Making of the Russian Avant-Garde." *RES: Anthropology and Aesthetics* 36 (Autumn 1999): 32–59.

Hanse-Löve, Aage. "Faktura, Fakturnost." *Russian Literature.* 17, no. 1 (1985): 29–38.

Henderson, Linda Dalrymple. *The Fourth Dimension and Non-Euclidean Geometry in Modern Art*. Princeton, NJ: Princeton University Press, 1983.

Hoenigswald, Ann. "Kazimir Malevich's Paintings: Surface and Intended Appearance." In *Conservation Research, 1996/1997*, pp. 109–125. Studies in the History of Art 57. Monograph Series II. Washington, D.C.: National Gallery of Art, 1997.

Janecek, Gerald. *Zaum: The Transrational Poetry of Russian Futurism*. San Diego: San Diego State University Press, 1996.

Joostens, J. M. "Malevich in the Stedelijk." In *Kazimir Malevich 1878–1935,* ed. Wim A. L. Beeren, pp. 44–54. Amsterdam: Stedelijk Museum, 1988.

Khalturin, Yulian. "Kazimir Malevich's Artistic Method and Evolution of His Painting Technique." Ph.D. diss., Lomonosov Moscow State University, 2006.

Kokkori, Maria. "Russian Avant-Garde Art: A Historical Contextualization of Selected Paintings by Kazimir Malevich, Ivan Kliun, and Liubov Popova c.1905–1925." Ph.D. diss., Courtauld Institute of Art, 2008.

Kokkori, Maria, and Alexander Bouras. "Charting Modernism: Kazimir Malevich's Research Tables." In *Malevich,* ed. Achim Borchardt-Hume, pp. 164–195. London: Tate, 2014.

———. "The Painting Techniques of Kazimir Malevich: 1900–1910." In *Painting Techniques, History, Materials and Studio Practice*. Amsterdam: Rijksmuseum, 2015 (Manuscript submitted for publication).

Malevich, Kazimir. *Ot kubizma i futurizma k suprematizmu: novyi zhivopisnyi realism*. Moscow: tip. Obshchestvennaia Pol'za, 1916.

Malewicz, Leonard, et al., v. City of Amsterdam. 517 F. Supp. 2d 322. D.D.C. 2007.

Markov, Vladimir. *Printsipy tvorchestva v plasticheskikh iskusstvakh: faktura*. Petrograd: Izdanie Obshchestva Khudozhnikov 'Soiuz Molodezhi', 1914.

Mayakovsky, Vladimir. *Parizh*. Moscow: Moskovskii rabochii, 1925.

Mazzeo, R., S. Prati, M. Quaranta, E. Joseph, E. Kendix, and M. Galeotti. "Attenuated Total Reflection Micro FTIR Characterisation of Pigment-Binder Interaction in Reconstructed Paint Films." *Analytical and Bioanalytical Chemistry*, 392, nos. 1–2 (2008): 65–76. http://dx.doi.org/10.1007/s00216-008-2126-5.

Miliani, C., K. Kahrim, B. G. Brunetti, A. Sgamellotti, A. Aldrovandi, M. R. van Bommel, K. J. van den Berg, and H. Janssen. "MOLAB, a Mobile Facility Suitable for Non-invasive in-Situ Investigations of Early and Contemporary Paintings: The Case-Study of *Victory Boogie Woogie* (1942–1944) by Piet Mondrian." In *ICOM-CC 15th Triennial Conference New Delhi, 22–26 September 2008,* ed. Janet Bridgland, pp. 857–864. New Delhi: Allied Publishers, 2008.

Miliani, C., F. Rosi, A. Burnstock, B. G. Brunetti, and A. Sgamelotti. "Non-invasive in-Situ Investigations Versus Micro-sampling: A Comparative Study on a Renoirs Painting." *Applied Physics A* 89, no. 4 (2007): 849–856. http://dx.doi.org/10.1007/s00339-007-4222-3.

Miliani, C., F. Rosi, A. Daveri, and B. G. Brunetti. "Reflection Infrared Spectroscopy for the Non-invasive in Situ Study of Artists' Pigments." *Applied Physics A* 106, no. 2 (2012): 295–307. http://dx.doi.org/10.1007/s00339-011-6708-2.

Monico, L., F. Rosi, C. Miliani, A. Daveri, and B. Brunetti. "Non-invasive Identification of Metal-Oxalate Complexes on Polychrome Artwork Surfaces by Reflection Mid-infrared Spectroscopy." *Spectrochimica Acta Part A: Molecular and Biomolecular Spectroscopy* 116 (December 2013): 270–280. http://dx.doi.org/10.1016/j.saa.2013.06.084.

Rerberg, Fedor. *Kraski i drugie khudozhestvennye sovremennye materialy.* Moscow: Izd. Moskovskago tovarishchestva khudozhnikov′, 1905.

———. *Palitra sovremennogo khudozhnika*. Moscow: Gosizdat, 1921.

Rosi, F., A. Burnstock, K. J. Van den Berg, C. Miliani, B. G. Brunetti, and A. Sgamelotti. "A Non-invasive XRF Study Supported by Multivariate Statistical Analysis and Reflectance FTIR to Assess the Composition of Modern Painting Materials." *Spectrochimica Acta A* 71, no. 5 (2009): 1655–1662. http://dx.doi.org/10.1016/j.saa.2008.06.011.

Rosi, F., C. Miliani, C. Clementi, K. Kahrim, F. Presciutti, M. Vagnini, V. Manuali, A. Daveri, L. Cartechini, B. G. Brunetti, and A. Sgamellotti. "An Integrated Spectroscopic Approach for the Non-Invasive Study of Modern Art Materials and Techniques." *Applied Physics A* 100, no. 3 (2010): 613–624. http://dx.doi.org/10.1007/s00339-010-5744-7.

Vagnini, M., C. Miliani, L. Cartechini, P. Rocchi, B. G. Brunetti, and. A. Sgamellotti. "FT-NIR Spectroscopy for Non-invasive Identification of Natural Polymers and Resins in Easel Paintings." *Analytical and Bioanalytical Chemistry* 395, no. 7 (2009): 2107–2118. http://dx.doi.org/10.1007/s00216-009-3145-6.

Vikturina, Milda, and Alla Lukanova. "A Study of Technique: Ten Paintings by Malevich in the Tretiakov Gallery." In *Kazimir Malevich, 1878–1935*, pp. 187–197. Los Angeles: Armand Hammer Museum of Art and Cultural Center, 1990.

Wijnberg, Louise. "Do We See What We Know or Do We Know What We See? Conservation of Oil Paintings in the Stedelijk Museum Amsterdam." In *Issues in Contemporary Oil Paint*, ed. Klaas Jan van den Berg, Aviva Burnstock, Matthijs de Keijzer, Jay Krueger, Tom Learner, Alberto de Tagle, and Gunnar Heydenreich, pp. 21–23. Cham, Switzerland: Springer, 2014.

Index

Page numbers in *italics* indicate tables and figures.

SUMMARY OF REQUIREMENTS FOR SMITHSONIAN CONTRIBUTIONS SERIES

For comprehensive guidelines and specifications, visit www.scholarlypress.si.edu.

ABSTRACTS must not exceed 300 words.

TEXT must be prepared in a recent version of Microsoft Word; use a Times font in 12 point for regular text; be double spaced; and have 1" margins.

REQUIRED ELEMENTS are title page, abstract, table of contents, main text, and references.

FIGURES must be numbered sequentially (1, 2, 3, etc.) in the order called out; have components lettered consistently (in size, font, and style) and described in captions; include a scale bar or scale description, if appropriate; include any legends in or on figures rather than in captions. Figures must be original and must be submitted as individual TIF or EPS files.

FIGURE FILES must meet all required specifications in the Digital Art Preparation Guide. Color images should be requested only if required.

TAXONOMIC KEYS in natural history manuscripts should use the aligned-couplet form for zoology. If cross referencing is required between key and text, do not include page references within the key, but number the keyed-out taxa, using the same numbers with their corresponding heads in the text.

SYNONYMY IN ZOOLOGY must use the short form (taxon, author, year:page), with full reference at the end of the manuscript under "References."

REFERENCES should be in alphabetical order, and in chronological order for same-author entries. Each reference should be cited at least once in main text. Complete bibliographic information must be included in all citations. Examples of the most common types of citations can be found at SISP's website under Resources/Guidelines.